Cho Kin Wong
Doctor of Philosophy
1980

Summary

Increased antitumour selectivity may be expected from the combination of radiotherapy and cancer chemotherapy. Radiosensitizing agents which have been employed for this purpose are reviewed in the first chapter.

The acridine nucleus with its purported DNA intercalation capability has been used in the design of antitumour agents. A review of the extensive structure-activity relationship studies in this area is found in Chapter 2.

Irreversible and selective attachments of acridine molecules to the DNA of cancer cells is expected to inhibit the proliferation of these cells permanently. Nitrenes are electrophilic species which may react with nucleophilic centres in DNA, and can be generated by irradiation of azido compounds. Azido derivatives of 9-anilinoacridine should therefore prove to be effective irreversible antitumour radiosensitizing agents. The chemistry and pharmacology of azides and nitrenes are discussed in Chapter 3.

In the Discussion, the synthesis and characterisation of 9-anilinoacridines are described. Raney nickel-hydrazine hydrate reduction of nitroanilino derivatives gives the corresponding amines. Azido derivatives are formed when the para and meta aminoanilino-acridines are diazotised and reacted with aqueous sodium azide. Diazotisation of the ortho aminoanilinoacridine affords 9-(benzotriazol-1-yl)acridine; thermolysis of this compound produces 13H-quin[4,3,2-kl]acridine. Photolysis studies of the azides suggest that their degree of decomposition is proportional to the irradiation time and inversely proportional to the irradiation wavelength.

L1210 mouse leukaemic cell culture is selected as the biological model for the detection of photosensitization by azides. The growth characteristics of L1210 cells are presented in Chapter 6. The additional cytotoxicity of the photosensitization by azido compounds is probably due to the photogeneration of reactive (nitrene) species since it is proportional to the irradiation time of cell cultures treated with these azido agents. Both the model azide azidobenzenesulphonamide and the azidoanilinoacridines exhibit photosensitization effects. Thorough control experiments demonstrate and isolate such photosensitization properties.

Key words: *tumour*
chemotherapy
radiosensitization
azidoanilinoacridines
nitrenes

Acknowledgements

The author wishes to express his gratitude to Professor M.F.G. Stevens, BPharm, PhD, DSc, MPS for his interest, advice and encouragement throughout the course of this work.

Thanks are extended to members of the Pharmacy Department especially members of the Cancer Chemotherapy Research Group for their criticisms and support.

Ms. L. Page is thanked for typing the script.

The funding of this research project and the award of a postgraduate studentship by the Lord Dowding Fund for Humane Research are gratefully acknowledged.

A tous ceux que j'aime


N + N + N
≡ N3

Contents

* * * * * * * *

Part 1

Introduction

Part 1 Introduction

Chapter 1

1.1 Selectivity in the chemotherapy of cancer

Cancer is a disease of multicellular organisms which is characterised by the uncontrolled multiplication and spread within the organism of apparently abnormal forms of the host's own cells[1]. This definition encompasses the three key characteristics of cancer; namely cellular multiplication, invasiveness and autonomy.

Cell division and growth in healthy animals and man are regulated precisely by control mechanisms of the body[2]. A cell becomes malignant when it escapes from these control mechanisms[3]. As the tumour grows larger and ages, especially in rapidly dividing tumours, the cells become undifferentiated. Persistent growth is followed by invasion of surrounding normal tissues and clumps of cancer cells may break off into the circulation and be carried to distant sites to form metastases[4]. When the tumour growth involves vital organs, or if the disease has disseminated, chemotherapy is perhaps the only remaining therapeutic armament[5].

There are several reasons for the lack of selective toxicity[6] of drugs used in cancer chemotherapy[7]. Cancer cells have originated from the host and are not truly foreign. Therefore they do not arouse an immunological response as in bacterial infections. Biochemical and morphological differences between normal and cancer cells appear to be quantitative rather than qualitative, and agents which damage cancer cells also harm the host. Cancer cells rapidly develop resistance to antitumour agents[8] and further intensive chemotherapy at this stage can often

lead to the emergence of more malignant cell lines. Drugs then have to be used at higher doses and even become selectively toxic towards the host. Most available antitumour agents produce a wide range of untoward effects[9], e.g. immunosuppression, bone marrow toxicity, nausea and vomiting etc.

Despite this lack of selectivity of the existing antitumour agents, improved therapeutic results have followed the rational combination of drugs with different mechanisms of action and toxicities. This approach has at least partially combatted the problem of tumour cell resistance to single agents. The correct timing of pulsed combination chemotherapy allow maximum exploitation of the differential in recovery times between normal and malignant tissues leading to maximum tumour cell kill with minimum of toxicity. This relative lack of toxicity allows pulsed therapy to be continued for much longer periods and therefore increases the chance of cure[10, 11].

Drugs elicit their biological responses by first reacting or interacting with the chemical groupings of rigid or semirigid three dimensional biochemical structures called receptors *in vivo*. These receptors may be specific proteins (e.g. enzymes), nucleic acids or other cellular macromolecules. Most reactions between drug and receptor are reversible and they are due to binding of drug and receptor molecules by weak intermolecular forces such as hydrogen bondings, ionic bondings, hydrophobic interactions and van der Waals' forces[12].

Covalent binding of drug and receptor molecules are not unknown, e.g. arsenicals, mercurials and antimonials which act on parasites by combination with mercapto-groups; penicillins, the phosphorus-containing anticholinesterases and the nitrogen mustards, all of which either acylate or alkylate certain receptors[6].

Covalent bonds are very strong bonds which involve the sharing of one or more pairs of electrons between two atoms. These bonds can only be broken by heat, reactive chemicals or certain enzymes. Drugs which evoke their biological response by the formation of covalent bonds form permanent or irreversible complexes with their receptors. These drugs are often electrophilic (or they produce electrophilic species) and react with nucleophilic centres of cell components. The cellular macromolecules which carry vital information and possess abundant nucleophilic centres are proteins and nucleic acids.

The aim of the present work is to develop new drugs which are structurally specific - that is, they have specific affinity for their receptors. This specificity of action should be determined by a precise combination and steric arrangement of chemical groups in the drug molecule which could facilitate interaction by chemical bonding and physical interaction with appropriate receptor molecules[13].

It is a further aim of this project to seek chemical agents, carrying a masked reactive function, which are preferentially concentrated in tumour cells; these agents should then form reversible drug-receptor complexes with vital tumour cellular components. The masked reactive function is so chosen that it may be activated by low doses of penetrating radiation to liberate a highly reactive electrophilic species. Upon irradiation of the tumour treated with these agents, the reactive electrophilic species should then be generated *in situ* resulting in irreversible covalent binding of the drug to its receptor. This process should then afford a bonus selectivity since only the chemical agents (or drug-receptor complexes) in the path of the radiation beam are

affected and surrounding normal cells are spared. Therefore high degree of selectivity results from accurate focusing of the radiation beam as well as the intrinsic selectivity of these "pro-drug" molecules (determined through structure-activity relationship considerations) for tumour cells.

The receptors of interest to this work are the nucleic acids; the drug moiety which has specific affinity for nucleic acids employed here is the acridine nucleus and the masked reactive chemical function is the azido group.

1.2 Interplay of radiotherapy and chemotherapy

The inactivation of the proliferative capacity of mammalian cells by radiation is a complex process. It is represented schematically in Figure 1. The cellular target may be one of the vital cellular components, e.g. DNA.

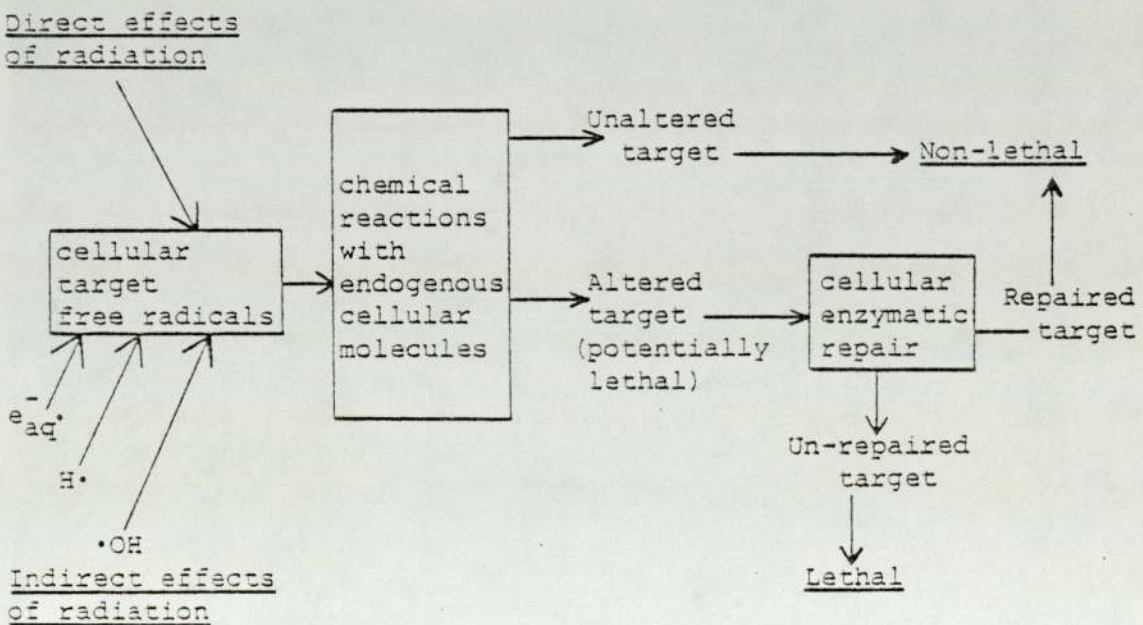

Figure 1

Radiation causes ionisations and excitations in these targets with resultant alteration to their chemical structures. These events have been classified as due to the direct effects of radiation. However, much of the energy absorbed by a cell is absorbed in water molecules. This results in highly reactive free radical species. These free radicals diffuse to and react with vital cellular molecules leading again to altered chemical structures. These are the indirect effects of radiation[14]. The most important free radical species generated in the radiolysis of water are H·, ·OH, and e^-_{aq}·. (For a further review on the radiolysis of chemicals and biochemicals, see reference 15.)

Both radiation and chemicals are commonly used in the treatment of malignant diseases. There can be considerable therapeutic gain by the combination of chemical and radiation therapy. The term "Radiosensitizer" is defined here as a chemical agent which increases the sensitivity of cells to the cytotoxic effect of radiation in radiotherapy. It may or may not possess antitumour activity in its own right, but when employed in combination, confers a greater than additive effect of the drug treatment and radiotherapy separately.

Figure 2

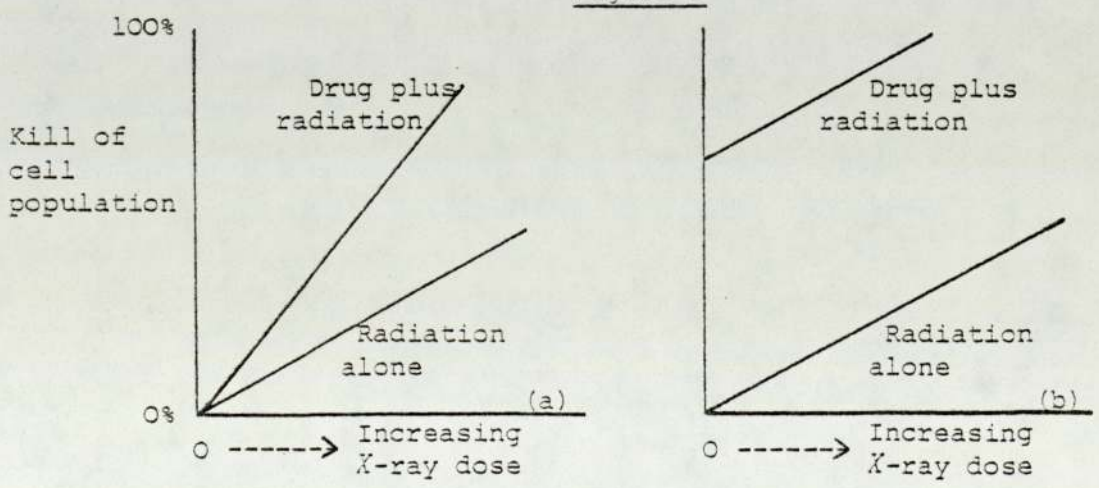

The hypothetical dose-response curves in Figure 2 demonstrate the two basic mechanisms of combined chemical and radiation effects. In Figure 2a, addition of drug has changed the slope of the dose-response curve; this slope is a measure of the radiation sensitivity of the cell population. The drug increases the sensitivity of the cells to the effects of radiation. In Figure 2b, the drug has added to the effect of radiation by acting independently on the cell population[16].

Most of the chemical agents used in combined chemo- and radio-therapy show both mechanism of action depicted above; it is the type of agents which show predominantly type 2a mechanism of action which will be discussed and described here as radiosensitizers. Bridges[17] has reviewed the earlier development of radiosensitizing agents.

1.3 Review of radiosensitizing agents

One of the first radiosensitizers investigated was a synthetic vitamin K substitute, Synkayvit, which is the tetra sodium salt of 2-methyl-1,4-naphthalenediol diphosphoric acid ester (1.1), abbreviated MNDP. It was found that MNDP was concentrated to some extent selectively in viable malignant cells in relation to normal cells, in certain types of tumours in man and animals[18]. Mitchell and Simon-Reuss reported significant potentiation of the effects of X-radiation by MNDP in inhibiting mitosis in chick fibroblast cultures and in some patients with squamous cell carcinoma of the buccal cavity[19].

In the hypoxic centres within a solid tumour, cells are resistant to therapeutic ionising radiations such as X- and γ-radiations[20,21]. Several methods of overcoming this problem

have been devised. Churchill-Davidson *et al.* used adjuvant hyperbaric oxygen treatment in clinical radiotherapy[22]. Neutron and π-meson therapies are expensive and not without disadvantages. Fractionated *X*-radiotherapy was shown to allow reoxygenation in the hypoxic fractions of some rodent tumours[23,24]. As tumour cells die after the doses of radiation given early in the course, the demand for oxygen is reduced, and as the tumour begins to shrink the flow and distribution of blood is improved. Thus a proportion of the cells which were hypoxic become oxic and so more sensitive to the radiation given in the next treatment.

Some drugs are purported to mimic the radical-forming ability of oxygen, but are not readily metabolised by the cells in the tumour through which they diffuse; they are thus able to reach hypoxic centres in a tumour. This group of electron affinic radiosensitizers include:

1-(2-nitro-1-imidazolyl)-3-methoxy-2-propanol

or Ro-07-0582, Misonidazole ----------(1.2)

2-methyl-5-nitroimidazole-1-ethanol

or metronidazole, Flagyl ----------(1.3)

(±)-1,2-bis(3,5-dioxopiperazin-1-yl)propane

or ICRF-159, Razoxane ----------(1.4)

4-nitroacetophenone

or PNAP ----------(1.5)

5-nitro-2-furaldehyde semicarbazone

or nitrofurazone ----------(1.6)

N-(5-nitro-2-furfurylidine)-1-aminohydantoin

or nitrofurantoin ----------(1.7)

ICRF-159 has anti-mitotic/anti-tumour activity both *in vitro* and *in vivo*[25,26] as well as a radiosensitizing effect. Misonidazole

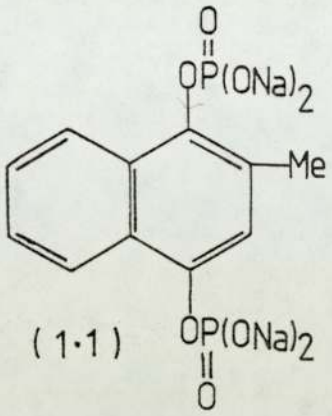

(1·1)

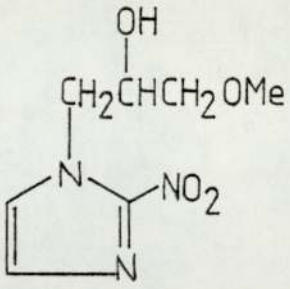

(1·2)

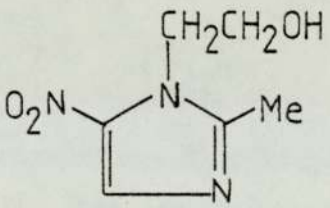

(1·3)

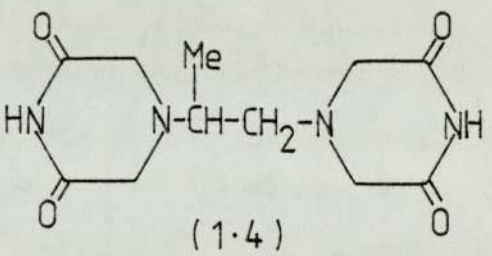

(1·4)

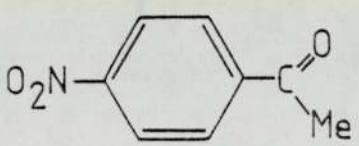

(1·5)

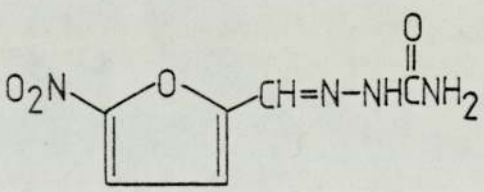

(1·6)

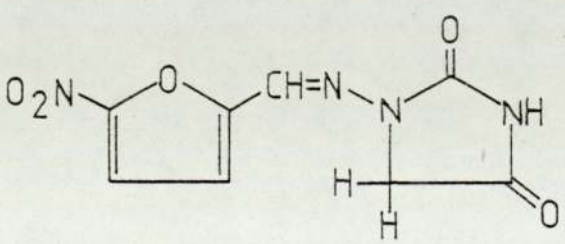

(1·7)

and metronidazole at therapeutic doses have low toxicity and are undergoing clinical trial[21,27,28] in adjuvant radiotherapy of seminoma of the testis, Hodgkin's disease, supratentorial glioblastomas and other local tumours. In a study of nitrofurans as radiosensitizers, Chapman *et al.*[29] described the necessity of the electron affinic properties and the nitro functions of compounds (1.5), (1.6) and (1.7). Hypoxia was shown to enhance the rate of radiation-induced binding of nitrofurazone to bovine serum albumin, DNA, polynucleotides and whole Chinese hampster cells. Kinetic studies[30,31] suggest that ionising radiations elicit the formation of primary reactive species (H·, ·OH, e^-_{aq}·) in hypoxic areas, and cellular components, e.g. DNA, and radiosensitizer molecules may react with these species to form radicals. It is the reactions between radiosensitizer radicals and cellular component radicals which result in cell deaths. In an oxic environment, O_2 molecules may react with e^-_{aq} to form the oxygen radical anion O_2^-· which then combines with cellular components resulting in biochemical lesions[32].

Pyrimidin-2,4-diones substituted in the 5-position with halogen atoms, and their deoxyribosides, may be incorporated into DNA in place of the pyrimidine bases and their deoxyribosides respectively[33]. Table 1 shows their structures, their names or abbreviations, and the van der Waals radii of the atoms in the 5-position. The bond dissociation energies of CH_3-X are included for comparison.

Stereochemical considerations suggest that BUdR is the best thymidine analogue since the van der Waals radius of bromine is very close to that of the methyl group; while FUdR is an analogue of deoxyuridine since the radius of fluorine is much closer to

Table 1

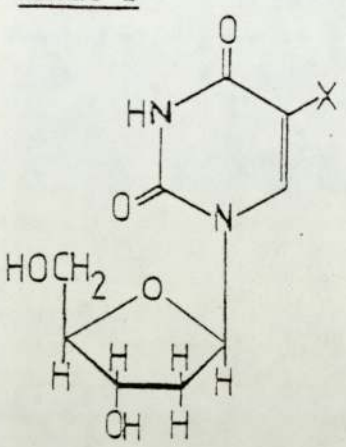

Names or abbreviations	X	van der Waals radii[34] (Å)	Bond dissociation energies[39] of CH_3-X (Kcal/mole)
Deoxyuridine	H	1.2	104
Deoxythymidine	Me	2.0	88
FUdR	F	1.35	108
CUdR	Cl	1.80	84
BUdR	Br	1.95	70
IUdR	I	2.15	56

the radius of hydrogen in uracil than of the methyl group in thymine[34].

The incorporation of these 5-halogeno deoxyuridines, namely 5-chlorodeoxyuridine (CUdR), 5-bromodeoxyuridine (BUdR) and 5-iododeoxyuridine (IUdR) were shown to increase cellular sensitivity to ultra violet and *X*-radiation *in vitro*[35]; the incorporation of 5-fluorodeoxyuridine (FUdR) is controversial[36] and FUdR has insignificant radiosensitizing effect, but it does inhibit the *de novo* synthesis of thymidylic acid[37]. The enhancement of sensitivity to *X*-radiation parallels the size of the halogen atom in these compounds, that is IUdR has greater radiosensitizing effect than BUdR whereas CUdR has the least effect. The anti-metabolic properties of these compounds may be quite separate from their radiosensitizing properties as Erikson and Szybalski[38] reported that the human bone marrow D98/AG line cells can grow for an unlimited number of generations at IUdR concentrations below 10^{-5} M, but at these same conditions with irradiation by

ultra violet or *X*-radiation, there were significant radiosensitizing effects as compared with controls. One could speculate that radiation may cause homolytic fission at the carbon-halogen bond; such dehalogenation releases halogen radical which may inflict damage to the post-irradiation repair mechanisms. If this is the explanation, it would account for the greater sensitizing effect of IUdR than BUdR and CUdR and the inactivity of FUdR, since the carbon-iodine bond has lower bond dissociation energy than the carbon-bromine, carbon-chlorine and carbon-fluorine bonds[39], as shown in Table 1.

From the various types of radiosensitizers discussed, the ideal radiosensitizer in combined chemo/radio therapy should be concentrated selectively by tumour cells. It may or may not possess antitumour activity itself, but in the presence of radiation it should be converted to a noxious reactive species independent of the degree of oxygenation of the tumour tissue, and should then cause irreversible damage to vital tumour cell components. Such a reactive species should preferably be short-lived so it may cause biochemical injuries only at the immediate vicinity where it is formed. Surplus reactive species should then form non-toxic metabonates and/or metabolites which will not interfere with surrounding normal tissues.

The development of such agents provide the basis of the research work described in this thesis and it will be shown in various parts of this work that even *in vitro* it is possible to satisfy some of the criteria some of the time, but very difficult to satisfy all the criteria at the same time.

Chapter 2

2.1 History of acridines

Graebe and Caro isolated acridine from coal tar in 1870[40]. Graebe's system of numbering the acridine ring has been adopted by IUPAC and it will be used throughout this work. The numbering of the 9-anilinoacridine (2.1) structure is given here as an example.

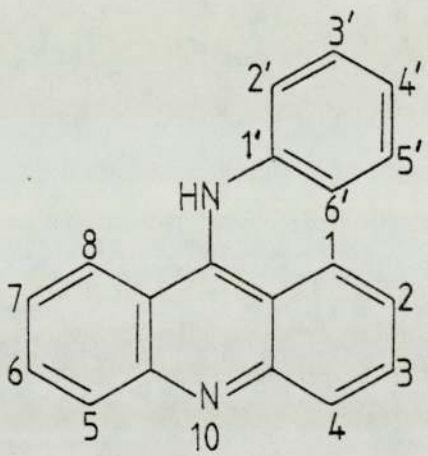

(2·1)

The utilization of acridines in medicine dates back to the early decades of this century. The outbreak of the first world war led to an increased demand for antibacterials. Proflavine (2.2) and acriflavine (2.3) were considered valuable drugs for the prevention and treatment of sepsis in wounds. During the second world war the neutral form of proflavine was developed and aminacrine (2.4) hydrochloride was introduced. In 1942, the shortage of quinine stimulated the widespread use of the anti-malarial, mepacrine (2.5). The chemotherapeutic activities of these acridines were attributed to their interactions with nucleic acids. The selective toxicities to the parasitic organisms -

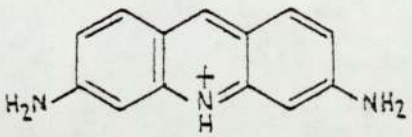

Proflavine (2.2)
3,6-diaminoacridinium ion

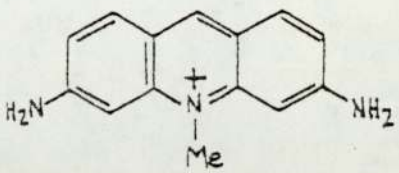

Acriflavine (2.3)
3,6-diamino-10-methylacridinium ion

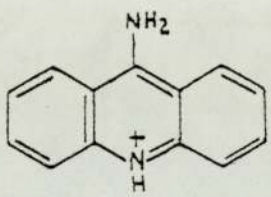

Aminacrine (2.4)
9-aminoacridinium ion

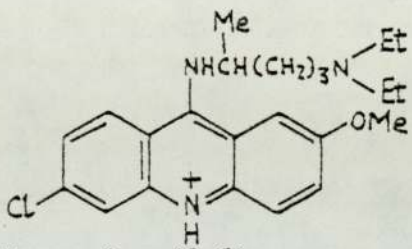

Mepacrine (2.5)
3-chloro-7-methoxy-9-(1-methyl-4-diethylaminobutylamino)-acridinium ion

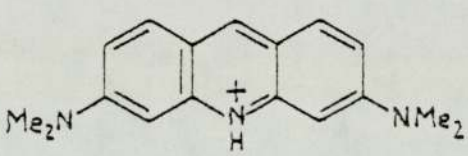

Acridine orange (2.6)
3,6-bisdimethylamino-acridinium ion

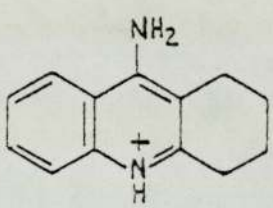

9-Amino-1,2,3,4-tetrahydro-acridinium ion (2.7)

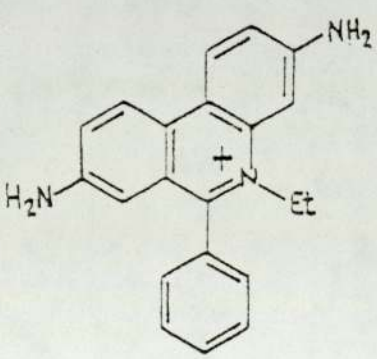

Ethidium bromide (2.8)

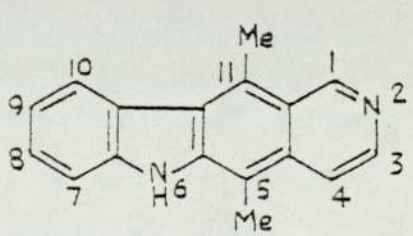

Ellipticine (2.9)

that is, bacteria and protozoa etc., were due to the lipophilic-hydrophilic balance of these drugs and their steric features which enabled them to concentrate in the cells of the parasites to cause fatal damage to these cells. Excellent reviews on the earlier studies of antibacterial and antimalarial acridines are provided by Albert[41] and by Acheson[42].

2.2 Cellular interactions and DNA intercalation

In the past fifty years, many experiments were carried out to reveal the site of action of acridine drugs. Acridine orange (2.6) was found to stain nucleic acids in cells and it could differentiate deoxyribonucleic acid (DNA) and ribonucleic acid (RNA) which fluoresce green and red respectively under a fluorescence microscope[43]. Mammalian cells have been observed to take up aminoacridines and concentrate them in the nucleus[44,45]. Furthermore, the antibacterial action of aminoacridines *in vitro* is not lowered by serum protein[46] but strongly inhibited by exogenous nucleic acids[47]. These results imply an affinity of acridines for nucleic acids. It has been shown *in vitro* that proflavine (2.2) inhibits bacterial DNA polymerase by 85% and RNA polymerase by 30%[48]. The mechanism of action was proposed to be the binding of proflavine to the DNA starter.

Albert demonstrated that the planarity of the three rings of acridine with a minimum planar area of 38 sq Å is required for antibacterial activity. Hydrogenation of one ring of aminacrine (2.4) to form 9-amino-1,2,3,4-tetrahydroacridine (2.7) practically eliminated its activity[49]. Conversely, ethidium bromide (2.8) which has similar stereochemical features to proflavine, inhibits the same two DNA-dependent polymerases by combining with the DNA

template[50,51]. By a spectrophotometric method and by equilibrium dialysis, Peacocke and Skerrett[52] established that proflavine is bound to DNA by two mechanisms: (a) a first-order reaction that reaches equilibrium at one proflavine molecule per four or five nucleotides; and (b) a weaker, high-order process that leads to a drug/phosphate binding ratio of 1:1. They also observed the bathochromatic shift induced by aminacrine (2.4) when associating with DNA, and the absence of such spectral change when the hydrogenated derivative (2.7) was allowed to mix with DNA under the same conditions, confirming Albert's assertion that the biological activities of acridines are correlated with their stereochemical structures[49]. The binding process (b) apparently is due to the adsorption of further acridine molecules onto those already attached to the DNA hence forming drug aggregates[53].

The intercalation model[54] of drug/DNA interaction formulated by Lerman is identified with the binding process (a). This model suggests that a proflavine molecule is sandwiched between two layers of nucleotide base-pairs of the Watson-Crick spiral. The primary amino groups contribute to the binding by forming ionic linkages with the phosphate residues of DNA[55], and are protected from attack by nitrous acid as adjudged by a greatly reduced rate of diazotisation. Lerman also showed that the ratio of the fluorescence intensities of flowing and stationary proflavine/DNA solutions agrees with the proposal that the flat acridine ring is slotted into the DNA structure perpendicular to the helical axis[56].

For intercalation to occur, the helix should become locally unwound to accommodate the acridine ring. The proflavine molecules so intercalated should cause the helix to be extended, stiffened and straightened which accounts for the threefold increase in

viscosity. The DNA-proflavine complex was found to have a lower sedimentation coefficient than free DNA. This was attributed to loss of mass per unit length since a proflavine molecule has less than half the mass of the same volume of DNA. *X*-ray diffraction patterns of oriented fibres drawn from the complex were much simpler than those given by pure DNA. The retention of the 3.4 Å meridonal spots as the sole meridonal reflexion suggested that the acridine molecules occupy the same 3.4 Å space corresponding to the separation between stacked layers. The new positions of the first equatorial reflections indicated that each DNA molecule was now more closely packed than pure DNA[54].

The sheer elegance of Lerman's model of DNA intercalation and its potential applicability to explain the binding to DNA of many other drugs were soon appreciated. Criteria are set out to examine chemicals before they are ascribed as intercalating agents.

The unwinding of the helix can be evidenced by the consequential removal and reversal of the supercoiling of closed circular duplex DNA as the drug-DNA binding ratio increases; that is, the number of right-handed supercoils steadily decreases at first, then at a critical ratio of added molecules the supercoils are all removed and the DNA molecule behaves as an untwisted open circle. As further additions of agents are made, the accumulated stretching of the DNA ring re-introduces supercoiling, but this time it is right-handed. This sequence of events in supercoiling is reflected in characteristic changes in the sedimentation coefficient of such drug-DNA complexes[57]. The predicted extension of the DNA helix can be investigated by measuring changes in the viscosity and sedimentation coefficient of sonicated rod-like DNA fragments. An intercalating agent, e.g. proflavine, would increase

the viscosity and decrease the sedimentation coefficient of native calf thymus DNA[58].

Neither of these two techniques alone is sufficient to establish unequivocally an intercalative mode of binding, for non-intercalative unwinding of the DNA helix by steroidal diamines has been observed[59,60]. Conversely, viscosity enhancement indicative of helix extension by the antibiotic netropsin has been reported, though no effect on the winding of the helix could be detected[61,62,63]. Only when both of these experiments offer positive results should a compound be justifiably classified as an intercalating agent. One such compound is the antitumour plant alkaloid, ellipticine[64] (2.9). Experimental results on this compound are in accord with the intercalation model epitomised by the intercalative action of proflavine[57,58]. The unwinding angle on binding to supercoiled DNA is estimated to be 7.9°, similar to that of proflavine. Another study on the ellipticine series of antitumour agents[65] suggests a positive correlation between their DNA affinity[66], their optimal unwinding angles and their antitumour activities[67].

2.3 Antitumour acridines and structure-activity relationship

The development of antitumour agents containing the acridine ring has been recent. The realisation that intercalation into DNA may constitute the major molecular mode of action of acridine drugs has provided a satisfactory basis for their interference with nucleic acid synthesis *via* distortion of the structure and function of the DNA template, but it nevertheless highlights the question of their selective toxicity. It is reasonable to assume that the biochemical and morphological differences between normal and tumour cells, however slight and subtle, could be exploited

to evolve a series of selective antitumour agents by studying the relationship between their chemical structures and the biological response they may evoke. This approach has been the foundation of much extensive work in acridine research.

Peck, O'Connell and Creech examined the effect of several 9-aminoacridines with monofunctional sulphur mustard or nitrogen mustard groups linked through an aminoalkyl side chain[68]. Davis and Soloway developed a series of neutron-capture agents based on carborane containing acridines which were intended for use in the neutron-therapy of cancer[69]. More significantly, the work of Ledochowski's group in Poland and the contribution from Cain and colleagues in New Zealand have put acridines very much on the map of cancer chemotherapy.

The Polish work started in 1960 in a search for antitumour activity amongst 9-aminoacridines followed by the synthesis of numerous derivatives resembling the structure of mepacrine (2.5). The inhibition of growth of Sarcoma 180 in mice was used as a primary screen. After much deliberation and many molecular modifications, the 3-chloro and 7-methoxy groups were rejected and a nitro group was introduced[70]. The one compound in this series which exhibits highest antitumour activity is Ledakrin, 1-nitro-9-(3-dimethylaminopropylamino) acridine dihydrochloride (2.10).

In the course of studies on the biological activities of Ledakrin and its nitro isomers, that is, the 2-nitro (2.11) and 3-nitro (2.12) derivatives, it was observed that (2.10) was more active than (2.12) and (2.11) was inactive in various cell and animal cytotoxicity screening systems. This could be positively correlated to the inhibitory effect on the incorporation of

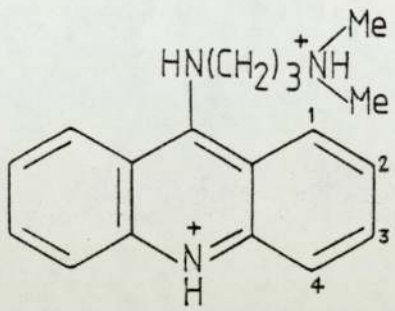

(2.10) = 1 - NO_2

(2.11) = 2 - NO_2

(2.12) = 3 - NO_2

(2.13) = 1 - NHOH

tritiated thymidine (a DNA precursor), uridine (a RNA precursor), and leucine (a protein precursor), but a study on the influence of these compounds on isolated DNA-polymerase and RNA-polymerase activities, offered contradictory results. A spectrophotometric analysis of the drug-DNA binding ratio also suggested that Ledakrin was less efficient in DNA binding than its isomers. However, it was proposed that the 1-nitro group may be more susceptible to reduction than a 2-nitro or 3-nitro function and the high antitumour activity of Ledakrin could be due to its reduced product, the 1-hydroxylamino analogue (2.13)[71].

Using the method of Boyland and Nery for the detection of hydroxylamines[72], it was found that Ledakrin was indeed metabolised to the hydroxylamine (2.13) by the action of the post-mitochondrial fraction from mouse liver homogenate. Furthermore, there was significant correlation between the amount of hydroxylamine produced and the biological activity of Ledakrin. This is in accord with the findings of Konopa *et al.* that Ledakrin binds covalently to DNA of Ehrlich ascites tumour cells *in vivo*, but not *in vitro*[73].

Ledakrin was admitted for clinical evaluation in 1967 after careful toxicological studies[74]; unfortunately, the agent was reserved only for patients near the terminal stages of their disease and the clinical studies so far have produced disappointing results[75,76,77,78].

Cain and his collaborators marked their entry to the acridine arena with a structure-activity relationship (SAR) study of a series of coplanar, fully ionised cationic agents in 1971. They proposed that the acridine ring structure enables the agent to lodge temporarily in the minor groove of the DNA duplex, Figure 3; subsequent intercalation leads to cell death. They also recognised that cellular penetration of the agent is the limiting factor and dependent on the concentration of neutral species - that is, the rate of passive diffusion is related to high lipophilicity and low ionisation of the agent at physiological pH. An agent with the optimal overall lipophilic/hydrophilic balance should then be able to reach its correct site of action[79].

The first acridine derivatives synthesised by Cain had aromatic groups interspersed with amino and amido functions, attached to the 9-position of the acridine ring[79,80]. Molecular simplification produced 9-anilinoacridine (2.1)[81] and its derivatives. The 9-anilinoacridine structure (2.1) has since been adopted as the parent in their series of potential antitumour agents. The screening system for antitumour activity consists of inoculation of 10^5 L1210 cells either (a) intraperitoneally (*ip*), (b) subcutaneously (*sc*) above the right axilla, or (c) intracerebrally (*ic*) through a temporal fissure into C_3H/DBA_2F_1 hybrid mice[82]. *Ip* drug treatment starts 24 hours later and continues for 5 days. Results are expressed as a % increase in life-span comparing with untreated animals.

Figure 3

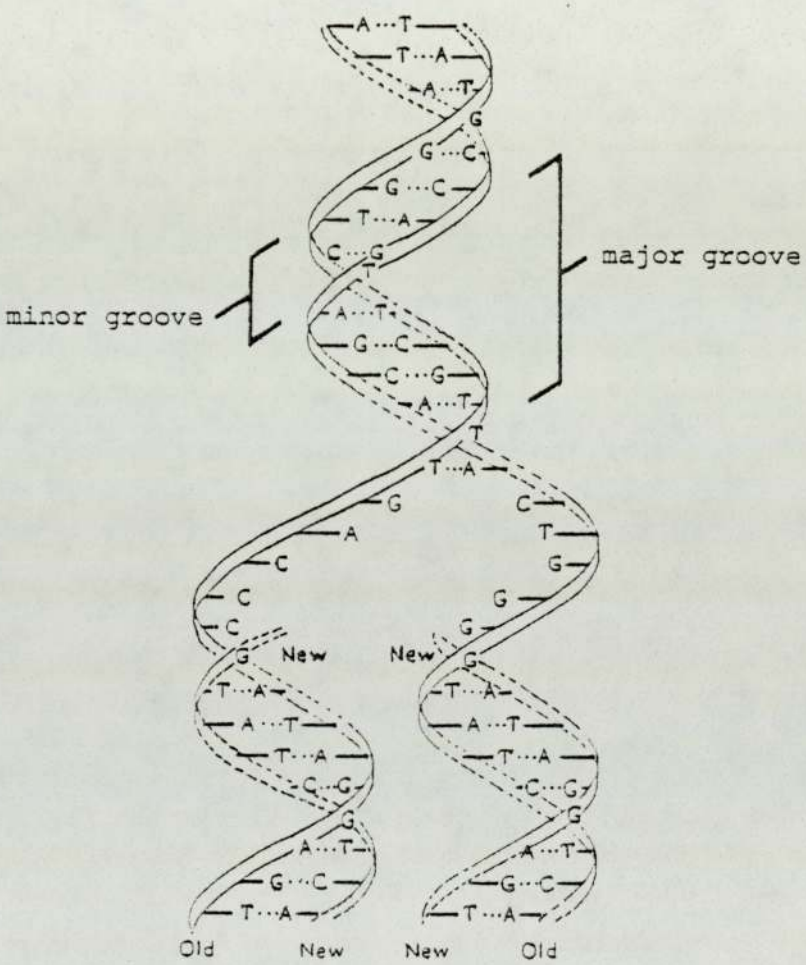

A replicating DNA duplex

The elucidation of antitumour activity by SAR is empirical but effective. Addition of a substituent to the parent compound of a drug series would invariably alter the overall lipophilic/hydrophilic balance. Additionally, this may alter steric, electronic and hydrophobic drug-receptor interactions, as well as affecting the rates of either metabolic or direct chemical activation and/or deactivation. The basicity of the compound may also be changed as a result[83].

Since correct lipophilic/hydrophilic balance of a drug is essential in the delivery of the molecule to its site of action[79], an attempt was made to determine and isolate its effect from those due to other factors mentioned above. A homologous series, e.g. compounds (2.14) to (2.17) in Table 2 was prepared. A plot of the biological activity of the members of the series against a measure of their partition properties (e.g. $-\Delta Rm^*$) will then provide a standard curve, Figure 4[84].

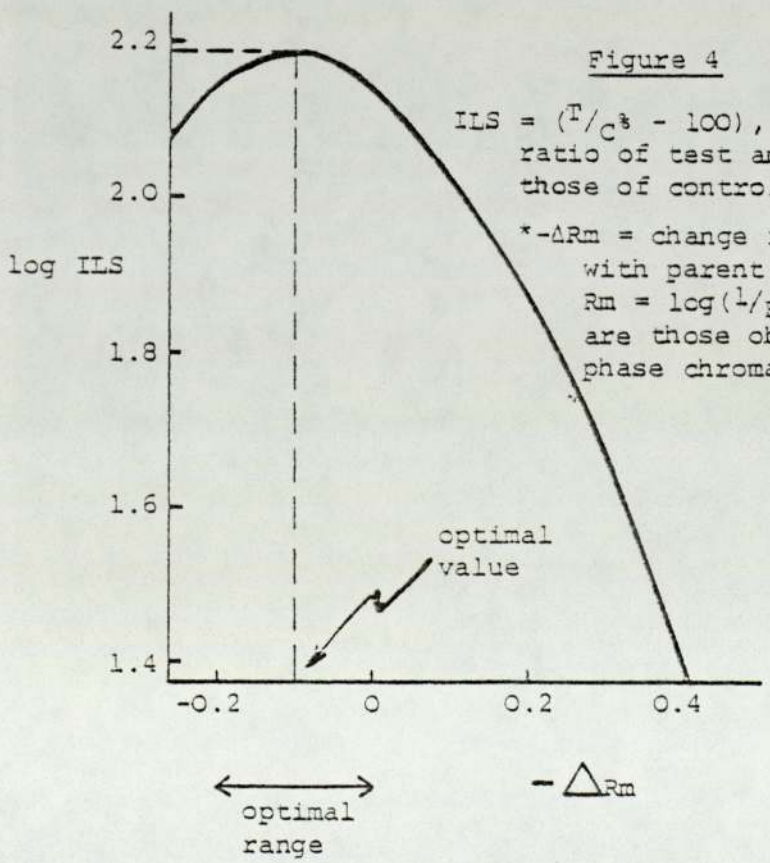

Figure 4

ILS = $(^{T}/_{C}\% - 100)$, where $^{T}/_{C}$ is the ratio of test animal life-span to those of controls.

*-ΔRm = change in Rm values compared with parent compound, where $Rm = \log(^{1}/_{R_f} - 1)$, and R_f values are those obtained from reversed phase chromatography[85].

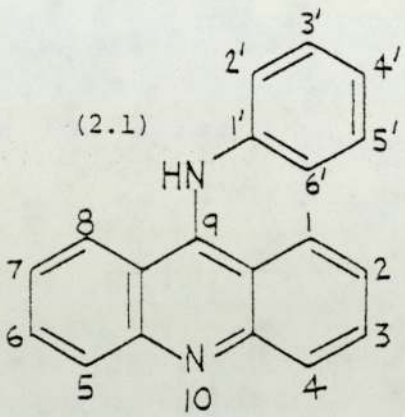

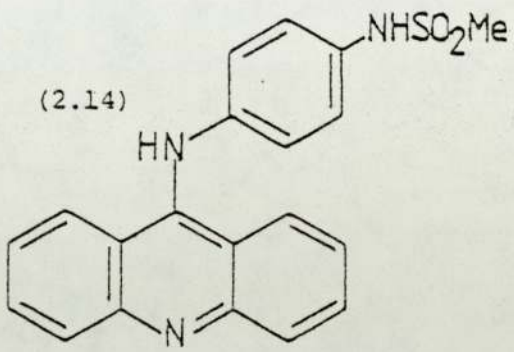

AMSA

Agents	Substituent in (2.1)
2.14	4'-$NHSO_2Me$
2.15	4'-$NHSO_2CH_2Me$
2.16	4'-$NHSO_2(CH_2)_2Me$
2.17	4'-$NHSO_2(CH_2)_3Me$

Agents	Substituent in (2.14)
2.18	2'-OMe
2.19	1-Me
2.20	2-NO_2
2.21	2-NH_2
2.22	2-NHAc
2.23	2,7-$(NH_2)_2$
2.24	2-Me
2.25	1-OMe
2.26	2-OMe
2.27	2-Cl
2.28	2-F

Agents	Substituent in (2.14)
2.29	1-NO_2
2.30	3-Cl,7-OMe
2.31	3-NO_2,7-OMe
2.32	3-NH_2,7-OMe
2.33	2,6-$(NHAc)_2$
2.34	3-NO_2
2.35	3-Cl
2.36	3-Br
2.37	3-I
2.38	3-CF_3
2.39	3,6-$(Me)_2$
2.40	3'-OMe,3-I,5-$OCH_2CHOHCH_2OH$
2.41	4-NO_2
2.42	3'-NH_2
2.43	2'-OEt
2.44	2'-Me

Table 2

In order to obtain maximum biological activity, the lipophilic/hydrophilic balance of an agent must be adjusted to or near the optimal ΔRm. This adjustment can be made by additional compensatory substitution with lipophilic or hydrophilic functions as necessary.

Intercalation has been adduced as being the molecular mode of action and representative members of this drug series, e.g. AMSA (2.14) and *m*-AMSA (2.18) were shown to bind strongly to double stranded DNA and can unwind closed circular PM-2 bacteriophage duplex DNA in a manner characteristic of intercalative drugs[86]. This is confirmed by equilibrium dialysis, spectrophotometric methods, fluorescence studies and thermal denaturation studies. Further, (2.18) inhibits DNA polymerase and RNA polymerase activities *in vitro*[87]. The DNA synthesis inhibitory action of (2.18) was also indicated by an inhibition of the incorporation of labelled thymidine into DNA of L1210 cells both *in vivo* and *in vitro*[88].

An *X*-ray crystallographic analysis of (2.14) demonstrated a considerable distortion of the C(9)-N-C(1') bond angle and showed that the 9-anilino function rotated so that the ring plane lay at right angle to the plane of the acridine system[89]. If this steric arrangement is a requisite for activity[84], appropriate molecular modification by chemical substitution may augment biological activity by providing an optimal fit of the drug molecule to its receptor site provided that the correct lipophilic/hydrophilic balance is maintained. Equally valuable, the information from these modifications should contribute towards the construction of a picture of the environment of the receptor site and aid in future drug design.

The effect of substitution in the various positions of 9-anilinoacridine (2.1) on its antitumour activity is summarised:

Acridine ring

Positions 1, 2, 7 and 8

There is a lack of bulk tolerance at these positions, and biological activities of compounds substituted in these positions are either depressed as in (2.19) - (2.23) or abolished as in (2.24)- (2.33)[84].

Positions 3 and 6

There appear to be hydrophobic sites corresponding to these positions[84], but these sites are restricted in size[90]. Therefore (2.34) - (2.37) have enhanced activity compared with the parent (2.14) while (2.38) with its bulky CF_3 group exhibits no activity. High activity of the 3,6-disubstituted compound (2.39) suggests that both these positions correspond to hydrophobic sites in the receptor.

Positions 4 and 5

There is considerable bulk tolerance for hydrophilic functions here since the large polar 5-substituent of (2.40) affords an active agent[83]. However, a 4-nitro substituent in (2.41) gives a compound of low activity[84].

Anilino ring

Positions 3' and 4'

Only electron donating groups here produce active agents, especially those in the 4' position as in (2.14)[80]. An electron deficient site in the receptor near the 5' position of the drug molecule was proposed[90]. Since an electron donating function at 3' will increase electron-density at the 5' position, an agent such as (2.42) has augmented activity.

Position 2'

Substitution at this position with a methoxy group (2.18) increases dose potency possibly due to reduction of thiolytic cleavage at the C(9)–N bond by steric inhibition of thiolysis[91], with full retention of antitumour activity[92]. However, this region of the receptor site tolerates limited bulk since the larger ethoxy group in (2.43) offers low potency[93]. It was also suggested that this region has a polar nature thereby tending to bind more to the methoxy function of (2.18) than a methyl function in (2.44), since (2.44) was inactive.

This SAR information has enabled an image of the receptor site environment to be constructed, Figure 5.

Compound (2.18), also known as Cain's acridine is undergoing phase 1 clinical trials[94,95] and phase 2 studies have already been planned. Responses were observed in patients with adenocarcinoma of the lung, melanoma, myeloblastic leukaemia and ovarian carcinoma. The main toxicities of this agent are haematopoietic, but these are readily reversible on cessation of the drug treatment.

From the evidence presented one can be confident that the 9-anilinoacridine structure has specific affinity for its receptor, the nucleic acids. This structure has been employed in this work as the carrier of a masked reactive function, the azido group. Hopefully, subsequent work will show that this combination - of acridine and azide - will result in compounds which are radiosensitizers for tumour cells.

Figure 5

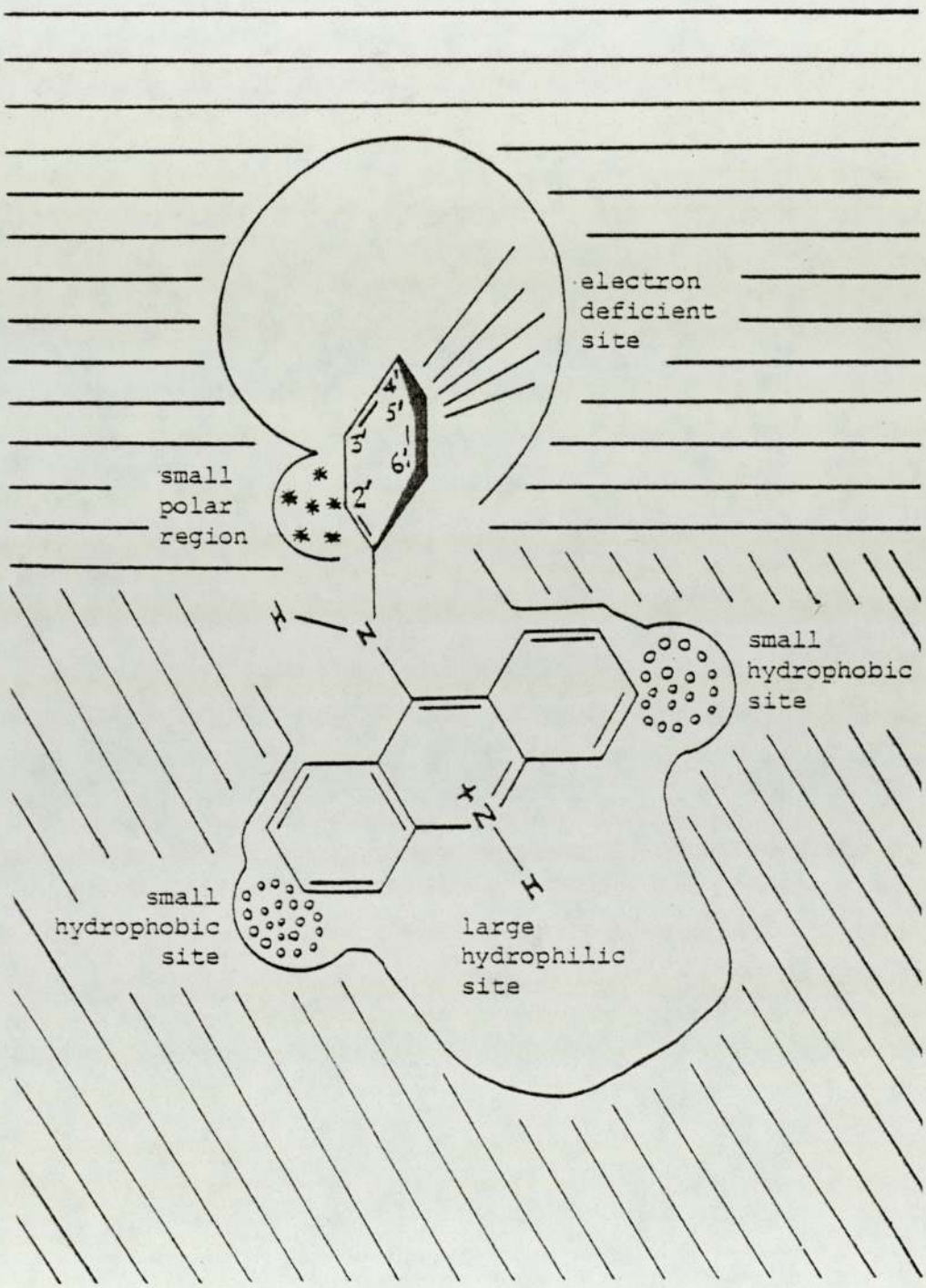
electron
deficient
site
small
polar
region
small
hydrophobic
site
small
hydrophobic
site
large
hydrophilic
site

Chapter 3

3.1 Arylnitrenes and their solution chemistry

Nitrenes are electron deficient, electroneutral monovalent nitrogen intermediates in which a nitrogen atom has one covalent bond to another group (e.g. an aryl group in arylnitrene), one lone pair of electrons and two non-bonding orbitals containing two electrons between them. These two orbitals of different energies may accommodate the two electrons in different ways:

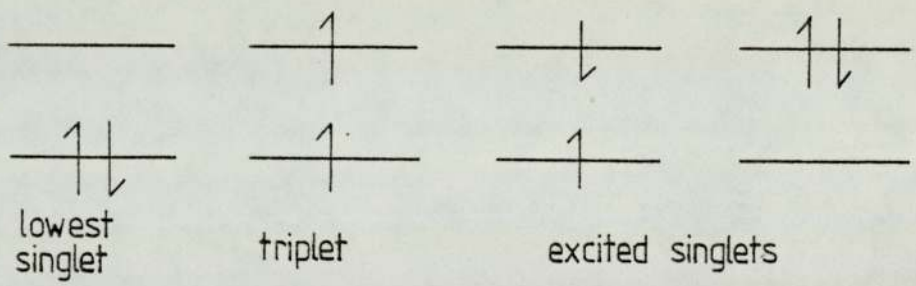

In the triplet nitrene, the two electrons have parallel spins; when these electrons are spin-paired, the nitrene is a singlet. Most nitrenes have triplet ground states. The triplet nitrene $R\ddot{N}\cdot$ is considered a diradical while the singlet nitrene $R\ddot{N}$: behaves as an electrophile.

The nitrenes of special interest are the arylnitrenes. They may be readily generated by reduction (or deoxygenation) of nitro and nitroso compounds or oxidation of amino compounds. Rose was the first to speculate that the carcinogenicity and cytotoxicity of hydroxylamines, amines and amides may be due to their bio-activation to form nitrene intermediates during metabolic oxidation and reduction reactions[96]; subsequent indiscriminate

interaction with cellular components may then be responsible for disorganisation of normal cellular processes. Alternatively, thermolytic and photolytic decomposition of appropriate aryl-azides may be employed to produce the corresponding arylnitrenes. The latter process is particularly useful because relatively mild conditions are required.

Arylnitrenes are short-lived with a half-life of microseconds[97] and once they are formed, they must react with nearby molecules or rearrange to more stable species. If the nitrene precursor could be activated after it has been specifically carried to the vicinity of vital biomolecules in tumour cells the irreversible combination of these nitrenes could then cause disruption of cellular functions and death. An understanding of the chemical properties of arylnitrenes is therefore important to illustrate the type of chemical functions with which these intermediates react and the way these reactions take place.

Some of the typical arylnitrene reactions include electrophilic attack on nucleophiles, abstraction (usually of hydrogen from solvent molecules), insertion (normally into C-H bonds), and rearrangement e.g. ring expansion[98,99]. The type of reaction in which the nitrene participates depends on its multiplicity - that is whether the nitrene reacts as a singlet (an electrophile) or a triplet (a diradical).

Photolysis of an arylazide substituted with a strongly electron-withdrawing group in the *para* position, e.g. *p*-cyanophenyl-azide, generates a nitrene (3.1) which exhibits singlet properties due to the destablising of the cyano group on mesomer (3.2)[100].

Thus if *p*-cyanophenylazide (3.3) is photolysed in dimethyl-amine, a nucleophilic solvent, the substituted hydrazine (3.4)

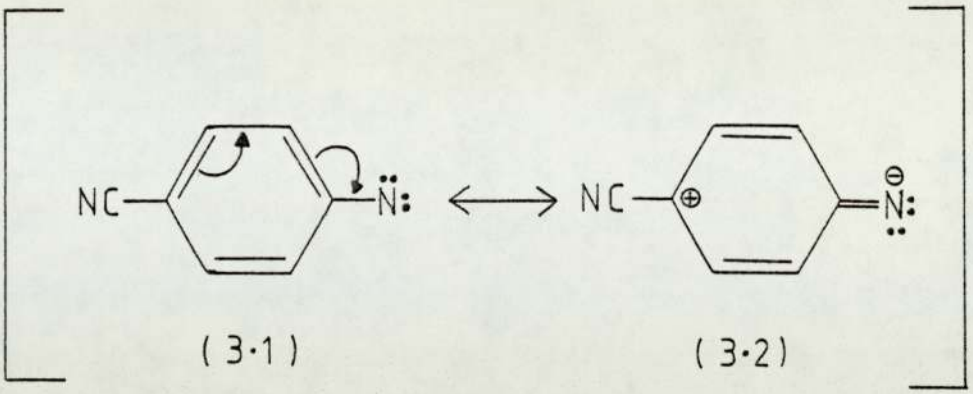

(3·1) (3·2)

is formed in high yield together with a small amount of the amine (3.5).

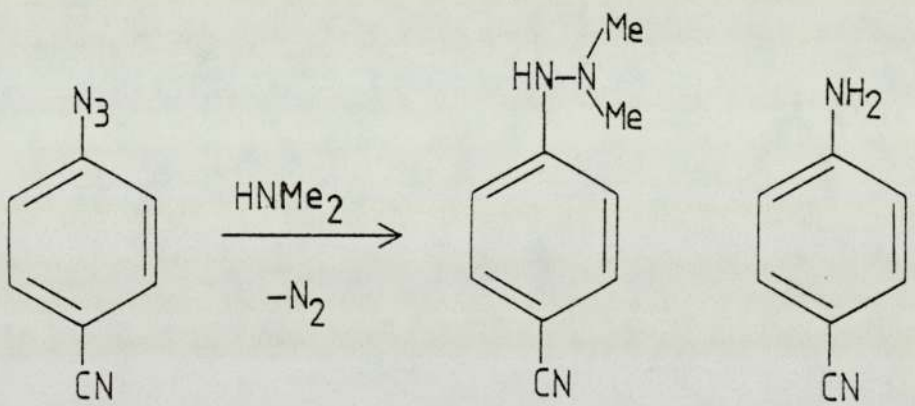

(3·3) (3·4) (3·5)

However, if the same reaction is carried out in the presence of xanthen-9-one, a triplet sensitizer, amine (3.5) is the major product. In this case, the predominating reaction is that of hydrogen abstraction from the solvent or from the starting azide[101].

	Reaction products	
Predominating nitrene species	(3.4)	(3.5)
SINGLET	70%	5%
TRIPLET	6%	70%

The singlet nitrene is responsible for the electrophilic attack on dimethylamine, while the hydrogen abstraction reaction is more typically a triplet reaction. Furthermore, the singlet may also contribute towards ring expansion reactions. This latter reaction could compete with hydrazine (3.4) formation depending on the wavelength of light used in the photolysis. This dependence has been ascribed as due to excess excitation by higher energy irradiation producing an over-excited "hot" nitrene[102].

The ring expansion reactions result in 5-cyano-2-dimethylamino- 3H-azepine (3.9) through intermediates (3.6), (3.7), and (3.8). This reaction sequence parallels that of the thermolysis of phenylazide in aniline[103].

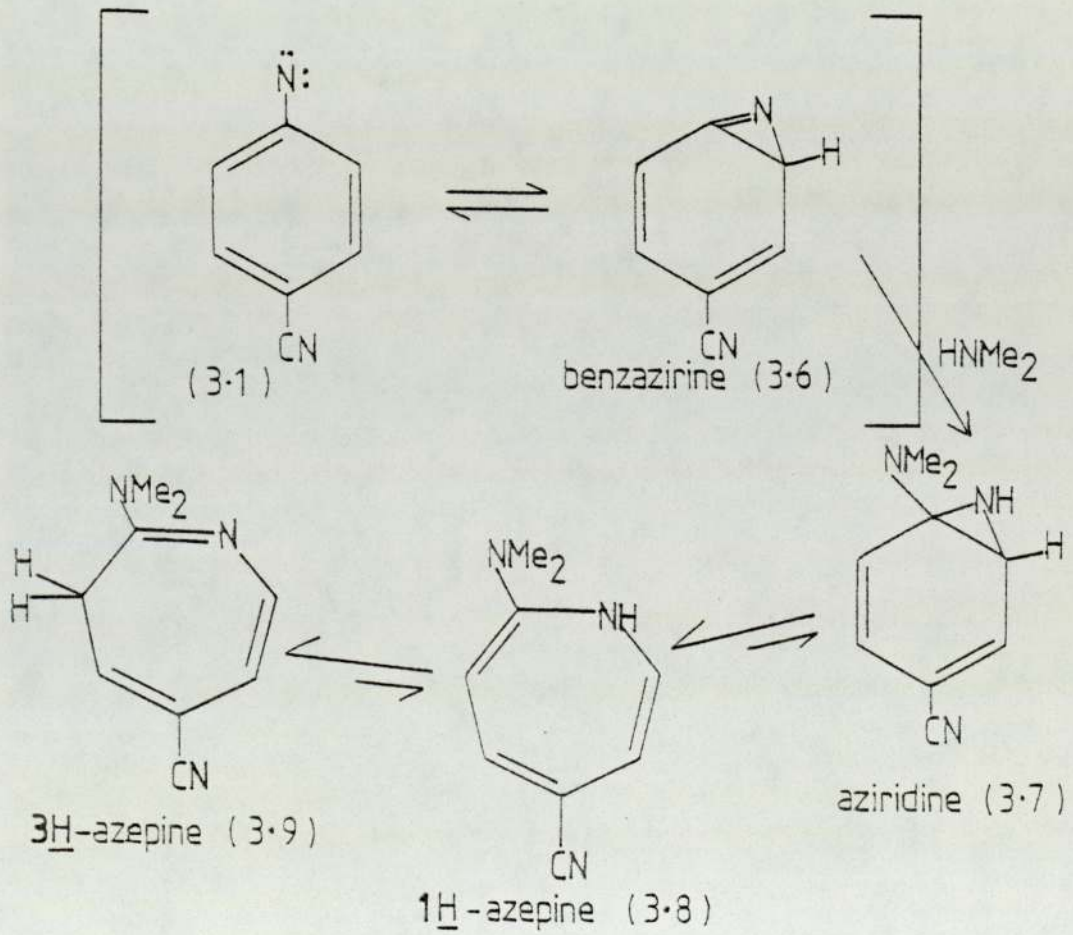

The amount of 3H-azepine formed through the sequence depicted also depends on the basicity of the solvent in which the photolysis

is carried out. Generally, solvent of high basicity tends to encourage this reaction, but it has been reported that methanol, a very weak base, reacts in the photolytic decomposition of phenylazide to afford a 10% yield of 2-methoxy- 3H -azepine[104].

Another type of nitrene reaction is the insertion by arylnitrene into C-H bonds. This was formerly associated with the singlet nitrene:

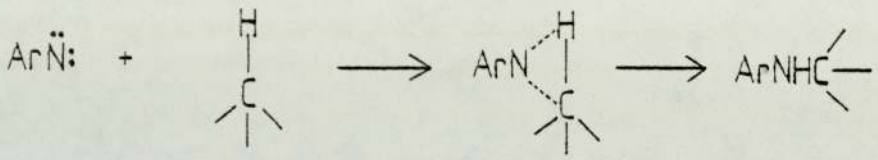

It can also be envisaged as a triplet reaction, an initial hydrogen abstraction followed by radical combination would produce the same product:

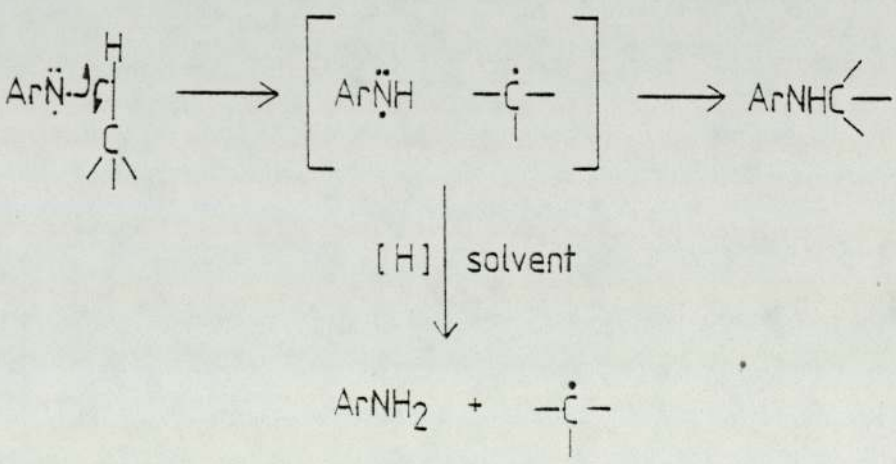

Thermolysis of phenylazide in *n*-pentane yields aniline (30%) and 10% N-(*n*-pentyl) aniline[105] which suggests the possibility of both singlet as well as triplet reactions. Another study of

this thermolysis in a cyclohexane-neopentane mixture resolves this mechanistic controversy[105]. If both mechanisms were operating, a decrease in the proportion of cyclohexane in the solvent mixture should result in a decrease in the formation of N-cyclohexylaniline (if it was formed from the singlet) and an increase in yield in aniline (a known triplet derived product) due to an increase in the probability of singlet $\longrightarrow$ triplet intersystem crossing. Variation in the solvent mixture proportions did not result in a change in the aniline/N-cyclohexylaniline ratio: therefore, the triplet must be the reactive species in this case.

This brief review of the solution chemistry of arylnitrenes likely to take place in the physiological environment should serve to demonstrate the reactivity and versatility of these intermediates. Further reading on the photochemistry of azides may be found in references 106 and 107.

3.2 Biological activities of azido compounds

These can broadly be placed into two categories in which (a) azido compounds are used as pharmaceutical agents, (consult Table 3) and (b) azido compounds are used as research tools (consult Table 4). Considering the diversity of their applications, it is pertinent to summarise the prevalent rationale for employing the azido function in each of these two groups of compounds.

(a) Pharmaceutical agents containing the azido function

In these compounds, the inclusion of an azido function in the drug molecule offers pharmacologically desirable features. The azido function belongs to a group of substituents called the pseudohalides, other members of the group are CN, NCO, SCN etc. They are so called because they all share certain

Table 3

Agents	Biological activity or use	References
5-Ethoxyethyl-2-amino-4-azido-6-phenylpyrimidine.	Diuretic activity in man.	108
6-Deoxy-6-azidodihydroisomorphine.	Potent narcotic analgesic in animals and man.	108 113, 114
6-Deoxy-6-dihydroazido-14-hydroxyisomorphine.	Experimental analgesic in animals.	111
6-Deoxy-6-azidodihydroisocodeine.	Experimental analgesic in animals.	109
7-Azido-5-phenyl-1,4-benzodiazepines.	Sedative and anticonvulsant activities in animals.	110
9-Azido-10-methylacridinium methosulphate.	Anticholinesterase activity *in vitro*.	112
Potassium-6-(D-α-azidophenylacetamido) penicillinate.	Antibiotic in man.	115
7-(D-α-aminophenylacetamido)-3-azidomethyl-3-cephem-4-carboxylic acid.	Broad-spectrum antibacterial activity in the mouse.	116

properties with the halogen atoms. N_3, like Br, is more electronegative than carbon; hence it exerts a negative inductive effect (-I) in organic compounds. It is also capable of conjugation through its non-bonding electrons and thus acts as an electron-donor; that is, it exerts a positive resonance effect (+M). That the overall electron-withdrawing property of N_3 is comparable to that of Br might be expected from their similar dipole moments[129]. In most of the following drugs, the azido group is just a novel substituent. Where the information is available, their pharmacological activity often parallels that of their halogeno counterparts[110]. From a drug metabolism study in man[114], the azido function (of azido morphine) was found to be relatively stable towards enzymatic and chemical change. It was largely excreted unchanged in the urine, although traces of reduction product, the amine, was also found.

(b) Azides used as research tools

Many biological processes involve the interaction of a small organic molecule (the ligand) with a biological macromolecule, the receptor. Enzymes catalyse reactions of their substrates and cofactors; antibodies bind their haptens; hormones interact with their receptors; macromolecular carriers transport ligands across biomembranes; and pharmaceutical agents also seek their sites of action. These receptor/ligand reactions can be made irreversible by covalent binding. The isolation of the permanent receptor/ligand complex and the elucidation of the exact point of attachment of the ligand to the receptor may offer information on their molecular mode of interaction[130].

All the compounds in Table 4 are azido derivatives of ligands which possess specificity for their appropriate receptors.

Table 4

Agent(s)	Biological use	Reference
ε-(4-Azido-2-nitrophenyl)-L-(4,5-^{3}H)lysine, and ε-(5-Azido-2-nitrophenyl)-L-(4,5-^{3}H)lysine.	To complex with an antibody which has been raised against the 4-azido-2-nitrophenyl function. Subsequent irradiation of the complex to result in photo-affinity labelling of the antibody-binding site, hence offer information of the environment of this site.	117, 118, 119
Quarternary ammonium arylazides.	Photo-affinity labelling of specific acetylcholine-binding sites on red blood cell membranes.	120
Peptides containing *p*-azido-L-phenylalanine	Photo-affinity labelling of chymotrypsin and amino-peptidases.	121
4-Azido-2-nitrophenyl glycosides.	Synthesised as potential photo-affinity labels.	122
[^{3}H]N-β-(*p*-azidophenyl) ethylnorlevorphanol.	Photo-affinity labelling of the opiate receptors.	123
Deformamidoazido antimycin A.	Photo-affinity labelling of the antimycin A receptor at the respiratory chain.	124
2-Azidoisopthalic acid, and 5-azidoisopthalic acid.	Photo-affinity labelling of the active site of glutamate dehydrogenase.	125
Ortho azido derivatives of estradiol, estrone and hexestrol.	Synthesised as potential photo-affinity labels of estrogen binding proteins.	126
Phenacyl-*p*-azide of 4-thiouridine.	Photo-affinity labelling of t-RNA binding sites on the ribosome (in E. coli).	127
4-Denitro-4-azido-chloramphenicol.	Synthesised as potential photo-affinity label of the peptidyl transferase binding site at the ribosome.	128

They will form reversible receptor/ligand complexes. The azido function merely serves to generate the appropriate nitreno-ligand upon photo-irradiation *in situ*. The ability of nitrenes to attack nucleophiles and to insert into C-H bonds (to result in covalent bond formations) has already been discussed. These nitreno-ligands therefore behave as effective photo-affinity labelling agents.

3.3 Aims of the present work

In the introduction, it was suggested that nucleophilic centres in cellular receptors are prone to electrophilic attack. These nucleophilic centres are electron rich regions; the basic nitrogen functions such as N(7) of guanine and N(1) of adenine in nucleic acids are just two of the probable candidates[131]. The 9-anilinoacridine structure described in Chapter 2 will serve as a carrier to nucleic acids with a not insignificant selectivity for tumour cells. The nitrene function is a suitable electrophilic species to react with these nucleophilic centres. Furthermore, the reactive nitrene may also insert into C-H bonds in the immediate vicinity where it is generated. The azido function should serve as a convenient nitrene precursor since it is chemically stable under physiological conditions[132] and would readily generate the nitrene intermediate upon photo-irradiation. The amalgamation of these structural and functional ingredients should provide the makings of a potentially selective antitumour agent with radio-sensitizing activity *if the azido function behaves similarly when exposed to penetrative X- and γ-irradiation.*

Part 2

Results and Discussion

Part 2 Results and Discussion

Chapter 4 Synthesis of acridine derivatives

4.1 Synthesis of substituted 9-anilinoacridines

The advent of antitumour acridine drugs such as *m*-AMSA (2.18) and others cited in Chapter 2 stimulated further synthesis of other derivatives of 9-anilinoacridine (2.1) in the present work. Nucleophilic substitution of the labile chlorine atom in 9-chloroacridine (4.1) with the appropriate arylamines (4.2) produced the requisite 9-anilinoacridines (4.3). The hydrochloride salts (4.4) - (4.8) were prepared by heating molar equivalents of the reactants in boiling anhydrous methanol for 90 minutes. On addition of excess ether, the products crystallised from the reaction mixtures in high yields (Scheme 1).

Scheme 1

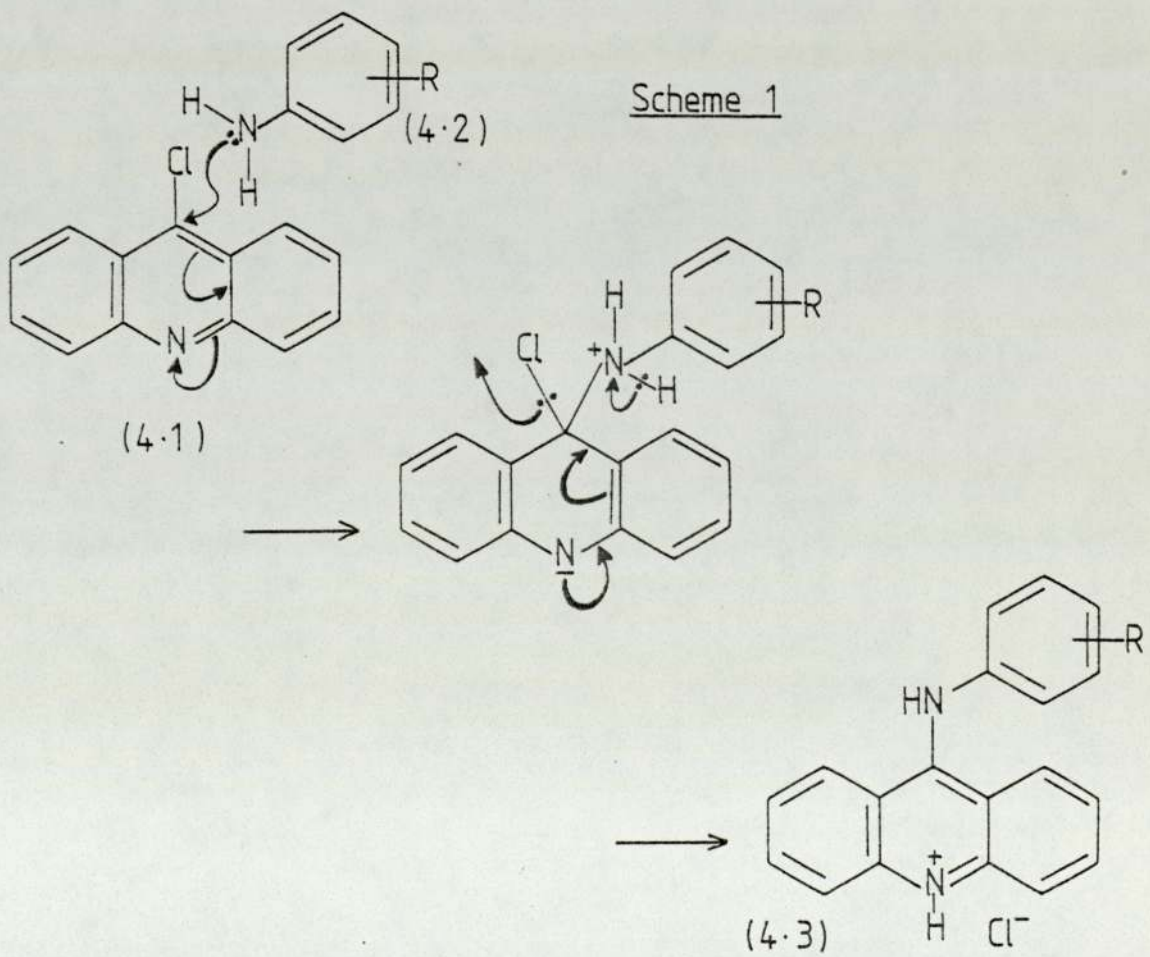

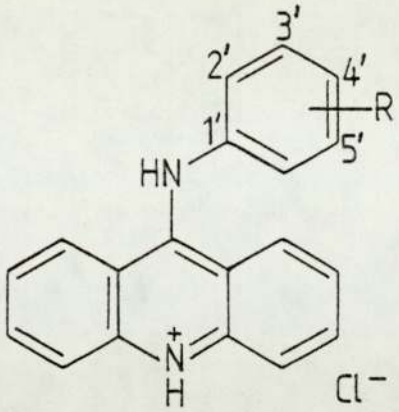

(4·3)

Structures	R in (4.3)[a]	Structures	R in (4.3)[a]
4.4	4' - NH_2	4.15	2' - OMe, 4' - NH_2
4.5	3' - NH_2	4.16	2' - OMe, 5' - NH_2
4.6	2' - NH_2	4.17	4' - N_2^+
4.7	4' - NO_2	4.18	3' - N_2^+
4.8	3' - NO_2	4.19	2' - N_2^+
4.9	2' - OMe, 4' - NO_2	4.20	4' - N_3
4.10	2' - OMe, 5' - NO_2	4.21	3' - N_3
4.11	2' - NH_2, 5' - NO_2	4.22	2' - OMe, 4' - N_3
4.12[b]	2' - NH_2, 5' - NO_2	4.23	4' - N_2O^-
4.13	2' - NH_2, 4' - NO_2	4.24	4' - F
4.14[c]	4' - NH_2	4.25	3' - F

a The ionic state (i.e. protonated or unionised), degree of hydration and other details may be found in the experimental section.

b (4.12) is the monohydrate of (4.11).

c (4.14) is the dihydrochloride of (4.4).

However, disubstituted anilines appeared less reactive in these condensations when one of the substituents was *ortho* to the amino function. If the above methods were used, 9-acridanone (4.26) was invariably produced in preference to the required anilinoacridine. Other polar solvents which were tried as replacements for methanol such as DMSO and DMF, which presumably contained traces of water, also promoted hydrolysis. This interfering hydrolysis (Scheme 2) could be minimised or even eliminated by employing a different solvent - acetonitrile - instead of methanol and by reducing the reaction time to 60 minutes. Compounds (4.9) - (4.12) were synthesised under these conditions.

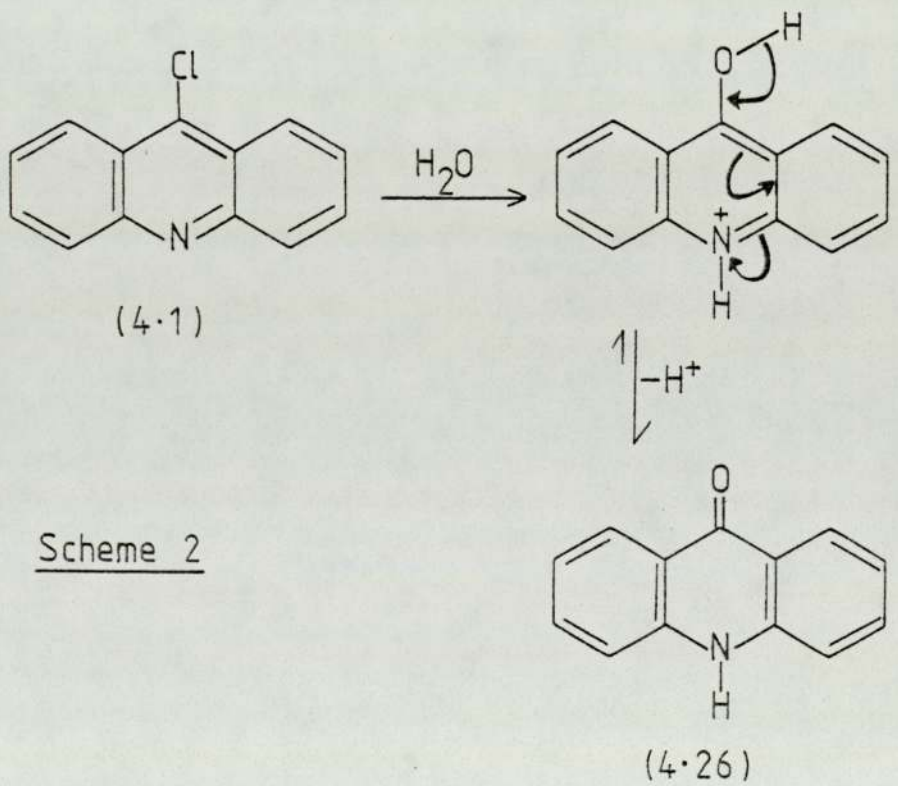

Scheme 2

Compound (4.11) has been assigned as substituted with a 2'-NH_2 and a 5'-NO_2 group in the anilino ring. This structure has not been proved unequivocally. The starting arylamine in

this case was 3,4-diaminonitrobenzene (4.27) and when coupled with 9-chloroacridine, a mixture of isomers (4.11) and (4.13) might be expected. Tlc examination of the reaction products revealed

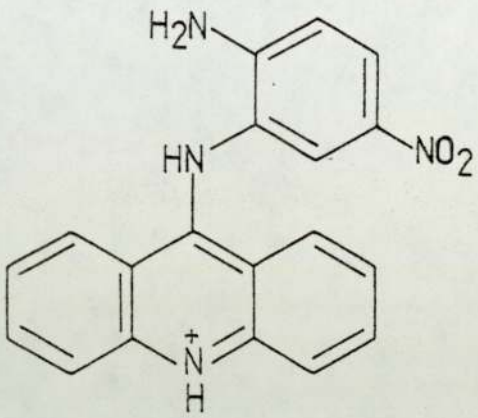

(4·11)

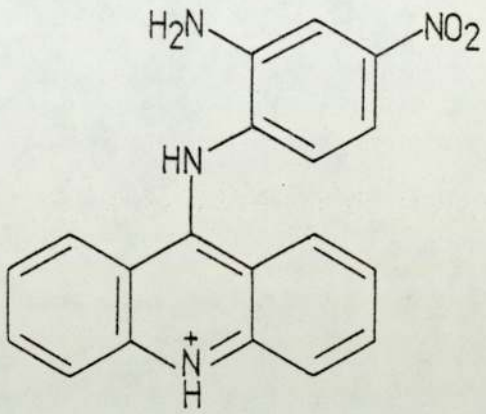

(4·13)

only one spot. The nitro group in (4.27) with its large (negative) inductive and mesomeric effects would reduce the electron density of the 4-amino nitrogen atom but have a lesser effect on the basicity of the 3-amino group hence increasing the probability of coupling at the 3-amino nitrogen to produce isomer (4.11).

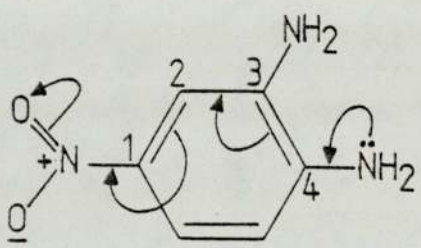

(4·27)

4.2 Reduction of nitro-substituted 9-anilinoacridines

Raney nickel-hydrazine hydrate was used successfully in the reduction of nitro compounds (4.7), (4.9) and (4.10) using DMSO as solvent at 160°. The crude amine was extracted into chloroform and purified by successive partition between chloroform and water at different pH. The purified amine free base was redissolved

in a minimum quantity of methanol saturated with HCl gas; the dihydrochloride salts (4.14) - (4.16) crystallised on addition of ether. Other reduction reagents were also used with unreliable results: reaction conditions and results are shown in Table 5. It appears that an alkaline reduction is superior to an acid reduction in minimising hydrolysis. Protonation at the N-10 position renders C-9 more prone to nucleophilic attack by hydroxyl ions (Scheme 3); this explains the acid lability of 9-anilinoacridines,

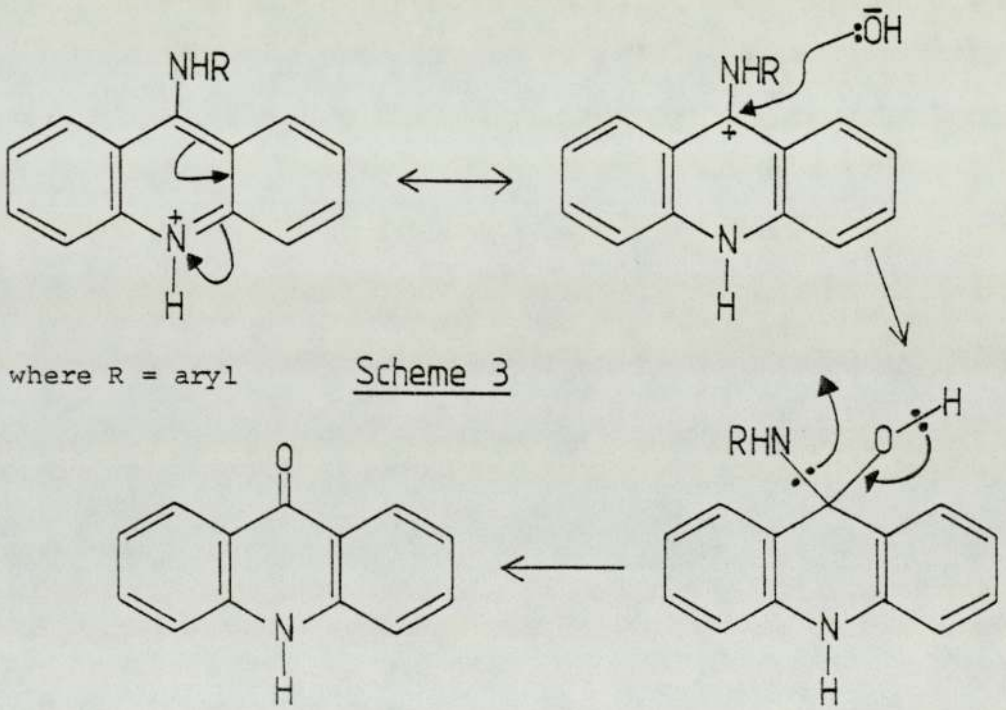

where R = aryl

Scheme 3

especially at elevated temperature. A powerful polar solvent such as DMSO was used in order to dissolve the nitro compounds. The free bases of nitroanilinoacridines were particularly insoluble in less polar solvents.

4.3 Diazotisation of amino-substituted 9-anilinoacridines

Diazotisation of the primary amino compounds (4.4) and (4.5)

Table 5 Reduction of nitro-substituted 9-anilinoacridines

Reagent	Substrate	Solvent	Condition	Remark
Raney nickel - hydrazine hydrate	Nitro compounds (4.7), (4.9), (4.10) and (4.11)	DMSO	160°, 30 minutes	Good yield of amine with only traces of 9-acridanone.
Zinc - aqueous ammonium chloride solution	Nitro compounds (4.7) and (4.9)	aqueous methanol	reflux, 30 minutes	Good yield of amines (4.7) and (4.9), but many by-products with (4.10).
Aqueous sodium dithionite - sodium hydroxide solution	Nitro compounds (4.7) and (4.9)	aqueous ethanol	room temperature, 10 minutes	Fast reduction but always gives 2 products (tlc). In the case with (4.10), 13 spots on tlc.
Stannous chloride - hydrochloric acid	-	aqueous ethanol	reflux, 30 minutes	Incomplete reduction due to insolubility of nitro compounds and low reaction rate, hydrolysis due to low pH.
Stannous chloride - hydrochloric acid	-	aqueous ethanol	room temperature, 48 hours	No observable reaction.

in tetrafluoroboric acid and aqueous sodium nitrite solution gave rise to the diazonium tetrafluoroborates (4.17) and (4.18). These compounds were sensitive to light, heat and moisture; they decomposed gradually even when kept in a refridgerated vacuum desiccator in the dark and the rate of decomposition was greatly accelerated if they were left in open air, ambient laboratory lighting and at room temperature. This decomposition was reflected in a colouration change and the loss of the characteristic diazonium absorption peak (at 2260 cm^{-1}) in the infra red (ir) spectrum. The diazotisation of the 2'-amino derivative (4.6) in hydrochloric acid and aqueous sodium nitrite solution did not give the expected diazonium compound (indicated by the absence of a diazonium peak in the ir spectrum), but 9-(benzotriazol-1-yl)-acridine (4.28) was produced instead. The diazonium derivative (4.19) could be envisaged as an intermediate and ring closure followed spontaneously.

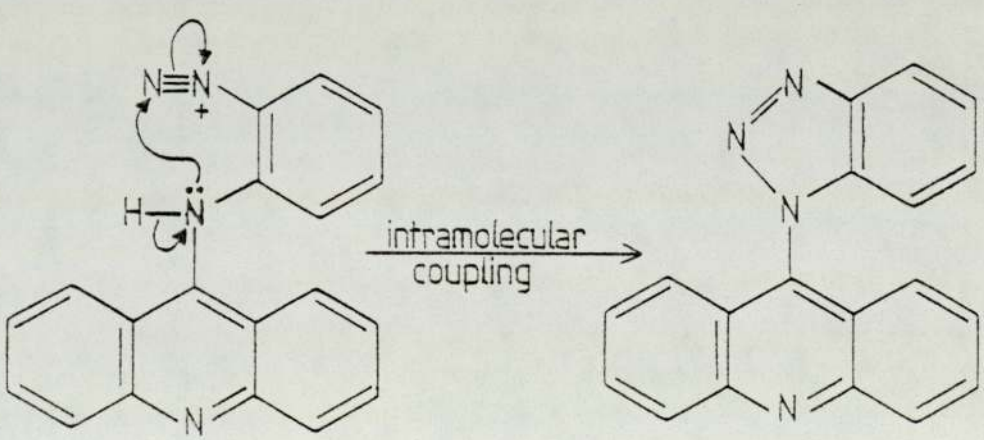

(4·19) (4·28)

When amines (4.4), (4.5) and (4.15) were diazotised in hydrochloride acid and aqueous sodium nitrite solution, the corrsponding diazonium chloride solutions were formed. On addition of an aqueous sodium azide solution, the azido derivatives (4.20),

(4.21) and (4.22) were produced. If the diazonium salt solution prepared from the diazotisation of amine (4.4) was treated with an (ice-cold) sodium hydroxide solution, the diazotate (4.23) resulted. Similar treatment of the 3'-diazonium salt (4.18) did not afford an analogous compound. These reactions of the diazonium ion with the azide and hydroxyl ions are summarised in Scheme 4.

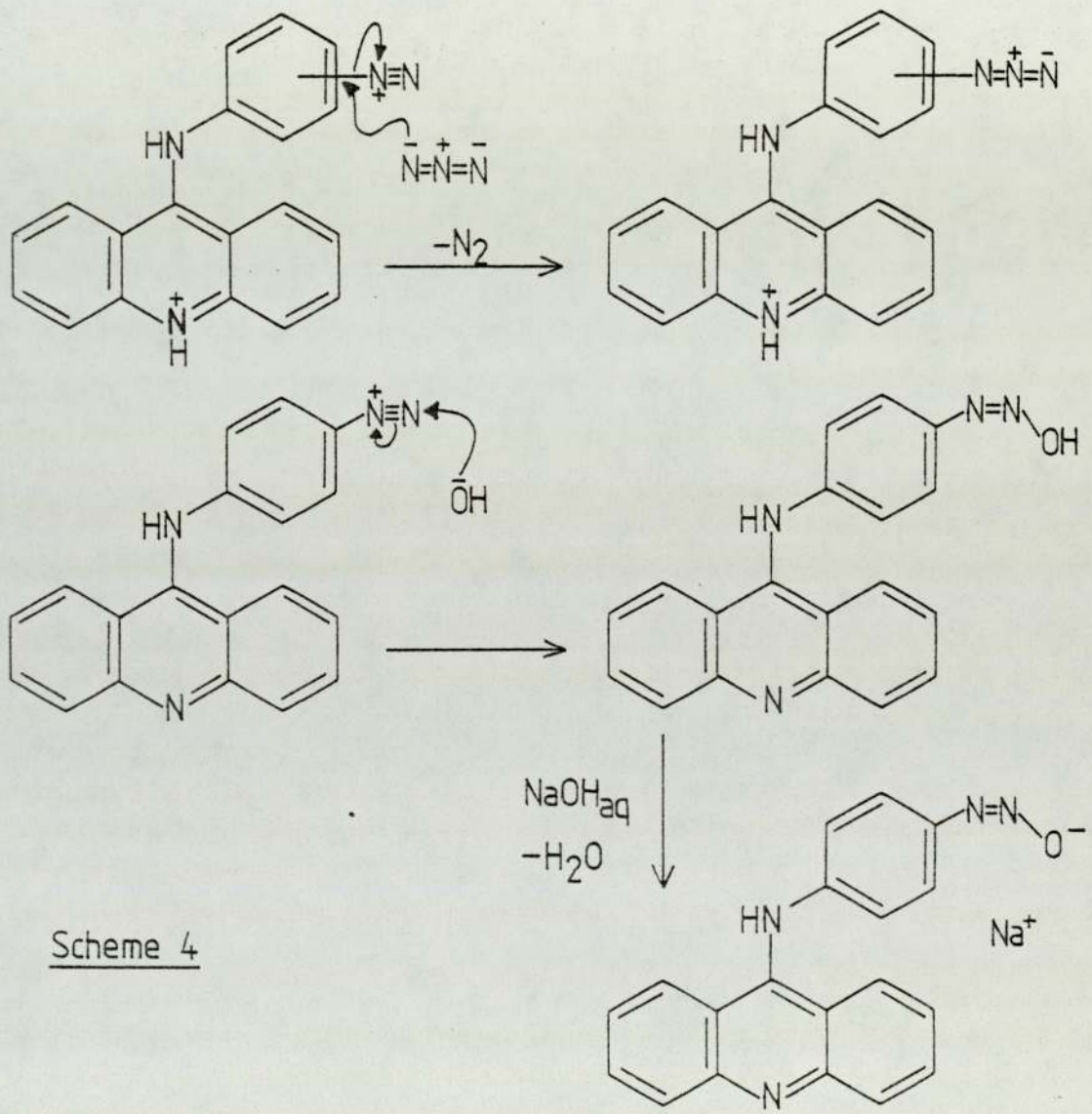

Scheme 4

Discussion of the mechanism of reaction between the diazonium ion and the azide ion, and the kinetics and mechanism of diazotate rearrangement can be found in reference 133.

4.4 Spectral characterisation of 9-anilinoacridines

9-Anilinoacridines have mass spectra, infra red (ir) and ultra violet (uv) spectra characteristic of these compounds as a group.

The mass spectra show molecular ions in high abundance and the common features are the peaks at $^{m}/e$ 269 (due to the anilino-acridinium ion often resulting from loss of substituents on the anilino ring) and $^{m}/e$ 178 (due to the acridinium ion resulting from the loss of the anilino fragment). Multiple-dehydrogenation is often encountered and is manifested as a cluster of peaks around the molecular ion and (therefore) its fragments. For example, the mass spectrum of amine (4.15) shows a cluster of peaks round the molecular ion at $^{m}/e$ 315. The fragmentation of the acridinium ion has been documented[134]. The mass spectra of particular interest in this work are those of the azides (4.20) and (4.21) and the diazonium tetrafluoroborates (4.17) and (4.18).

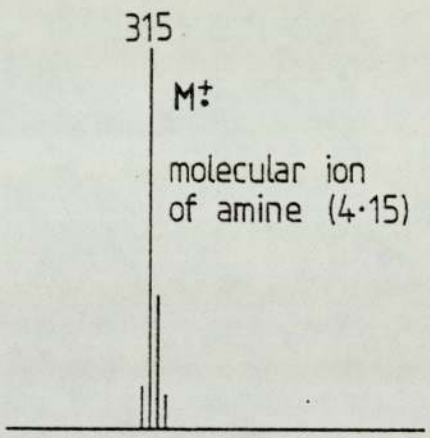

Molecular ions were not observed in the mass spectra of azides (4.20) and (4.21); a base peak at $^{m}/e$ 283 (M-28) corresponding to loss of a nitrogen molecule and a peak of high abundance at $^{m}/e$ 285 (M-26) were found instead. Peaks at M-26 have previously been observed in the mass spectra of azidopyrimidines[135] and have been shown to arise from thermal fragmentation of the azides to give nitrenes which by H-abstraction give the amine in an overall process $(M^{+\cdot} - N_2) + 2H^{\bullet}$. The usual 9-anilinoacridinium ion and the acridinium ion peaks were present accompanied by other peaks

of low abundance typical of 9-anilinoacridines; in addition a fragment at $^{m}/e$ 256 (M-55) was also found. This latter peak at M-55 has previously been observed in the mass spectrum of phenyl azide[136] and was correlated as the loss of HCN from the nitrene radical ion at M-28. This pattern of mass spectral behaviour is summarised in Scheme 5.

The mass spectra of the diazonium tetrafluoroborates (4.17) and (4.18) again showed no molecular ions and base peaks corresponding to the respective fluoroanilinoacridines (4.24) and (4.25) were found. The fragmentation of this ion ($^{m}/e$ 287) showed a pattern typical of 9-anilinoacridines. This suggests that thermal fragmentation of the diazonium ion occurs possibly in the injection chamber before reaching the ion analyser of the spectrometer. This type of thermal collapse of aryl diazonium tetrafluoroborates, which results in the formation of aryl fluorides, is known as the Schiemann reaction[137].

The infra red (ir) spectra of 9-anilinoacridines all possess numerous absorption peaks in the fingerprint region. The common features in the spectra of their hydrochloride salts are a strong absorption around 750 cm^{-1} and another at 1630 cm^{-1}. The broad band at 2900 cm^{-1} is associated with the protonated hetero nitrogen function in the acridine ring. Representative ir spectra in Figures 6 and 7 show these peaks as well as other characteristic absorptions due to individual functional groups. Details of ir absorptions of compounds synthesised in this work can be found in the experimental section.

The ultra violet (uv) spectra of 9-anilinoacridines are again similar amongst members of this group of compounds and are tabulated (Table 6). As expected for strongly basic compounds of this type

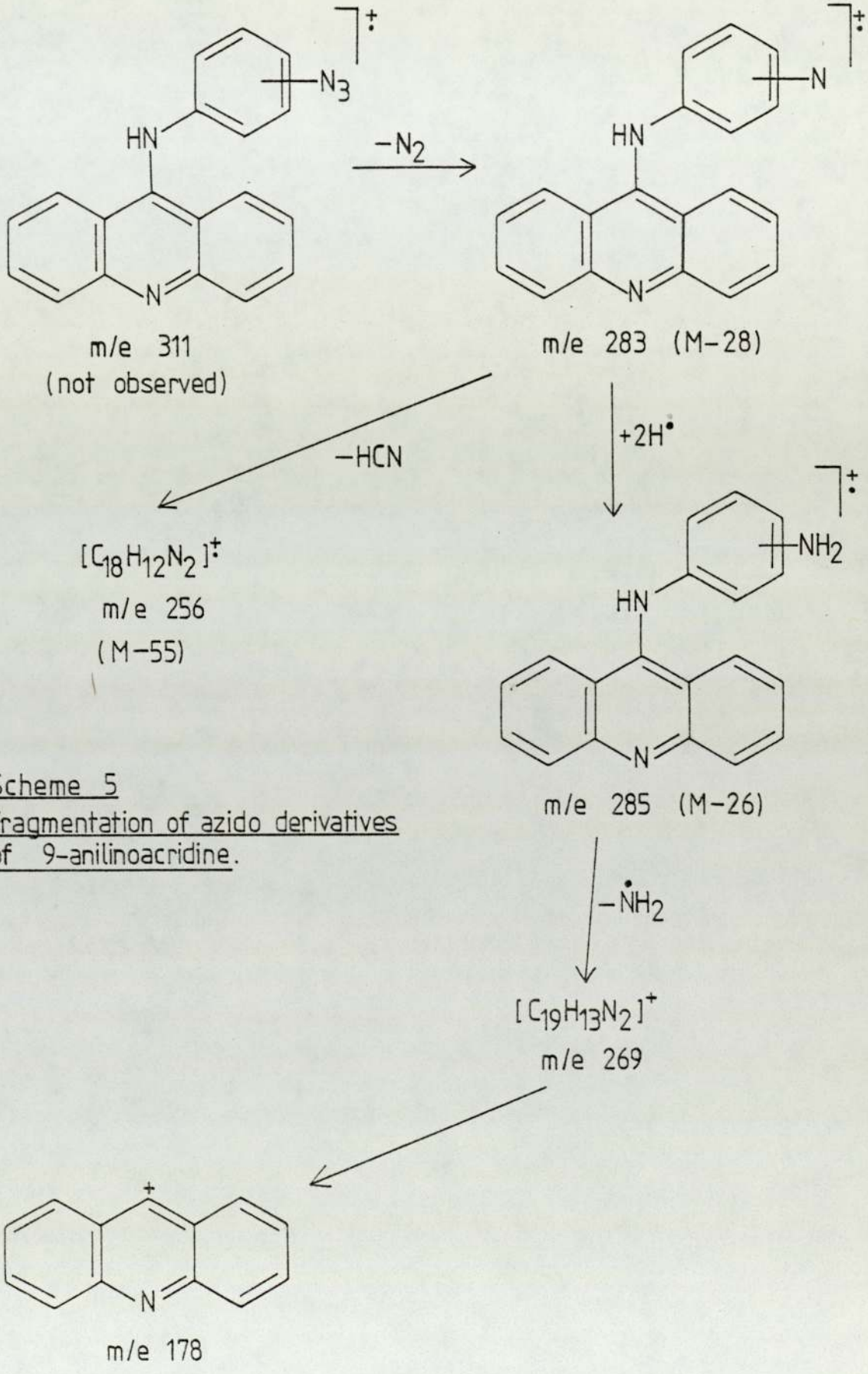

Scheme 5
Fragmentation of azido derivatives of 9-anilinoacridine.

Figure 6

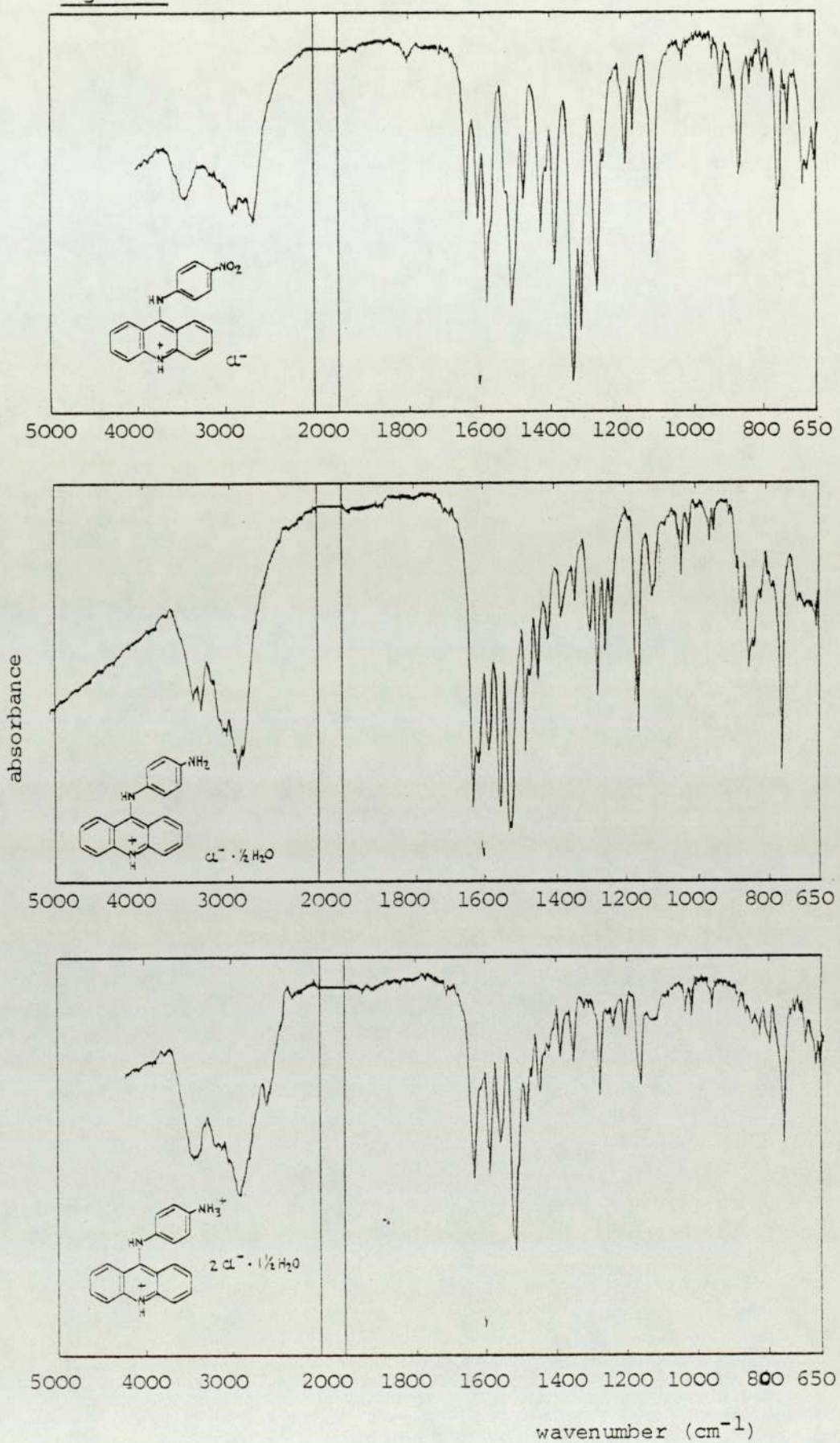
absorbance
5000 4000 3000 2000 1800 1600 1400 1200 1000 800 650
wavenumber (cm-1)

Figure 7

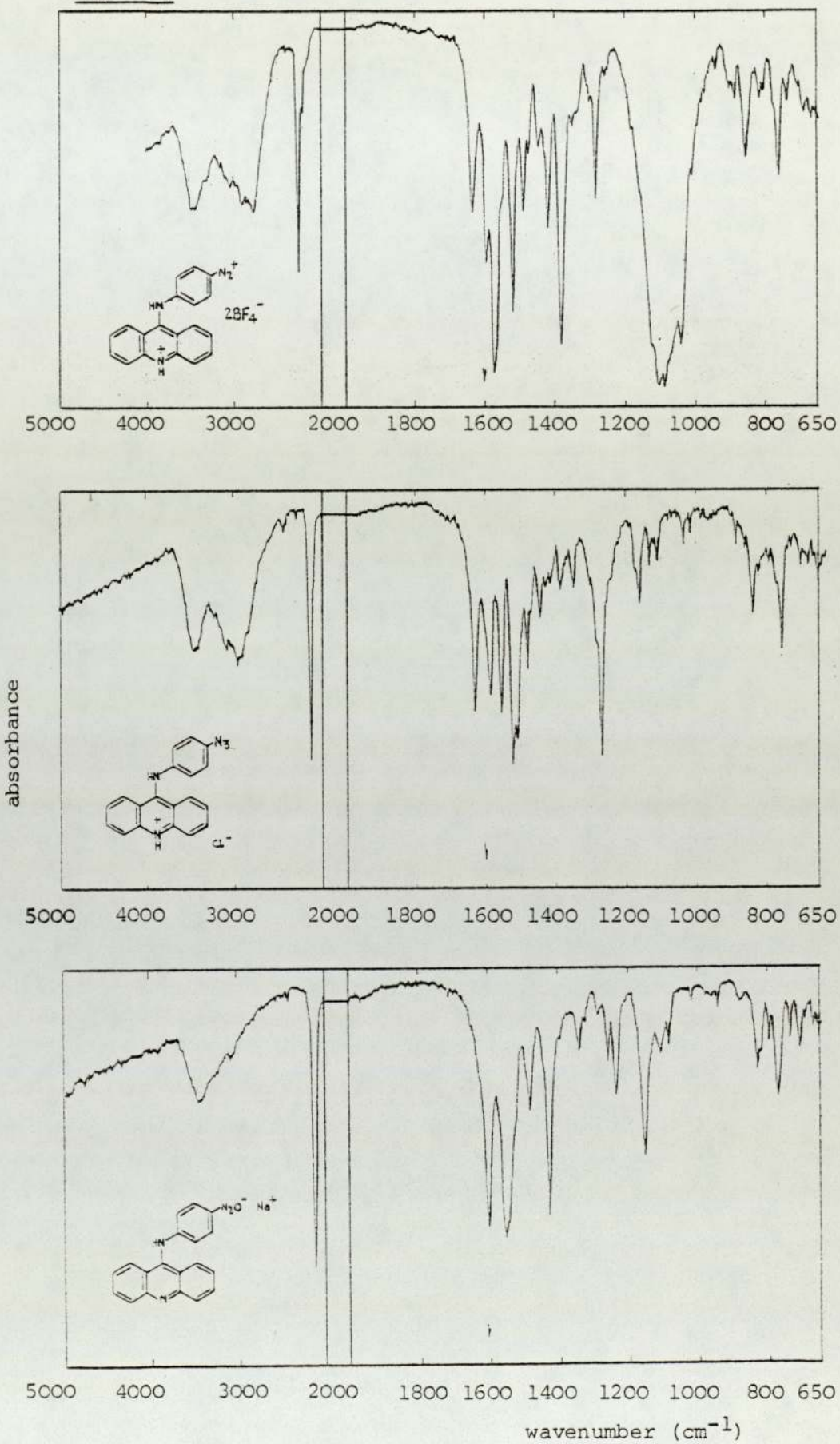
absorbance
5000 4000 3000 2000 1800 1600 1400 1200 1000 800 650
5000 4000 3000 2000 1800 1600 1400 1200 1000 800 650
5000 4000 3000 2000 1800 1600 1400 1200 1000 800 650
wavenumber (cm-1)

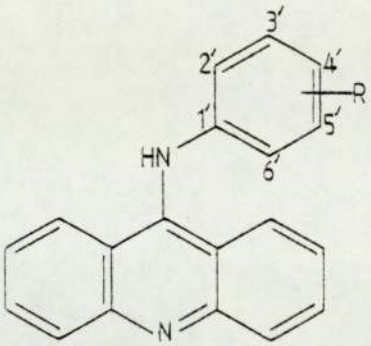

Table 6 Electronic absorption maxima of 9-anilinoacridine hydrochlorides.

Substituent R=	Solvent	λmax (nm) *Inflexion																				
4'-NH_2	a		253													422*		440				
3'-NH_2	a	249		266		336										420	438					
2'-NH_2	a		256*	262										413			436					
	c	249	256*									407										
4'-NO_2	a		252				345		362							422						
3'-NO_2	a	246		260*			344		362					414								
2'-OMe-4'-NO_2	b	248						358								421						
	c	248						358								421						
	d			265		335											435					
2'-OMe-5'-NO_2	b	247						358				406										
	c	247						358				406										
	d			264												420						
2'-NH_2-5'-NO_2	b	248			275*									411								
	c	248			275*									411								
	d			263					360					412			435					
2'-OMe-4'-NH_2	b		251			330											435					
	c	249														421						
	d			263		332										421	435					
2'-OMe-5'-NH_2	b	249		260				356						412			430*					
	c	248					340	356				403										
	d			264		333										422	434*					
4'-$N_2^+BF_4^-$	a		252	262*			346*		364*	372		403										521
3'-$N_2^+BF_4^-$	a	247		268		336										424*	439					
4'-N_3	b	245		265			340	356						414								
	c	245		267*			340	356						414								
	d	244		265		336											437					
3'-N_3	b	244		260*			340	356						410								
	c	244		260*			340	356						410								
	d	245		265		335											436					
2'-OMe-4'-N_3	b	247		262				357						414								
	c	247		260*				357				407										
	d	245		263		332										421	435					
4'-$N_2O^-Na^+$	a	250*	256						364					412								

Table 7 Electronic absorption maxima of acridine and allied compounds.

Compound	Solvent	λmax (nm) *Inflexion												
9-(benzotriazol-1-yl)acridine	a		250		344	360	388							
	c		250		344	360	388							
	d		250	257*	349	364	393	416						
13H-quin[4,3,2-kl]acridine	b	235	247*	261*		284	332	351	370	424	444			
	c	235	247*	261*		284	332	351	370	424	444			
	d	233	252*	262*	272	286	340*	355		433*	456	485		
9-aminoacridine	a		261			365*	381	402	425					
9-chloroacridine	a	252				346	360	387						
9-acridanone	a	254	295	307		366*	381	400						
acridine	a	250				325*	332*	339*	348*	356	380*			

Solvents: a = 95% ethanol; b = pH 7.4 buffer (Tris in 50% aqueous ethanol);
c = pH 11 buffer; and d = pH 4 buffer.
For details on these buffers, see notes in the experimental section.

the uv spectra are pH-sensitive; the cations absorb at longer wavelengths than the corresponding free bases. Similar features in the spectra of 9-aminoacridines have been quoted as evidence that 9-aminoacridines are protonated on the ring nitrogen[138]. A number of reference compounds including acridine itself are displayed in Table 7 together with 9-(benzotriazol-1-yl)acridine and 13H-quin[4,3,2-kl]acridine.

The protonated 9-anilinoacridine structure can be expressed as a hybrid of two resonance forms. This type of hybrid can also be envisaged in the case of 9-aminoacridine and 9-acridanone.

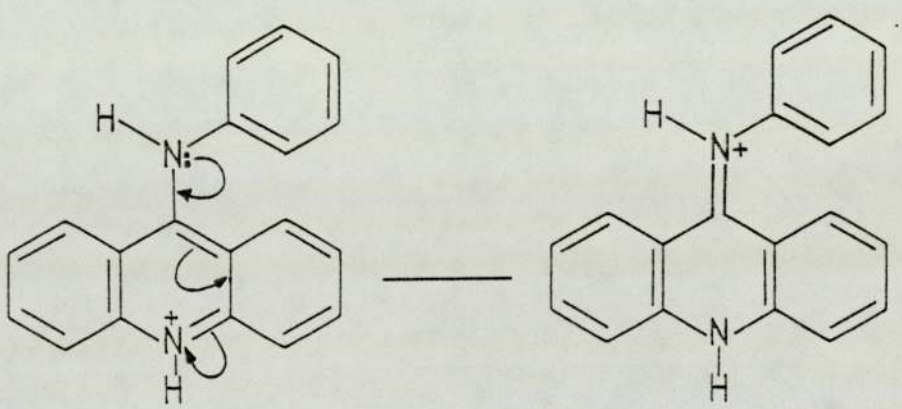

These systems possess substituents which can release a lone-pair of electrons for conjugation with the acridine nucleus and therefore impart a strong bathochromic effect on the parent acridine. On the other hand, no comparable resonance structures can be established for 9-chloroacridine which explains the similar absorption maxima of this compound to acridine itself. The close resemblance between the spectrum of 9-(benzotriazol-1-yl)acridine and that of 9-chloroacridine may suggest that the lone pair of electrons of the N-1 nitrogen of the benzotriazolo function does not contribute substantially in conjugation with acridine ring.

Chapter 5 Chemical decomposition studies

5.1 Photolysis of azido-substituted 9-anilinoacridines

The azidoanilinoacridines (4.20), (4.21) and (4.22) were designed for use as radiosensitizers and an understanding of the conditions necessary for the activation of these azides and their rate of photolysis was adjudged to be an important prelude to the study of their biological properties.

Hydrolysis of azidoanilinoacridine hydrochlorides (in common with other anilinoacridines) takes place very slowly in water; the hydrolytic products include 9-acridanone (4.26), 9-aminoacridine (2.4) and several unidentified products (tlc). If a fresh solution (in aqueous ethanol) of an anilinoacridine hydrochloride is kept in the dark at room temperature there is no discernible spectral change (uv) after 24 hours and only minimal hypochromic change after 1 week. Although no quantitative determination has been carried out, it can be assumed that the rate of hydrolysis under these conditions is very low. This is in contrast to the decomposition of these azides in light. If a similar solution is exposed to sunlight, the solution quickly changes colour accompanied by a hypsochromic shift in the uv spectrum.

An attempt was made to isolate the photolysis products of the azide (4.20). 500 ml of a solution (100 $\mu g\ ml^{-1}$) of this azide in 50% aqueous ethanol was photolysed in an Hanovia photochemical reactor (see notes on instruments for details) for several days until no further spectral change was observed. The solution was then concentrated by distillation at reduced pressure. Tlc examination of the photolysate showed four spots corresponding

to the amine (4.4), the starting azide and two unidentified compounds. There was no trace of 9-acridanone suggesting that hydrolysis was not a competing degradative pathway. Complete evaporation of the concentrated solution afforded a brown residue. Tlc examination of this residue showed numerous spots indicative of complete degradation of the products. The uv spectrum of this residue showed a characterless absorption pattern.

It has been proposed in Chapter 3 that arylnitrenes may be produced during the photolysis of arylazides; these short-lived intermediates must then react with nearby molecules or rearrange to more stable species. From the scanty chromatographic study of the photolysis products of (4.20), the identification of amine (4.4) is in agreement with the abstration of hydrogen atoms from the solvent by a triplet nitrene. It is tempting to speculate that a nitrene intermediate was generated and the unidentified compounds revealed by tlc were either the ring expanded product (5.1) from a singlet nitrene intermediate, or some triplet-derived products such as azo and hydrazo compounds analogous to those formed in the photolysis of other arylazides[101, 139] (Scheme 6). Unfortunately these compounds were not available as reference samples.

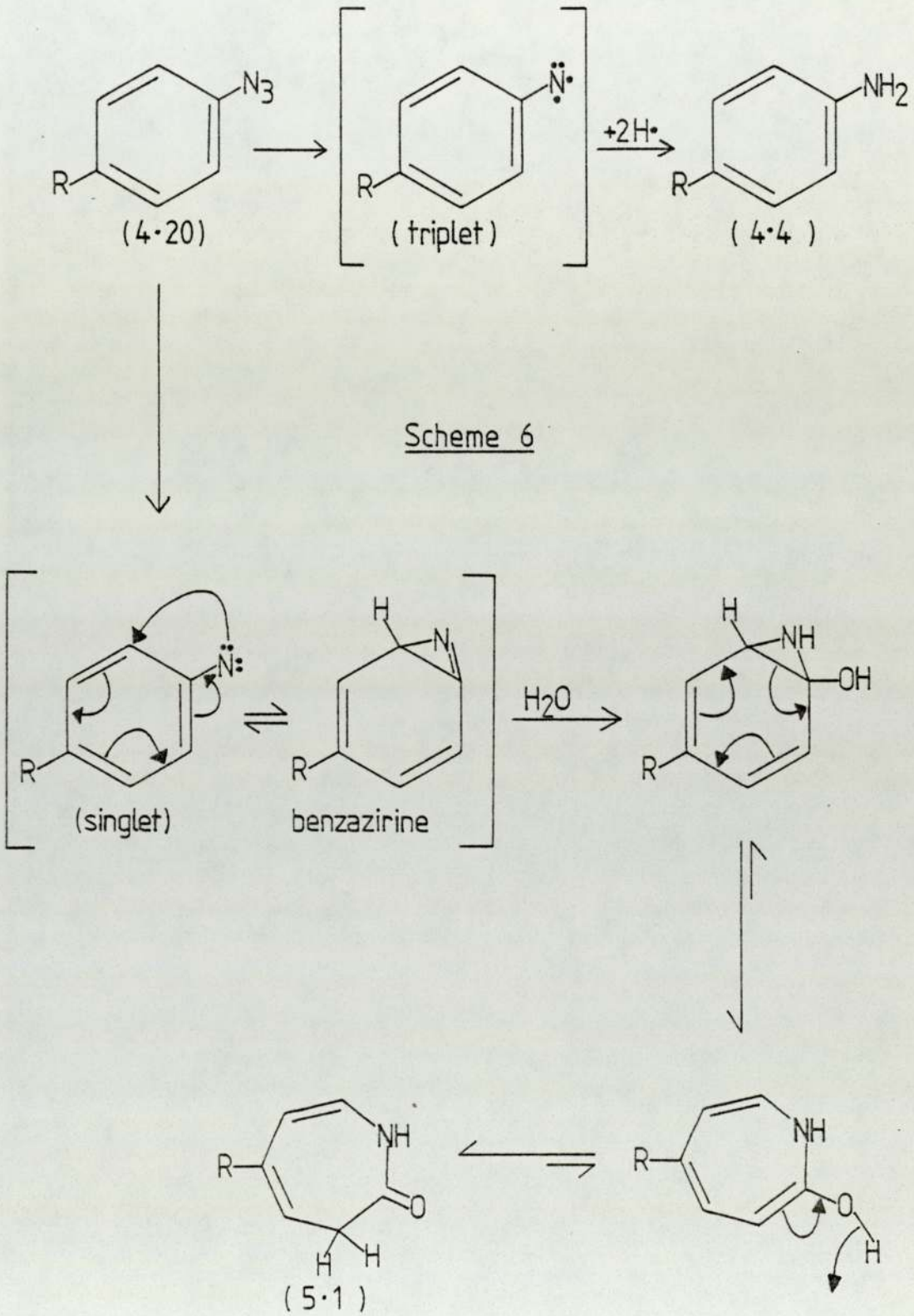

Scheme 6

R = acridin-9-ylamino

5.2 Rate of photolysis of azido compounds

In order to quantify the rate of photolysis of azides, a light box fitted with a fluorescent tube was used to serve as a light source of constant output (see notes on instruments). The azide solutions were then photolysed under standardised conditions (see Experimental Section). Three types of fluorescent tube were available with emission wavelengths of 253.7 nm, 366 nm and the visible range. Each compound was photolysed in either ethanol or one of the three buffers of pH 7.4, pH 4 and pH 11. Nine solvent/λirrad. (irradiation wavelength) combinations were used in each compound to investigate the effect of pH and wavelength of the applied radiation on the rate of photolysis. The progress of the photolyses was monitored by recording changes in their uv spectra.

The photolysis spectrum of the 4'-azido derivative (4.20) in pH 7.4 buffer (Figure 8) shows a hypsochromic shift from a peak at 411 nm to two peaks at 353 and 371 nm. This pattern is also seen in the photolysis of the 4'-azido-2'methoxy derivative (4.22) as shown in Figure 10 where a peak at 412 nm is transformed to two peaks at 354 and 373 nm. The photolysis of the 3'-azido compound (4.21) under the same condition shows qualitatively different behaviour (Figure 9); hypochromic change at 408 nm is accompanied by hyperchromic development at 355 nm and a general hyperchromic change at wavelengths below 385 nm. This suggests that the two 4'-azido compounds (4.20) and (4.22) may have a common mode of photolysis whereas the 3'-isomer (4.21) follows a different photolytic pathway.

There is close resemblance between the pH 7.4 spectra

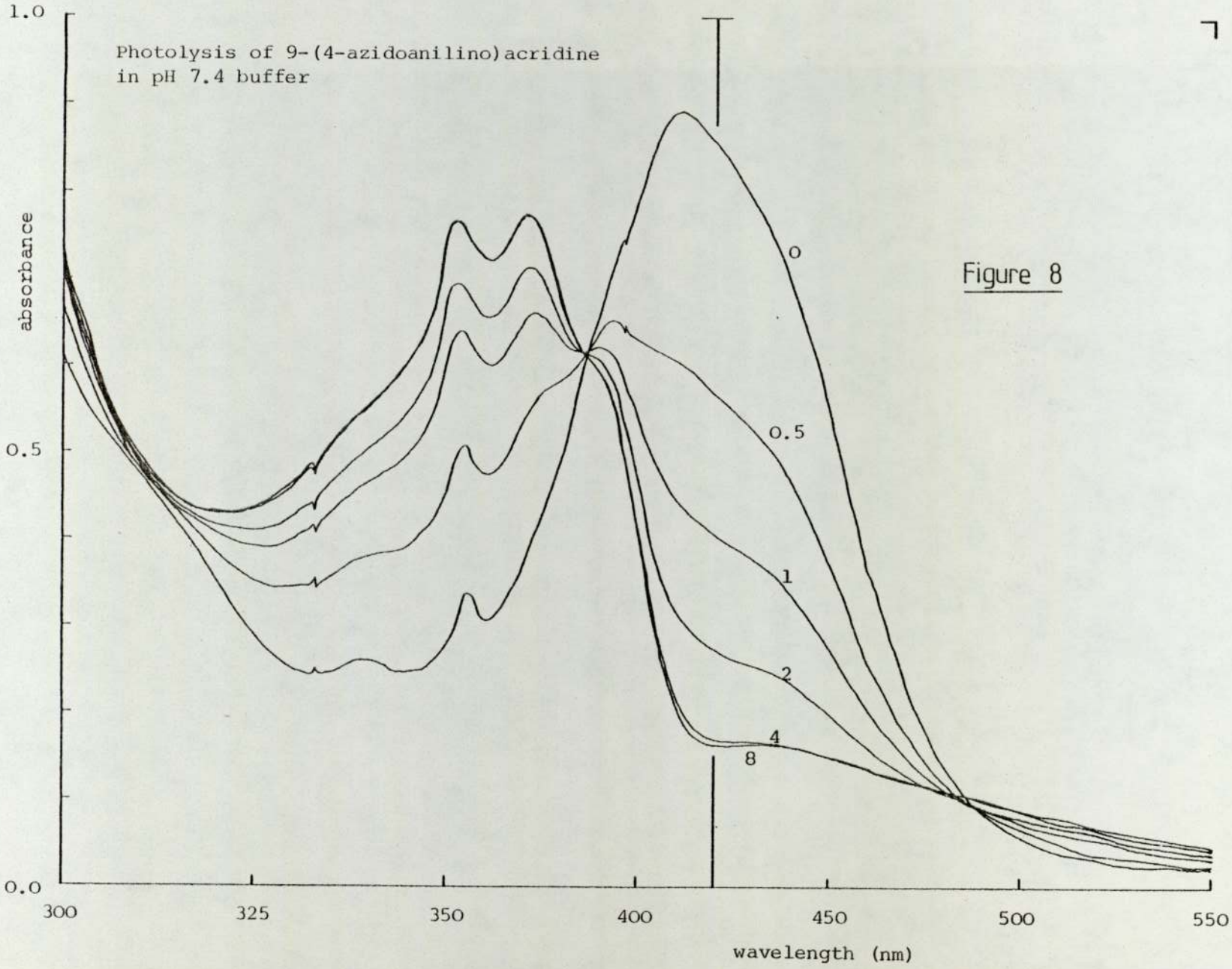
Photolysis of 9-(4-azidoanilino)acridine
in pH 7.4 buffer
absorbance
1.0
0.5
0.0
300
325
350
400
450
500
550
wavelength (nm)
0
0.5
1
2
4
8

Figure 8

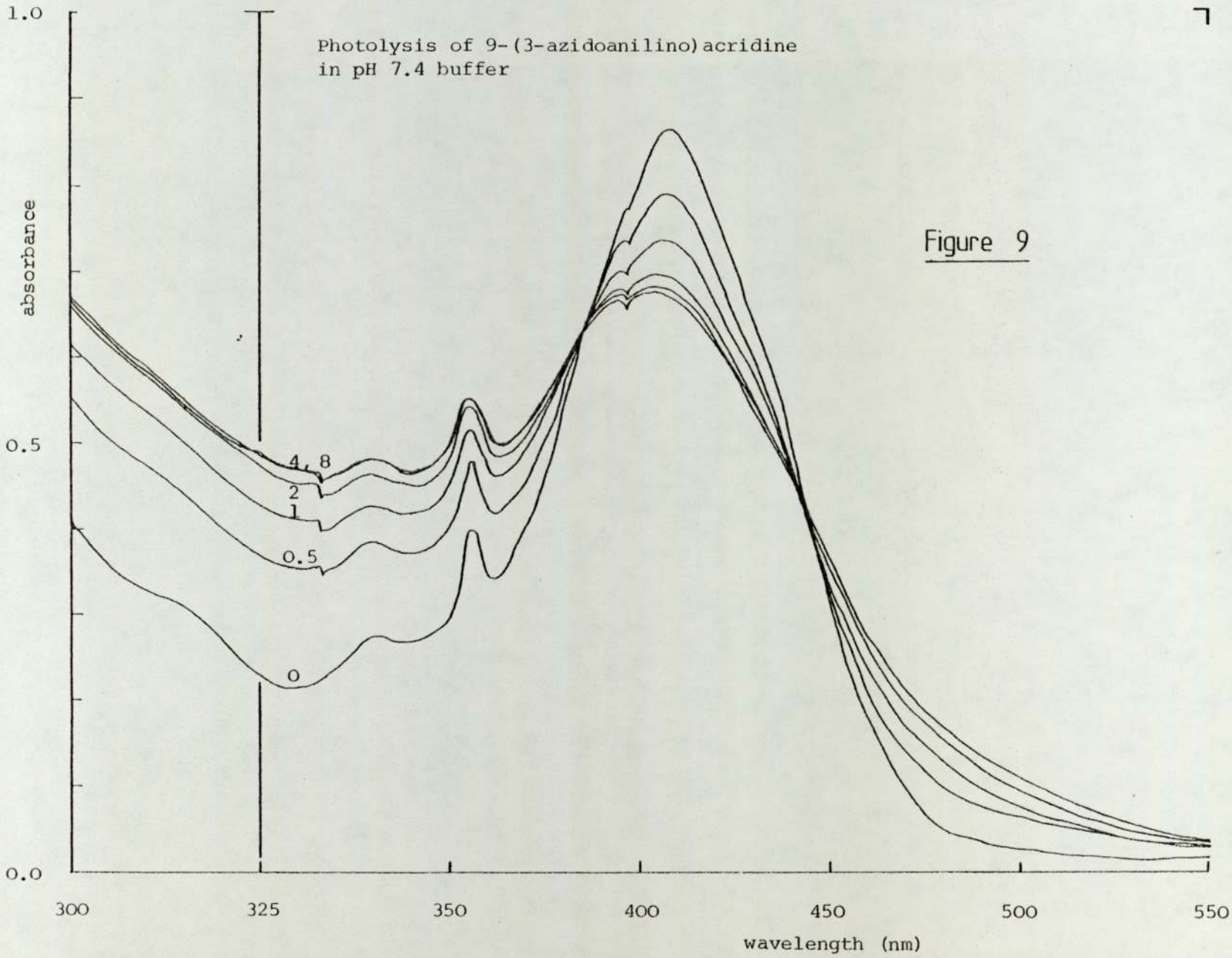
Photolysis of 9-(3-azidoanilino)acridine
in pH 7.4 buffer
1.0
0.5
0.0
absorbance
4, 8
2
1
0.5
0
300
325
350
400
450
500
550
wavelength (nm)

Figure 9

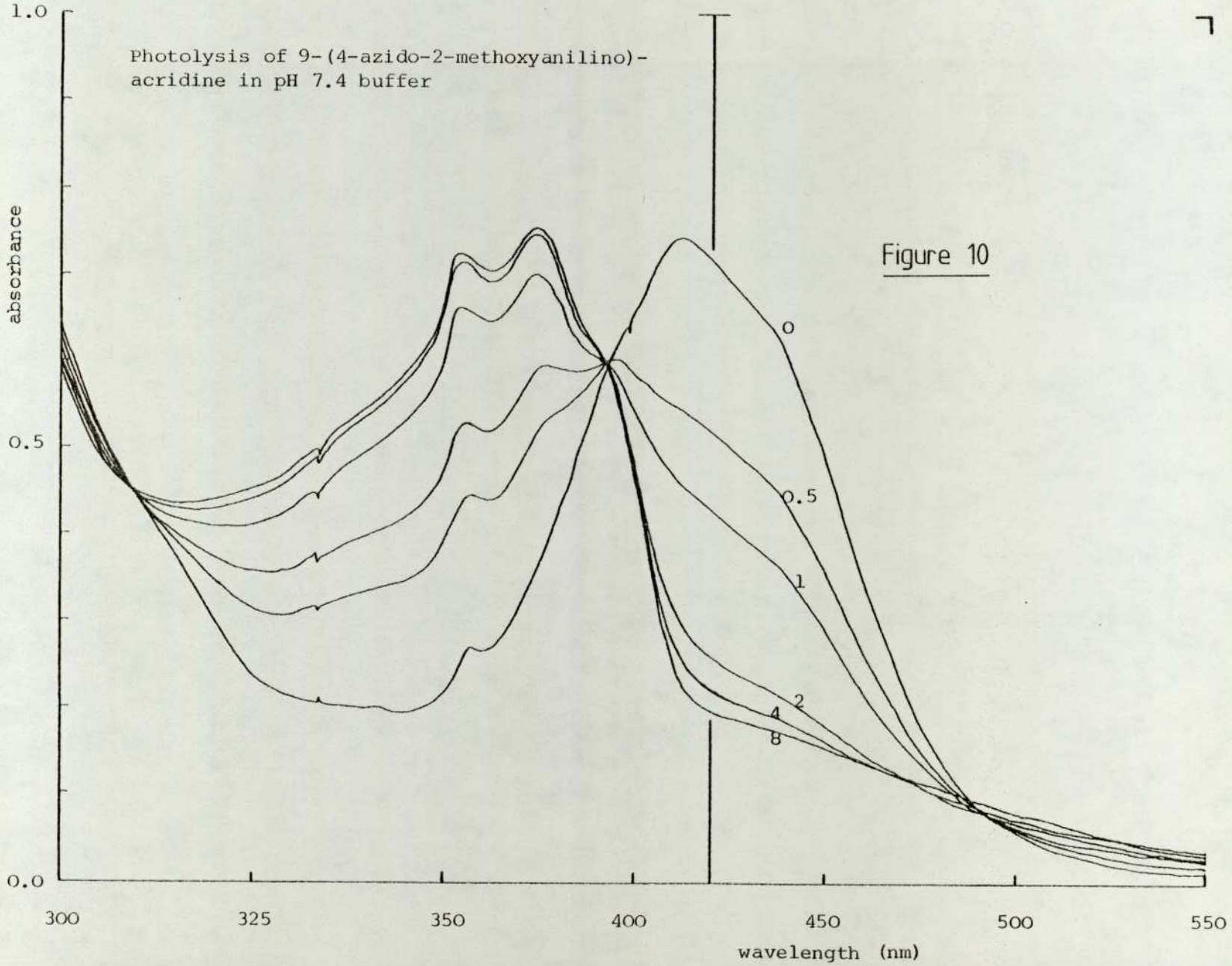
Photolysis of 9-(4-azido-2-methoxyanilino)-acridine in pH 7.4 buffer
absorbance
1.0
0.5
0.0
300
325
350
400
450
500
550
wavelength (nm)
0
0.5
1
2
4
8

Figure 10

(Figures 8, 9 and 10) and the corresponding pH 11 spectra in Figure 11. Evidently these azidoanilinoacridines are substantially unionised at the physiological pH of 7.4. This is in agreement with the pKa values of this type of compound (Table 8). These values were either measured spectrophotometrically[140] or predicted from the Hammett equation[141].

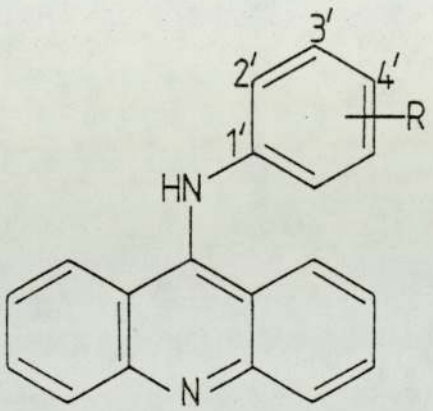

Table 8 The pKa values of 9-anilinoacridines

R=	pKa values		Reference
	experimentally determined	predicted	
H	7.41 ± 0.02	-	142
4' - NH_2	-	8.30	142
4' - Cl	7.04 ± 0.08	-	142
4' - Br	-	7.01	142
4' - N_3	7.07 ± 0.44*	7.25	143
3' - N_3	7.39 ± 0.77*	6.92	143
2' - OMe - 4' - N_3	-	7.25	143

* this high degree of variation is due to the low solubilities of these compounds.

Photolysis half-lives of the azides under specified conditions were obtained graphically from a plot of log absorbance against

Figure 11

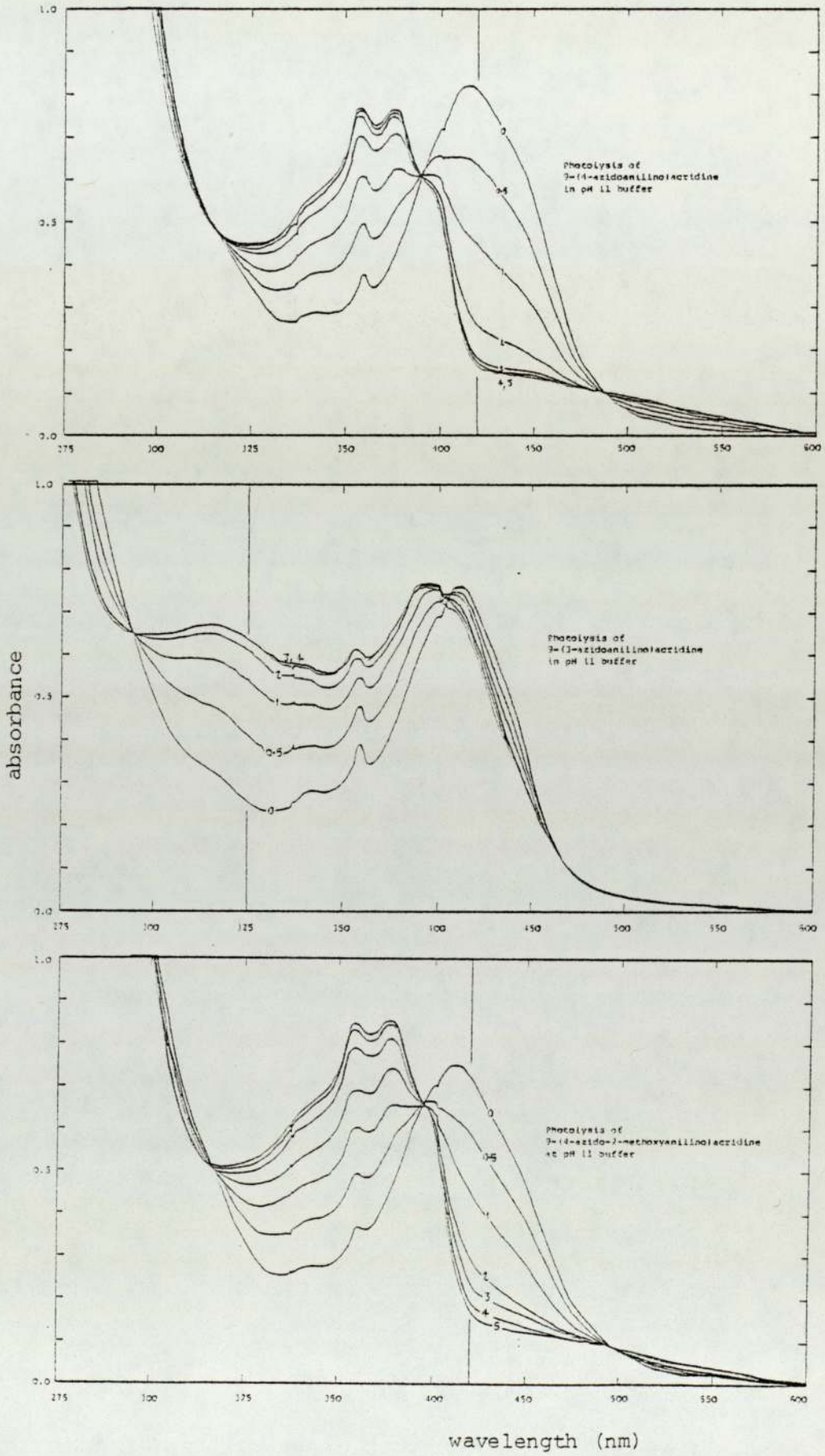
absorbance
wavelength (nm)
Photolysis of
9-(4-azidoanilino)acridine
in pH 11 buffer
Photolysis of
9-(3-azidoanilino)acridine
in pH 11 buffer
Photolysis of
9-(4-azido-2-methoxyanilino)acridine
in pH 11 buffer

irradiation time and are summarised in Table 9. From these results, it is evident that the rate of photolysis of these azides depends on the irradiation wavelengths - the shorter the wavelength the more energetic is the radiation and therefore the faster the rate of photolysis. There is little difference between photolysis rates at pH 7.4, 8.8 or 11, but at pH 4, an anomaly* arises. When solutions of the azides in pH 4 buffer

Table 9

Solvent	λirrad. (nm)	half-lives $t_{\frac{1}{2}}$ (second)		
		(4.20)	(4.21)	(4.22)
ethanol(pH 8.8)	253.7 366 visible	61 192 1419	55 357 2022	75 195 1423
pH 7.4 buffer	253.7 366 visible	42 153 667	29 279 1374	43 230 1087
pH 4 buffer	253.7 visible	* 5085	* 6060	* 6863
pH 11 buffer	253.7	48	32	60

*see text for explanation.

are photolysed (λirrad. = 253.7 nm) for up to 3 minutes, hypochromic changes occur and if these solutions are then basified they show uv spectral patterns resembling the spectra produced when photolyses are conducted at higher pH. This suggests that the route of photolysis is the same at all pH values. However if the photolyses at pH 4 are allowed to continue, hyperchromic changes occur followed by further hypochromic changes. This irregular spectral behaviour makes the determination of half-lives impracticable.

The observed irregularities are possibly due to a hydrolytic process taking place concurrently with photolysis. When solutions of the azides in pH 4 buffer are photolysed with visible light (Figure 12), gradual and slow decomposition indicated by a hypochromic change occurs. The very long half-lives under these conditions may suggest that these decompositions are due more to hydrolysis than photolysis at this acidic pH. However this is not the full explanation because the final uv spectra of these solutions after prolonged irradiation bear little resemblance to the spectrum of pure 9-acridanone, the usual hydrolysis product. It is interesting that at pH 4 (visible light) both 4'-substituted azides (4.20) and (4.22) behave similarly to the 3'-substituted azide (4.21).

5.3 Decomposition of 9-(benzotriazol-1-yl)acridine

The decomposition of benzotriazoles has long been of interest. Tsujimoto and co-workers[144] found that photolysis of various benzotriazoles gave products different from those formed by thermal decompositions. They concluded that the photochemical loss of nitrogen from benzotriazoles gave excited-state, 1,3-diradicals, while the thermolytic decompositions afforded ground-state diradicals.

9-(Benzotriazol-1-yl)acridine was pyrolysed at 250-300^{o} under reduced pressure in a vacuum sublimation apparatus; the cream-white flakes melted to form a black tar which effervesced vigorously. A yellow sublimate was gradually deposited on the central "cold finger" leaving a tarry residue. The yellow product was purified by vacuum sublimation. The mass spectrum of this yellow product was a fingerprint fit with the spectrum of the

Figure 12

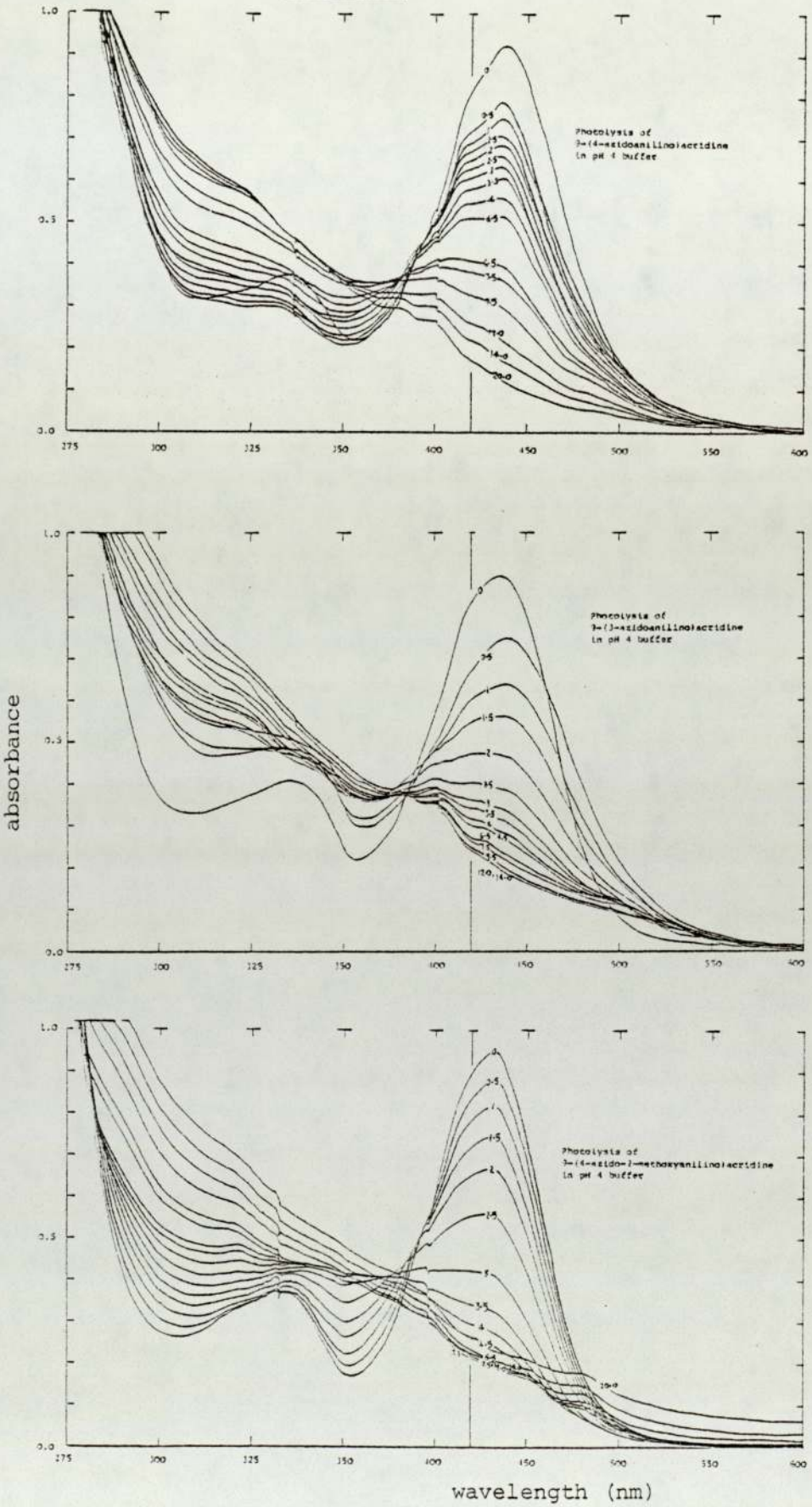

parent benzotriazole with the exception of the low abundance molecular ion peak of 9-(benzotriazol-1-yl)acridine at $^{m}/e$ 296. The base peak at $^{m}/e$ 268 in the spectrum of the triazole was probably due to loss of a nitrogen molecule which would explain the effervescence in the thermolysis of the title compound. Microanalysis of this yellow product further confirmed its chemical formula of $C_{19}H_{12}N_2$ corresponding to loss of one molecule of nitrogen from 9-(benzotriazol-1-yl)acridine ($C_{19}H_{12}N_4$).

When a sample of this yellow product was dissolved in ethanol, the solution fluoresced intensely under uv light. The uv spectrum of this compound showed bands at considerably longer wavelength than those of the parent benzotriazole indicative of a highly conjugated structure.

Electronic absorption maxima λmax (nm)

Parent benzotriazole (4.28)											
at pH 11		250				344	360	388			
at pH 4		250	257*			349	364	393	416		
Yellow product											
at pH 11	235	247*	261*		284	332	351	370	424	444	
at pH 4	233	252*	262*	272	286	340*	355		433	456	485

(* inflexion)

From the evidence presented, the yellow compound was identified as 13H-quin[4,3,2-kl]acridine (5.4) which was the first example of a new ring system. This thermo-cyclisation product provided a good parallel with the formation of phenanthridine (5.3) in the thermolysis of 1-benzylbenzotriazole (5.2)[145] (Scheme 7). The optimal yield of this quinacridine (5.4) from the thermolysis of the parent benzotriazole (4.28) was 60%.

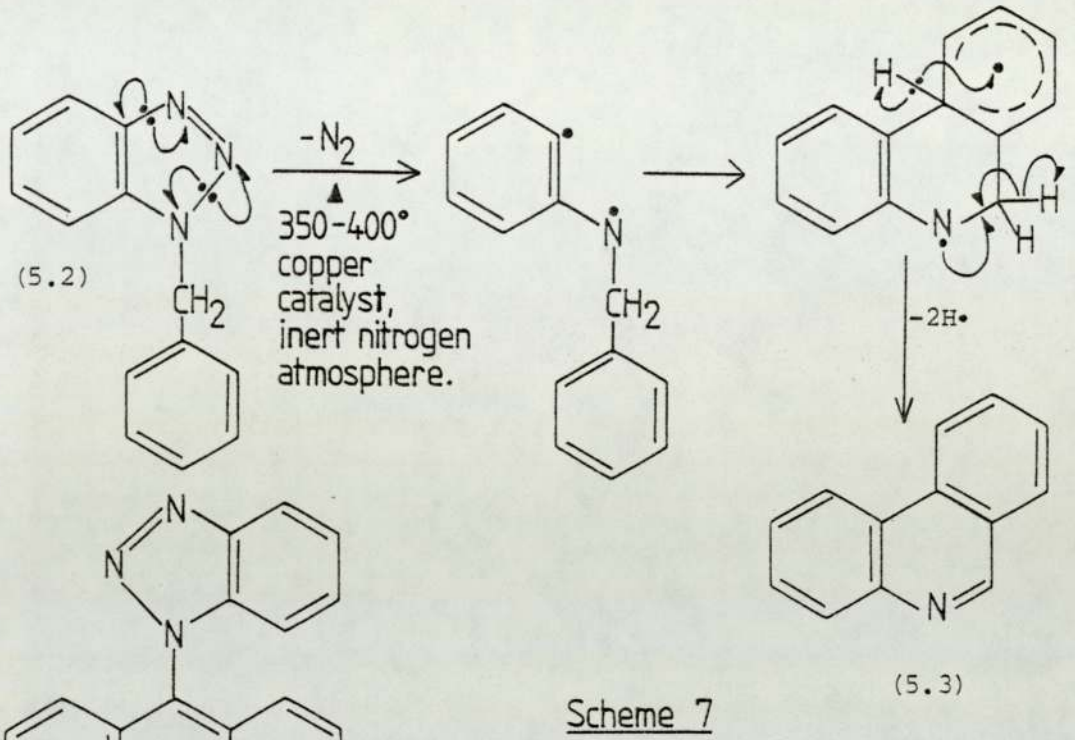

Scheme 7

(4·28)

250-300°
$-N_2$
under reduced
pressure

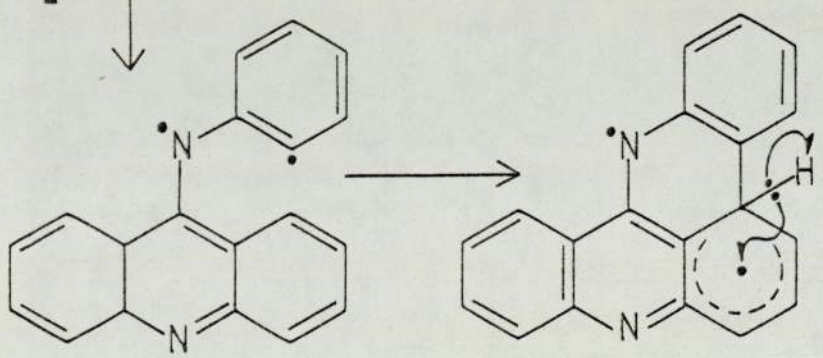

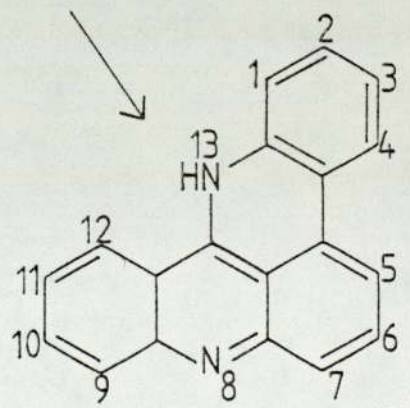

13H-quin[4,3,2-kl]acridine (5·4)

The photolysis of 1-benzylbenzotriazole (5.2) in protic solvents has been shown to afford the hydrogen abstraction product benzylaniline and its dehydrogenated analogue benzylideneaniline[144]. In the present work, the benzotriazole (4.28) was photolysed in ethanol in an Hanovia photochemical reactor. Tlc examination of the products showed seven spots which included the unchanged benzotriazole, quinacridine (5.4) and 9-acridanone (4.26), but no indication of the expected H-abstraction product— 9-anilino-acridine. Four spots remained unidentified. Decomposition studies on anilinoacridines and derivatives in general proved frustrating mainly due to the diversity and low yields of the various decomposition products.

Quantitative examination of the photolysis of the benzotriazole (4.28) was carried out in a similar fashion to the photolysis of azides described in the last section of this Chapter. Solutions of the substrate in ethanol were photolysed at three different irradiation wavelengths (λirrad.) and a typical uv change is shown in Figure 13. Photolysis half-lives of benzotriazole (4.28) under specified conditions were obtained graphically from a plot of log absorbance against irradiation time and are summarised in Table 10.

Table 10

λirrad. (nm)	$t_{\frac{1}{2}}$ (second)
253.7	85
366	100
visible	1450

From these results, it is deduced that the rate of photolysis is inversely proportional to the irradiation wavelengths.

Figure 13

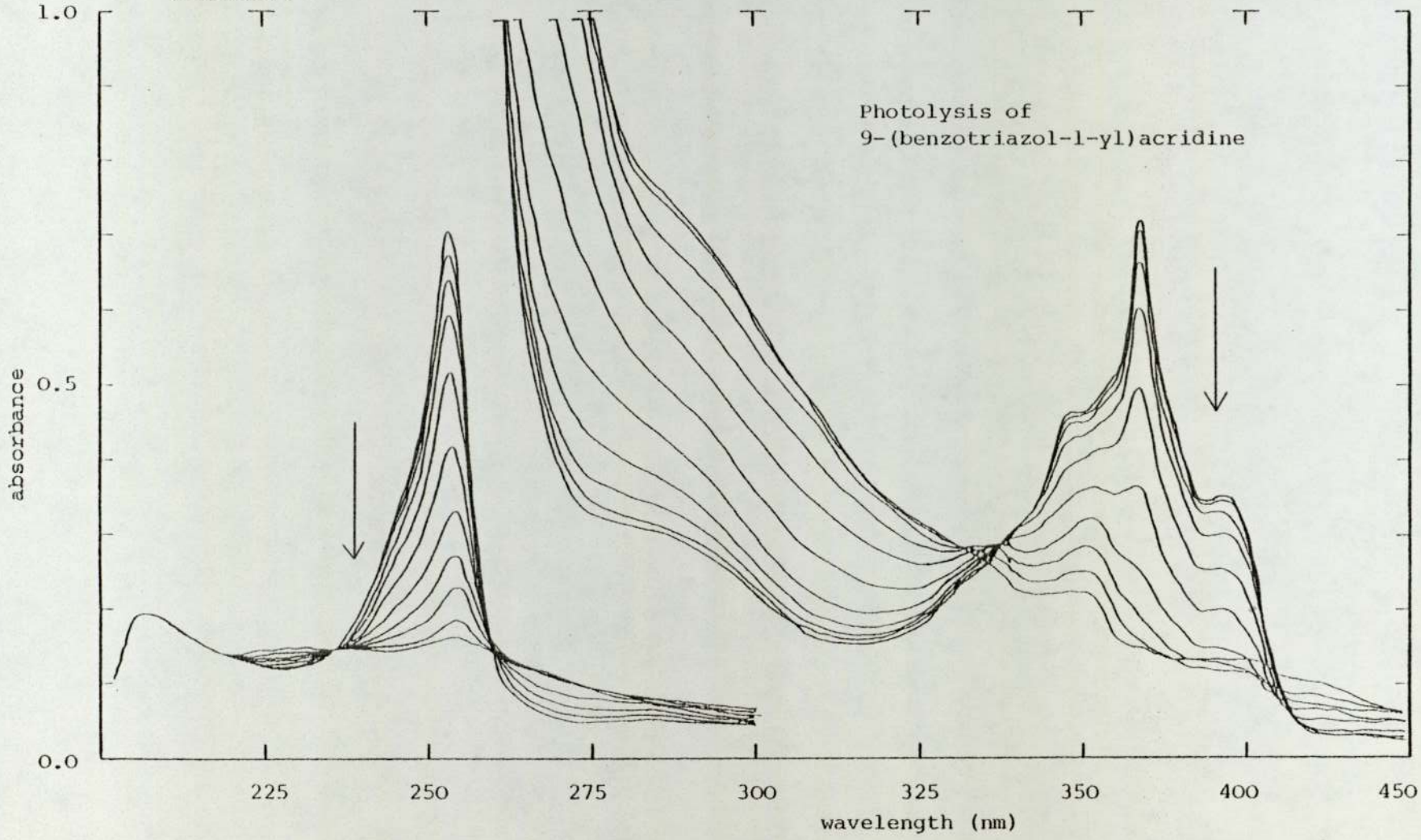
Photolysis of
9-(benzotriazol-1-yl)acridine
absorbance
1.0
0.5
0.0
225
250
275
300
325
350
400
450
wavelength (nm)

Chapter 6 Biological cell culture studies

6.1 The L1210 mouse lymphocytic leukaemic cell culture

The L1210 mouse leukaemic cell culture was employed in this work as a convenient biological system in which the cytotoxicity of potential antitumour agents could be examined. No pretence is implied that this *in vitro* system on its own could offer information on the *in vivo* antitumour activity of potential agents. L1210 cells were chosen because they can be easily maintained in the laboratory; they are robust to handling; their density can be determined accurately and quickly with a Coulter counter; they multiply rapidly, and, as a cell suspension they can be inspected while inside a culture flask with an inverted microscope without any chance of contamination. Indeed, another reason for using this cell line is its known sensitivity to acridine type compounds since the *in vivo* L1210 system is the current primary screening system for antitumour activity of 9-anilinoacridines at the Cancer Chemotherapy Laboratory of Auckland, New Zealand[82].

The time taken for the density of a cell population to double is termed the doubling time; this value is characteristic of a particular cell line. Figure 14 shows a growth curve of L1210 cells grown under favourable conditions (see experimental for conditions). The doubling time of L1210 cells under the conditions employed in this work was 10.5 ± 0.5 hours. Another distinctive feature of L1210 cells was that the average diameter of these cells during log phase growth determined using a Coulter counter or in conjunction with a Coulter channelyser was always 15 ± 0.5 μ. Periodical determinations of these two parameters throughout this work served to certify the identity of the stock

Figure 14

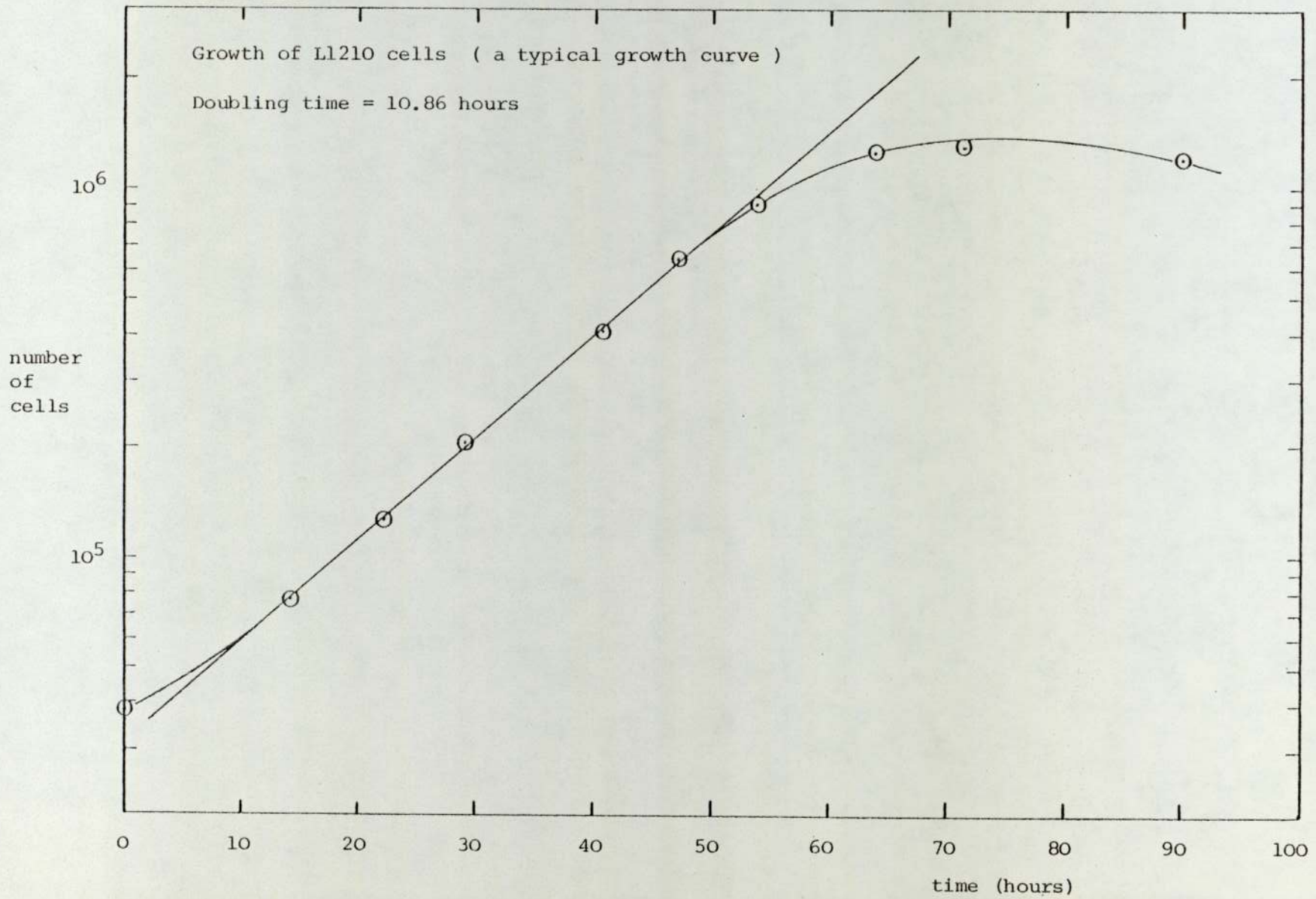
Growth of L1210 cells (a typical growth curve)
Doubling time = 10.86 hours
10^6
10^5
number of cells
0
10
20
30
40
50
60
70
80
90
100
time (hours)

culture. The dose/response relationship of a reference acridine agent - 9-(4-aminoanilino)acridine (4.14) - was used to check the sensitivity of L1210 cells to acridine type compounds throughout the course of this project.

6.2 Effect of DMSO on cell growth

Agents under investigation in this work (in the L1210 cell system) are quite insoluble in water, therefore, they were first dissolved in DMSO to prepare serial dilutions before treating the cells. DMSO was chosen because of its solvent power, its ability to penetrate cell membranes[146] and carry organic (drug) molecules with it[147]. However DMSO itself does have a cytotoxic effect against L1210 cells at high concentration. Figure 15 shows the effect of DMSO concentration on the growth of L1210 cells. In view of these results, 50 $\mu l\ ml^{-1}$ of DMSO in cell medium was chosen as a solvent for all subsequent cell culture experiments. This concentration of DMSO gave only 10% growth inhibition but was adequate to keep test compounds in solution.

6.3 Effect of 366 nm radiation on cell growth

The photosensitization experiments (to be discussed in the next Chapter) require a light source which would activate potential photosensitizing agents. A light box fitted with an 8 W fluorescent tube was designed for the purpose. Three types of fluorescent tubes with emission wavelengths of 253.7 nm, 366 nm and the visible-range were employed. It is evident from Chapter 5 that the photozensitizers under investigation were best activated by the first two irradiation wavelengths (λirrad.) while the visible-range was too slow in photolysing these agents, since the irradiation time must be within the 60 minutes allowed for the

Figure 15

Toxicity of DMSO in L1210 cell cultures

(results are the mean of 3 separate determinations)

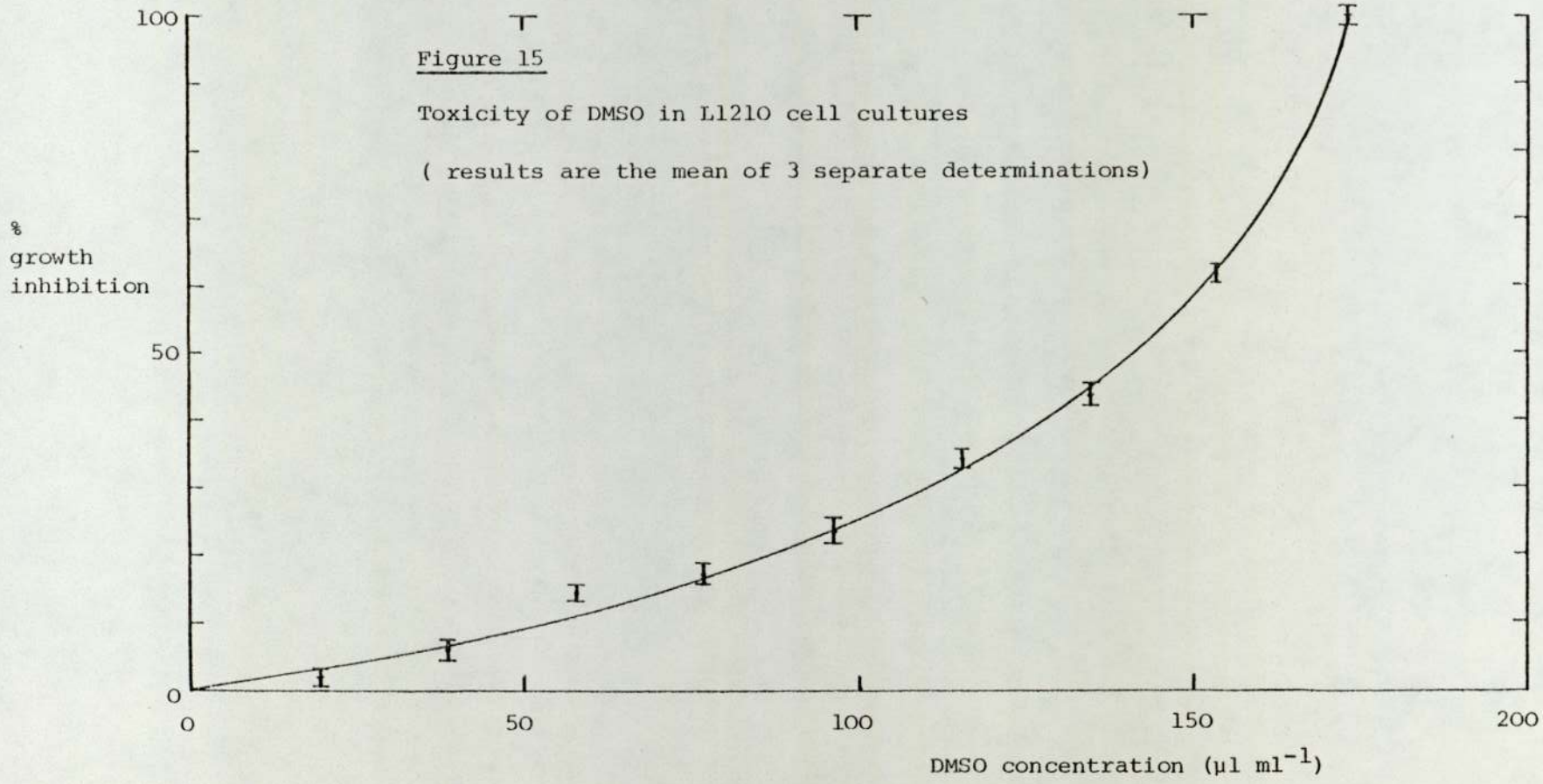

drug treatment (see Chapter 9 for cytotoxicity screening procedures). Of the two λirrad. (i.e. 253.7 nm and 366 nm), the ultra violet 253.7 nm radiation was not suitable for use in *in vitro* cell experiments because (a) the sterile plastic-ware used in these experiments efficiently absorbed electromagnetic radiation in the uv region (Figure 16); (b) even the small fraction of uv radiation which penetrated the plastic-ware afforded a lethal effect on L1210 cells at exposure time of 1 minute or less.

The blue light fluorescent tube (λirrad. = 366 nm) was the best compromise with a reasonably short irradiation time required to photolyse agents completely and the cytotoxic effect of this λirrad. is moderate. Figure 17 shows the effect of this λirrad. on cell growth. Irradiation time for cell experiments of not more than 5 minutes was selected corresponding to a cell growth inhibition of 5% or less. Both the "test" and "control" cell suspensions were irradiated for the same period of time under the same irradiation conditions to nullify this growth inhibitory effect of this radiation in these experiments.

Figure 16

Absorption of electromagnetic radiation by universal tubes plastic-ware in the ultra violet/visible region

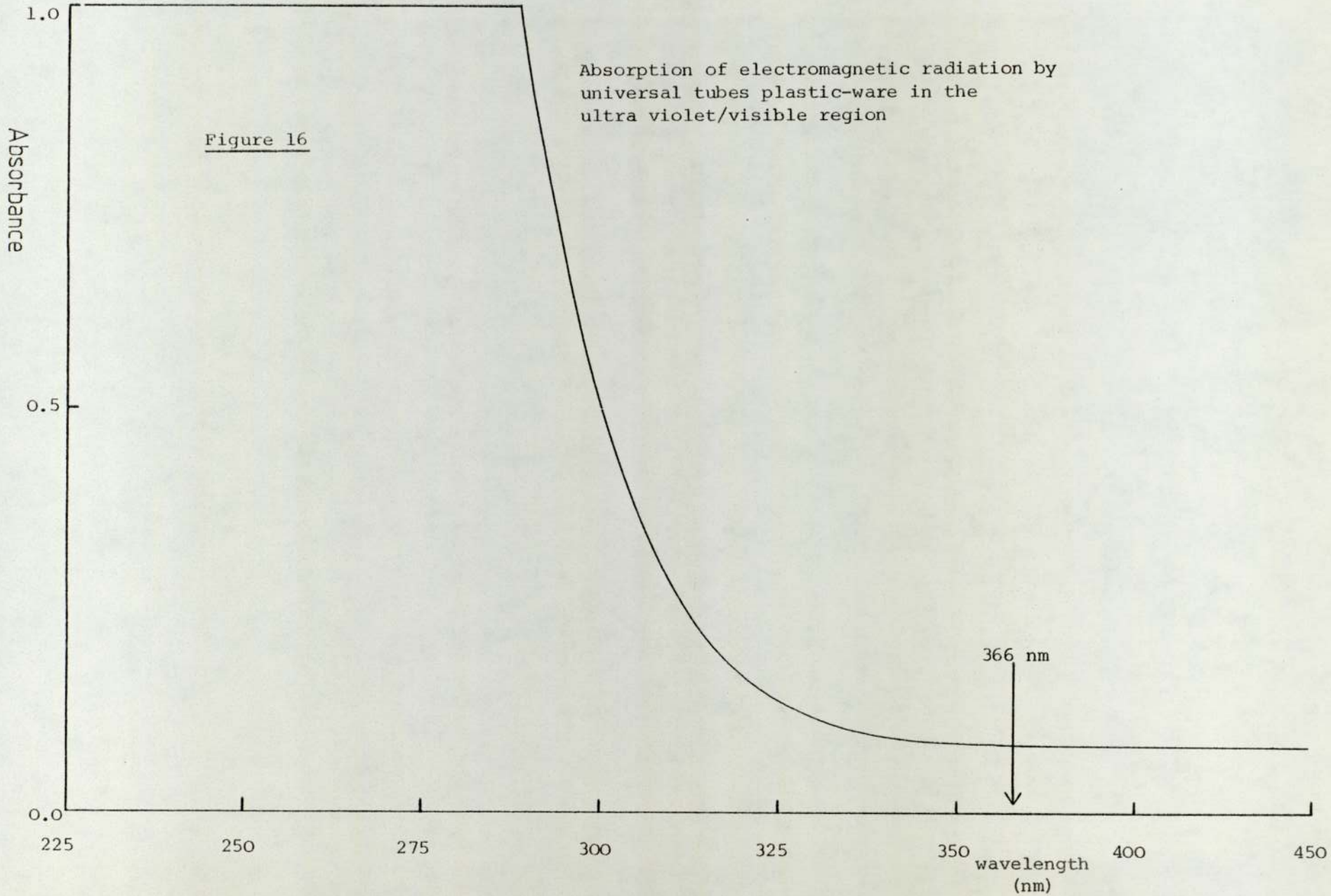

Figure 17

Effect of 366 nm radiation on the growth of L1210 cells

(results are the mean of 3 separate determinations)

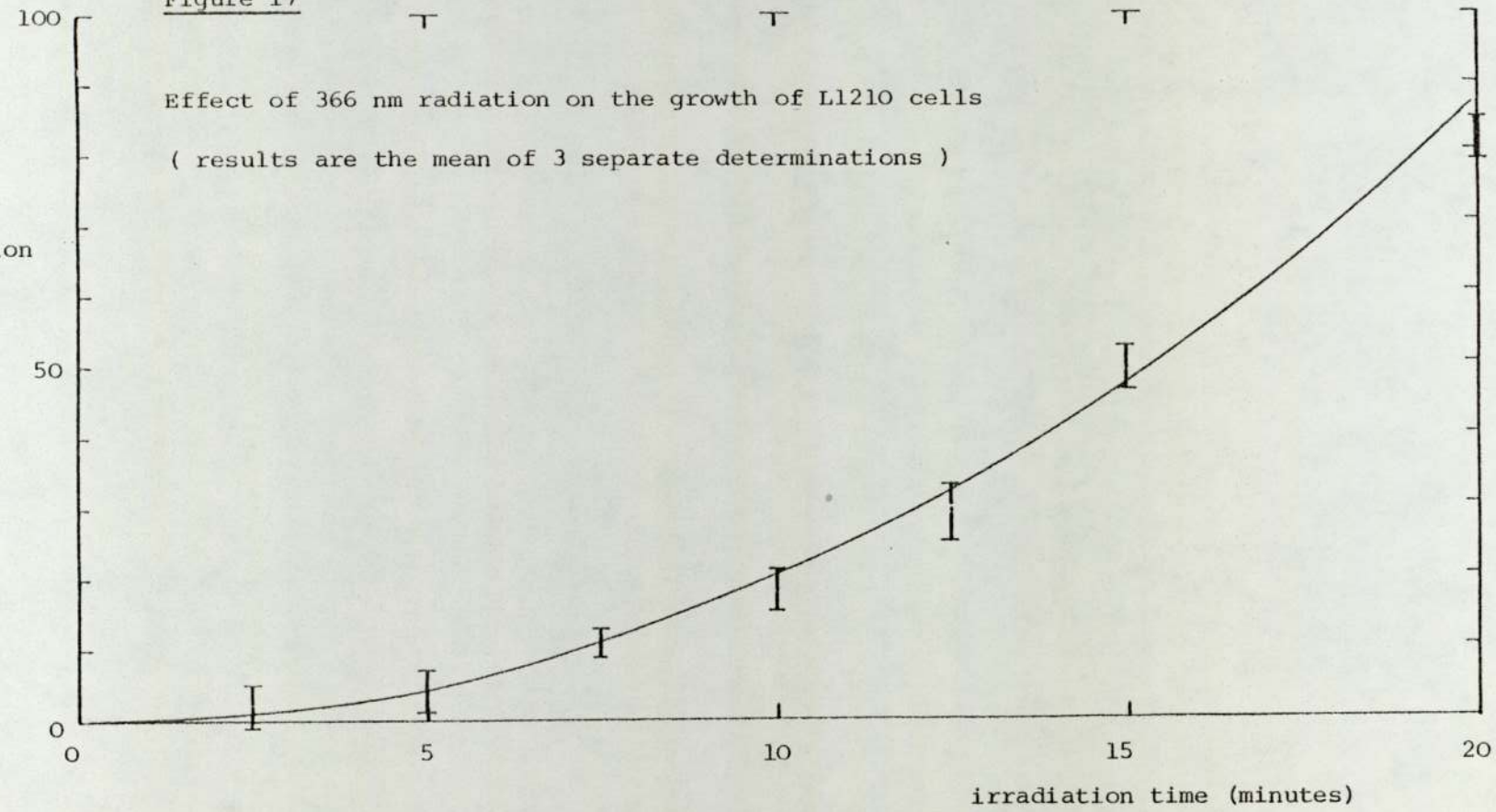

Chapter 7 Cytotoxicity and photosensitization

7.1 Cytotoxicity of potential antitumour agents

An ideal antitumour agent should interfere with the functioning of tumour cells, inhibit their proliferation and promote their destruction while leaving normal cells substantially unharmed *in vivo*. Unfortunately such an agent is not yet available and cytotoxic agents with only quantitative selectivity for tumour cells are currently the medicinal agents in use in the treatment of cancer. One such agent is *m*-AMSA (2.18). This compound together with a number of 9-anilinoacridines synthesised in the present work, doxorubicin (7.2) and daunorubicin (7.3) which are antitumour antibiotics of the rhodomycin group, and sulphanilamide (7.6), its azido derivative (7.5) and the azepino ring expanded product (7.7) have been examined in the *in vitro* L1210 cytotoxicity screening system in this work (see the Experimental section). A list of these 15 compounds together with their chemical structures is given in Table 11. Although an *in vitro* cytotoxicity screening system alone cannot afford information on the selectivity of antitumour agents, the inhibition of tumour cell growth is a desirable biological response in a potential antitumour agent. The cytotoxicity test results of the 15 agents listed in Table 11 are given in Tables 12-26 and are presented graphically in Figures 18-23.

It was observed in Figure 18 that the *p*-nitro compound (4.9) required a higher dose to achieve the same toxicity level as its *m*-isomer (4.10); another *m*-nitro derivative (4.11) showed a similarly shaped dose-response curve to compound (4.10) but again was less potent. These nitro compounds were not very soluble in

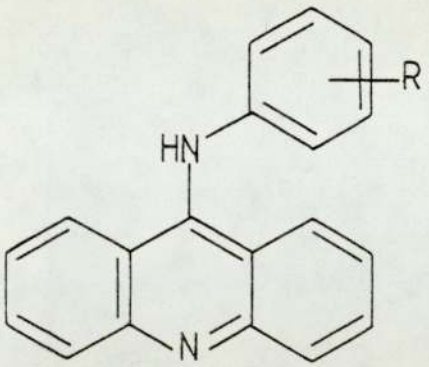

(4.3)

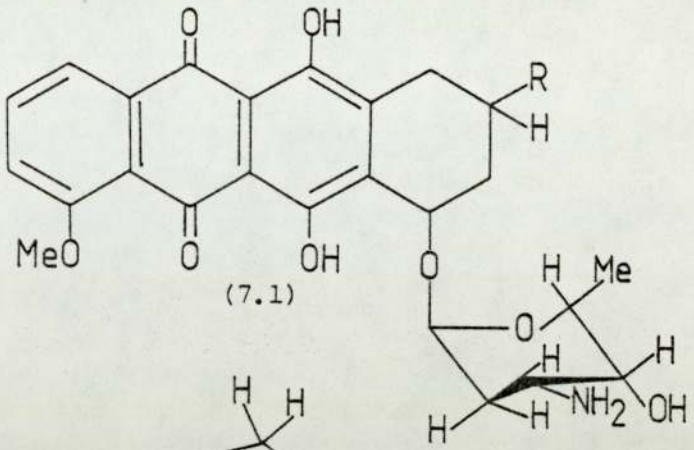

(7.1)

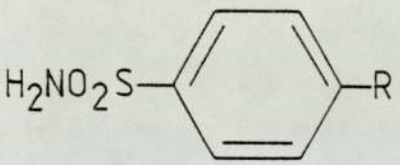

(7.4)

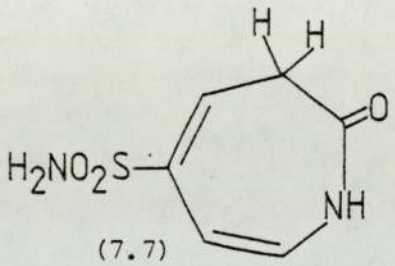

(7.7)

Table 11

Agents	Substituents(s) R in structure	
2.18	2'-OMe-4'$NHSO_2Me$	4.3*
4.9	2'-OMe-4'-NO_2	4.3*
4.10	2'OMe-5'-NO_2	4.3*
4.11	2'-NH_2-5'-NO_2	4.3*
4.14	4'-NH_2	4.3*
4.15	2'OMe-4'-NH_2	4.3*
4.16	2'OMe-5'-NH_2	4.3*
4.20	4'-N_3	4.3*
4.21	3'-N_3	4.3*
4.22	2'-OMe-4'-N_3	4.3*
7.2	-$COCH_2OH$	7.1
7.3	-COMe	7.1
7.5	-N_3	7.4
7.6	-NH_2	7.4
7.7	———	-

*As hydrochloride salts - see Experimental section.

Table 12 Cytotoxicity of agent (4.9)

Dose ($\mu g\ ml^{-1}$)	% inhibition			mean	S.D.
3.81×10^2	93.7	96.4	103.2	97.8	4.9
2.38×10^2	91.7	87.9	93.5	91.0	2.9
1.49×10^2	69.1	60.5	72.4	67.3	6.1
9.3×10^1	41.1	35.6	44.1	40.3	4.3
5.81×10^1	27.0	24.5	25.7	25.7	1.3
3.63×10^1	3.0	1.6	8.7	4.4	3.8
2.27×10^1	6.9	0.3	9.2	5.5	4.6

$ID_{80} = 1.94 \times 10^2\ \mu g\ ml^{-1}$

$ID_{50} = 1.035 \times 10^2$

$ID_{20} = 5.5 \times 10^1$

Table 13 Cytotoxicity of agent (4.10)

Dose ($\mu g\ ml^{-1}$)	% inhibition			mean	S.D.
3.81×10^1	99.9	107.8	98.9	102.2	4.9
2.93×10^1	78.6	84.9	62.1	75.2	11.8
2.25×10^1	41.9	46.3	30.5	39.6	8.2
1.73×10^1	14.6	16.9	8.3	13.3	4.5
1.33×10^1	7.9	9.6	0.33	5.9	4.9
1.03×10^1	1.3	6.6	-3.7	1.4	5.2

$ID_{80} = 3.09 \times 10^1\ \mu g\ ml^{-1}$

$ID_{50} = 2.4 \times 10^1$

$ID_{20} = 1.86 \times 10^1$

Table 14 Cytotoxicity of agent (4.11)

Dose ($\mu g\ ml^{-1}$)	% inhibition			mean	S.D.
9.5×10^1	102.5	98.9	99.3	100.2	1.97
7.94×10^1	95.4	79.6	79.4	84.8	9.2
6.61×10^1	69.4	58.3	56.8	61.5	6.9
5.51×10^1	42.2	28.1	30.6	33.6	7.5
4.59×10^1	29.5	14.7	10.4	18.2	10.0
3.83×10^1	14.7	11.5	7.6	11.3	3.6
3.19×10^1	9.8	10.4	11.2	10.5	0.7

$ID_{80} = 7.71 \times 10^1\ \mu g\ ml^{-1}$

$ID_{50} = 6.06 \times 10^1$

$ID_{20} = 4.76 \times 10^1$

Table 15 Cytotoxicity of agent (4.14)

Dose ($\mu g\ ml^{-1}$)	% inhibition			mean	S.D.
3.33	96.9	91.3	89.1	92.4	4.0
1.75	79.8	89.5	76.0	81.8	7.0
9.2×10^{-1}	67.7	76.2	61.0	68.3	7.6
4.9×10^{-1}	46.8	43.6	37.2	42.5	4.9
2.6×10^{-1}	23.9	28.4	22.3	24.9	3.2
1.3×10^{-1}	13.7	15.6	7.3	12.2	4.3

$ID_{80} = 1.81\ \mu g\ ml^{-1}$

$ID_{50} = 5.8 \times 10^{-1}$

$ID_{20} = 1.87 \times 10^{-1}$

Table 16 Cytotoxicity of agent (4.15)

Dose ($\mu g\ ml^{-1}$)	% inhibition			mean	S.D.
5.7	95.8	101.2	101.1	99.4	3.1
3.8	86.3	91.9	87.7	88.6	2.9
2.5	73.2	80.6	73.2	75.7	4.3
1.7	54.5	67.0	60.1	60.5	6.3
1.1	37.4	57.8	46.3	47.2	10.2
7.5×10^{-1}	25.6	42.1	33.3	33.7	8.3
5.0×10^{-1}	18.3	24.6	21.5	21.5	3.2
3.3×10^{-1}	13.1	8.9	11.2	11.1	2.1
2.2×10^{-1}	9.8	0.3	3.9	4.7	4.8
1.5×10^{-1}	7.5	3.7	3.6	4.9	2.2
1.0×10^{-1}	6.4	1.7	4.1	4.1	2.4

$ID_{80} = 2.90\ \mu g\ ml^{-1}$

$ID_{50} = 1.20$

$ID_{20} = 4.9 \times 10^{-1}$

Table 17 Cytotoxicity of agent (4.16)

Dose ($\mu g\ ml^{-1}$)	% inhibition			mean	S.D.
4.76×10^{1}	110.5	-	-	-	-
3.17×10^{1}	99.7	97.5	99.4	98.9	1.2
2.12×10^{1}	97.5	90.8	94.3	94.2	3.4
1.41×10^{1}	93.4	74.6	80.9	83.0	9.6
9.4	69.3	76.5	69.9	71.9	4.0
6.3	47.8	55.7	58.3	53.9	5.5
4.2	34.6	38.9	26.7	33.4	6.2
2.8	22.4	15.8	13.5	17.2	4.6
1.9	11.7	7.9	5.6	8.4	3.1

$ID_{80} = 1.23 \times 10^{1}\ \mu g\ ml^{-1}$

$ID_{50} = 6.0$

$ID_{20} = 2.9$

Table 18 Cytotoxicity of agent (4.20)

Dose ($\mu g\ ml^{-1}$)	% inhibition			mean	S.D.
1.43×10^{1}	97.3	101.2	89.1	95.9	6.2
7.1	57.6	61.5	48.0	55.7	6.9
3.6	33.3	42.8	29.7	35.3	6.8
1.8	18.5	9.3	6.2	11.3	6.4
9.0×10^{-1}	10.7	7.6	1.5	6.6	4.7

$ID_{80} = 1.09 \times 10^{1}\ \mu g\ ml^{-1}$

$ID_{50} = 5.1$

$ID_{20} = 2.4$

Table 19 Cytotoxicity of agent (4.21)

Dose ($\mu g\ ml^{-1}$)	% inhibition			mean	S.D.
9.52×10^{1}	107.0	105.2	102.3	104.8	2.4
5.29×10^{1}	54.8	82.3	71.5	69.5	13.9
2.94×10^{1}	37.6	45.7	42.4	41.9	4.1
1.63×10^{1}	5.9	15.9	6.2	9.3	5.7
9.1	2.7	3.2	4.8	3.6	1.1

$ID_{80} = 6.13 \times 10^{1}\ \mu g\ ml^{-1}$

$ID_{50} = 3.5 \times 10^{1}$

$ID_{20} = 1.99 \times 10^{1}$

Table 20 Cytotoxicity of agent (4.22)

Dose ($\mu g\ ml^{-1}$)	% inhibition			mean	S.D.
1.9×10^{1}	101.4	94.6	90.6	95.5	5.5
9.5	76.9	79.0	72.1	76.0	3.5
4.8	51.3	43.2	38.7	44.4	6.4
2.4	24.5	22.5	12.5	19.8	6.4
1.2	5.8	5.4	-2.5	2.9	4.7

$ID_{80} = 1.08 \times 10^{1} \mu g\ ml^{-1}$

$ID_{50} = 5.2$

$ID_{20} = 2.5$

Table 21 Cytotoxicity of agent (7.5)

Dose ($\mu g\ ml^{-1}$)	% inhibition			mean	S.D.
9.52×10^{2}	9.7	3.6	14.1	9.1	5.3
5.60×10^{2}	3.7	1.2	5.7	3.5	2.3
3.30×10^{2}	1.9	-0.2	5.5	2.4	2.9
1.94×10^{2}	2.4	0.8	8.7	4.0	4.2
1.14×10^{2}	1.1	-2.5	3.2	0.6	2.9
6.7×10^{1}	1.0	0.3	1.1	0.8	0.4
4.0×10^{1}	0.8	-0.3	3.6	1.4	2.0

$ID_{80} >> 1 \times 10^{3}\ \mu g\ ml^{-1}$

$ID_{50} >> 1 \times 10^{3}$

$ID_{20} >> 1 \times 10^{3}$

Table 22 Cytotoxicity of agent (2.18)

Dose ($\mu g\ ml^{-1}$)	% inhibition			mean	S.D.
1.905×10^{-1}	96.1	99.2	92.6	96.0	3.3
1.270×10^{-1}	93.2	97.6	87.9	92.9	4.9
8.47×10^{-2}	92.3	97.8	85.4	91.8	6.2
5.64×10^{-2}	82.4	76.5	73.2	77.4	4.7
3.76×10^{-2}	71.1	77.3	60.9	69.8	8.3
2.51×10^{-2}	48.4	51.9	41.8	47.4	5.1
1.67×10^{-2}	32.9	40.6	23.5	32.3	8.6
1.11×10^{-2}	20.7	29.9	25.5	25.4	4.6
7.4×10^{-3}	17.3	23.5	11.1	17.3	6.2
5.0×10^{-3}	3.1	9.6	2.4	5.0	4.0
3.3×10^{-3}	-0.8	0.0	2.2	0.5	1.6

$ID_{80} = 6.06 \times 10^{-2}\ \mu g\ ml^{-1}$

$ID_{50} = 2.38 \times 10^{-2}$

$ID_{20} = 9.3 \times 10^{-3}$

Table 23 Cytotoxicity of agent (7.2)

Dose ($\mu g\ ml^{-1}$)	% inhibition			mean	S.D.
4.76×10^{-1}	94.3	93.9	98.4	95.5	2.5
2.38×10^{-1}	89.3	87.8	83.2	86.8	3.3
1.19×10^{-1}	56.8	57.7	66.5	60.3	5.4
5.95×10^{-2}	17.4	21.9	28.6	22.6	5.6
2.98×10^{-2}	11.3	0.9	15.8	9.3	7.6

$ID_{80} = 1.974 \times 10^{-1}\ \mu g\ ml^{-1}$

$ID_{50} = 1.033 \times 10^{-1}$

$ID_{20} = 5.4 \times 10^{-2}$

Table 24 Cytotoxicity of agent (7.3)

Dose ($\mu g\ ml^{-1}$)	% inhibition			mean	S.D.
1.90×10^{-1}	97.6	97.8	96.9	97.4	0.5
9.52×10^{-2}	90.3	86.1	81.8	86.1	4.3
4.76×10^{-2}	36.3	44.8	42.7	41.3	4.3
2.38×10^{-2}	18.9	26.9	21.6	22.5	4.1
1.19×10^{-2}	-0.4	4.8	1.5	2.0	2.6

$ID_{80} = 9.16 \times 10^{-2}\ \mu g\ ml^{-1}$

$ID_{50} = 4.76 \times 10^{-2}$

$ID_{20} = 2.48 \times 10^{-2}$

Table 25 Cytotoxicity of agent (7.6)

Dose ($\mu g\ ml^{-1}$)	% inhibition		
9.52×10^{2}	-0.02	0.16	-
4.76×10^{2}	0.04	0.03	-
2.38×10^{2}	0.8	-0.2	-
1.19×10^{2}	0.1	0.2	-
60	0.06	0.8	-
30	-0.42	0.5	-
15	0.13	-0.4	-
7.4	0.01	0.00	-
3.7	0.08	0.12	-
1.9	-0.02	1.4	-

No growth-inhibition was detected at all doses up to $9.52 \times 10^{2}\ \mu g\ ml^{-1}$

Table 26 Cytotoxicity of agent (7.7)

Dose ($\mu g\ ml^{-1}$)	% inhibition			mean	S.D.
9.52×10^2	46.9	28.5	17.8	31.1	14.7
4.76×10^2	14.2	12.9	12.3	13.1	1.0
2.38×10^2	6.9	3.4	4.4	4.9	1.8
1.19×10^2	4.3	2.7	1.6	2.9	1.4
6.0×10^1	5.8	4.8	2.7	4.4	1.6
3.0×10^1	13.4	2.5	2.4	6.1	6.3
1.5×10^1	3.2	1.9	0.0	1.7	1.6

$ID_{80} >> 1 \times 10^3\ \mu g\ ml^{-1}$

$ID_{50} >> 1 \times 10^3$

$ID_{20} = 5.7 \times 10^2$

Figure 18

Agents of Table 11 : cytotoxicity in the dark

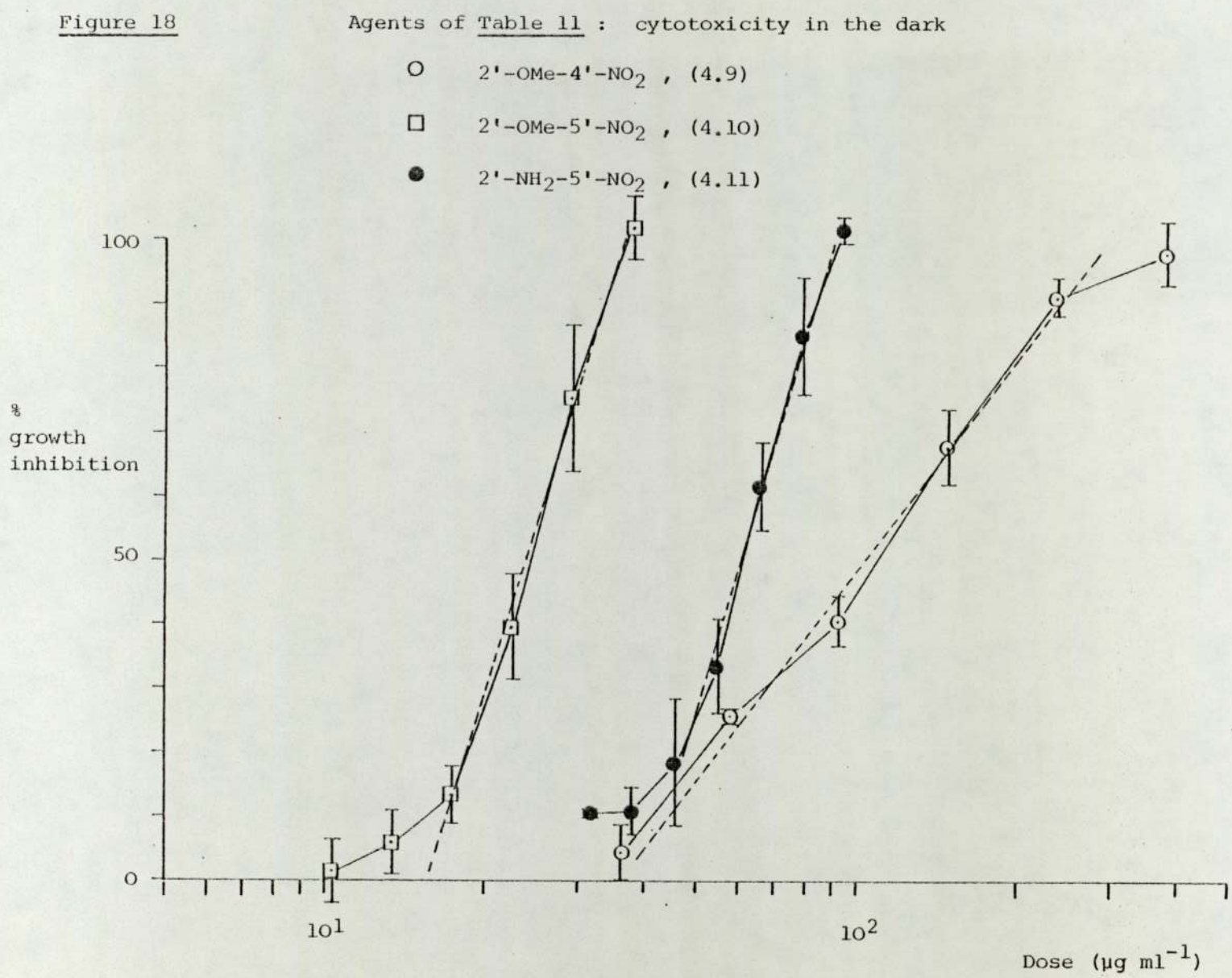

Figure 19

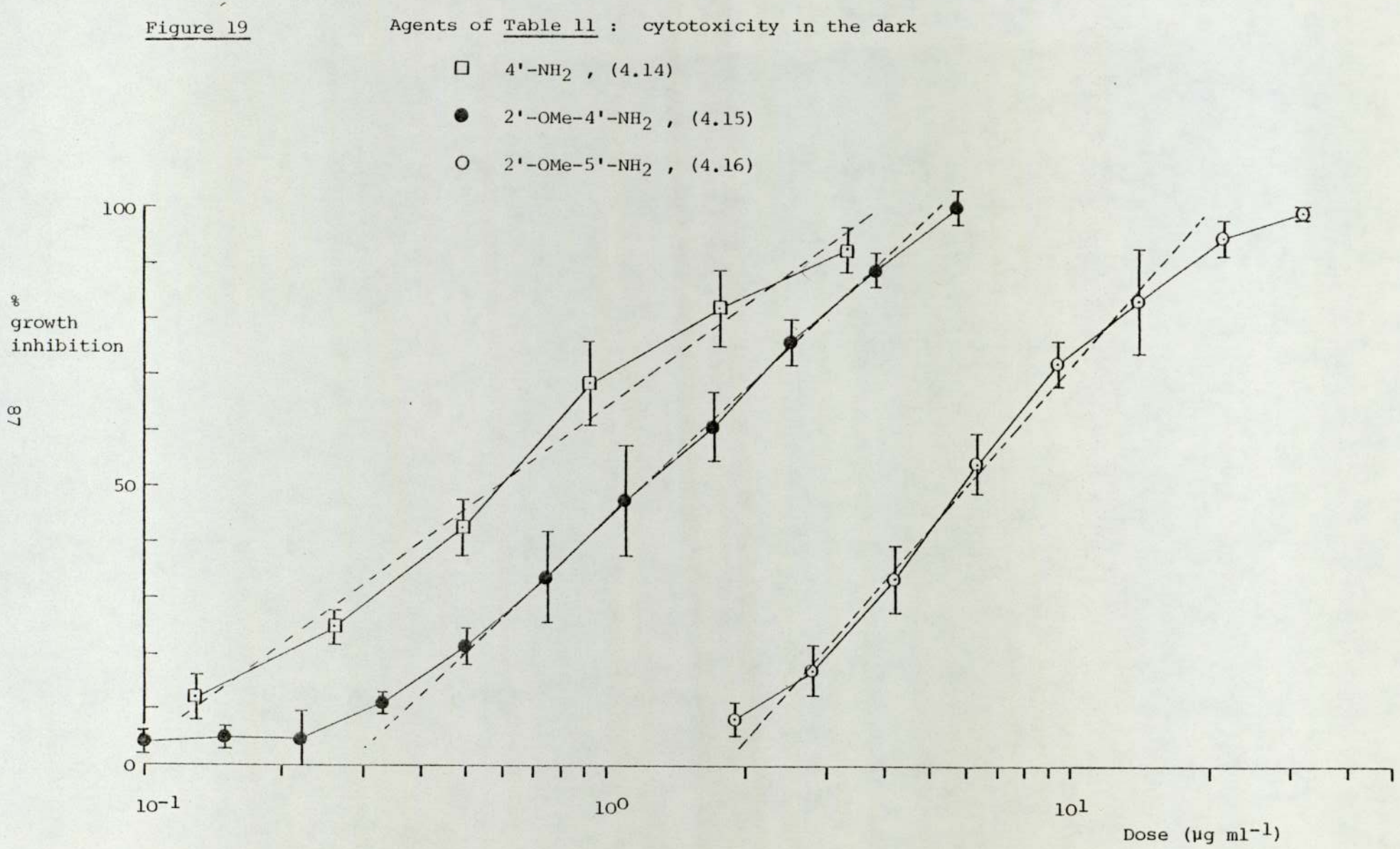
Agents of Table 11 : cytotoxicity in the dark
□ 4'-NH2 , (4.14)
● 2'-OMe-4'-NH2 , (4.15)
○ 2'-OMe-5'-NH2 , (4.16)
100
%
growth
inhibition
87
50
0
10-1
100
101
Dose (µg ml-1)

Figure 20

Agents of Table 11 : cytotoxicity in the the dark

□ 4'-N_3 , (4.20)

● 3'-N_3 , (4.21)

■ 2'-OMe-4'-N_3 , (4.22)

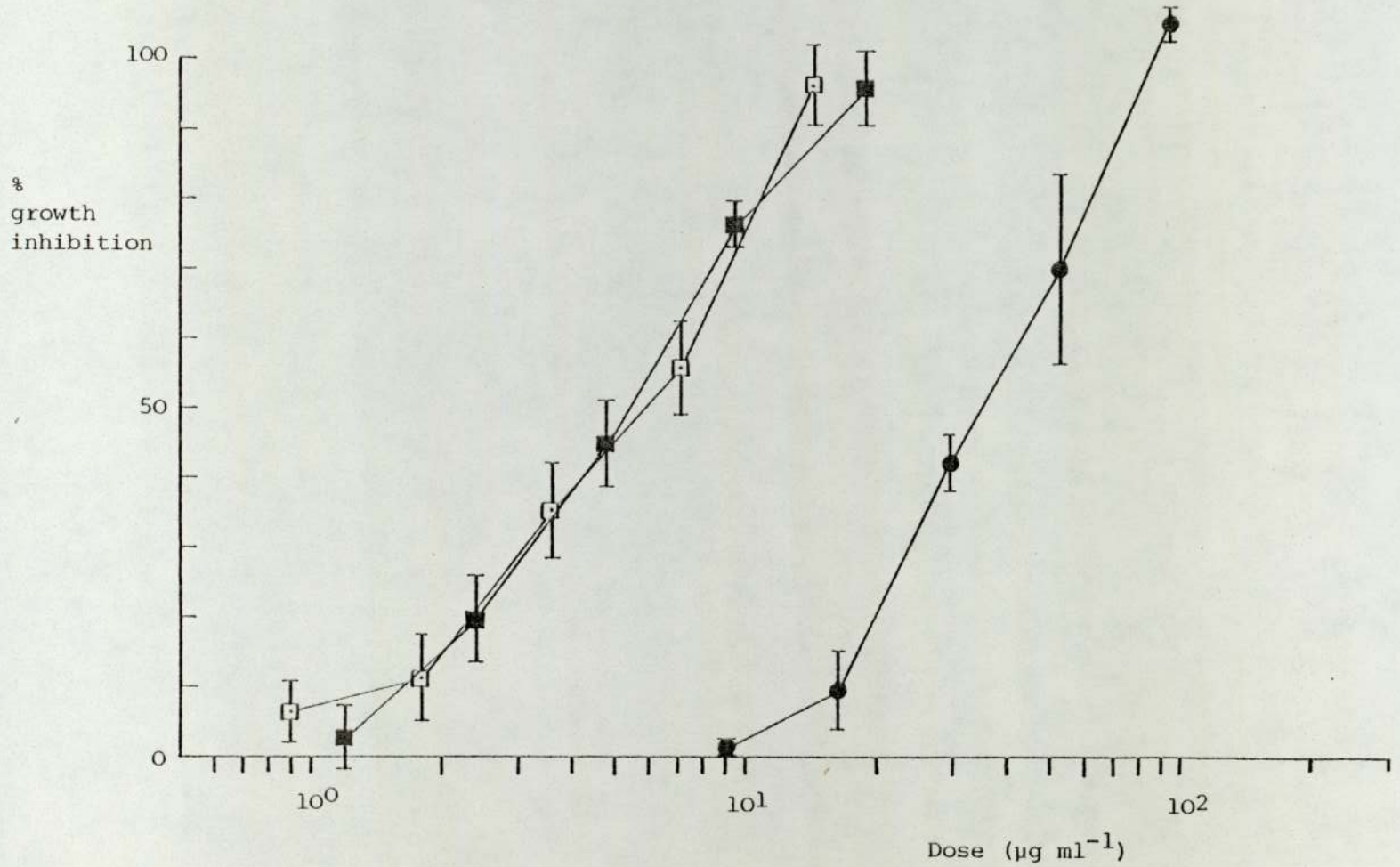

Figure 21

Agents of Table 11 : cytotoxicity in the dark

○ 4-Azidobenzenesulphonamide, (7.5)

◇ 5-Sulphonamido-3H-azepin-2(1H)-one, (7.7)

for the cytotoxicity of sulphanilamide (7.6), see Table 25

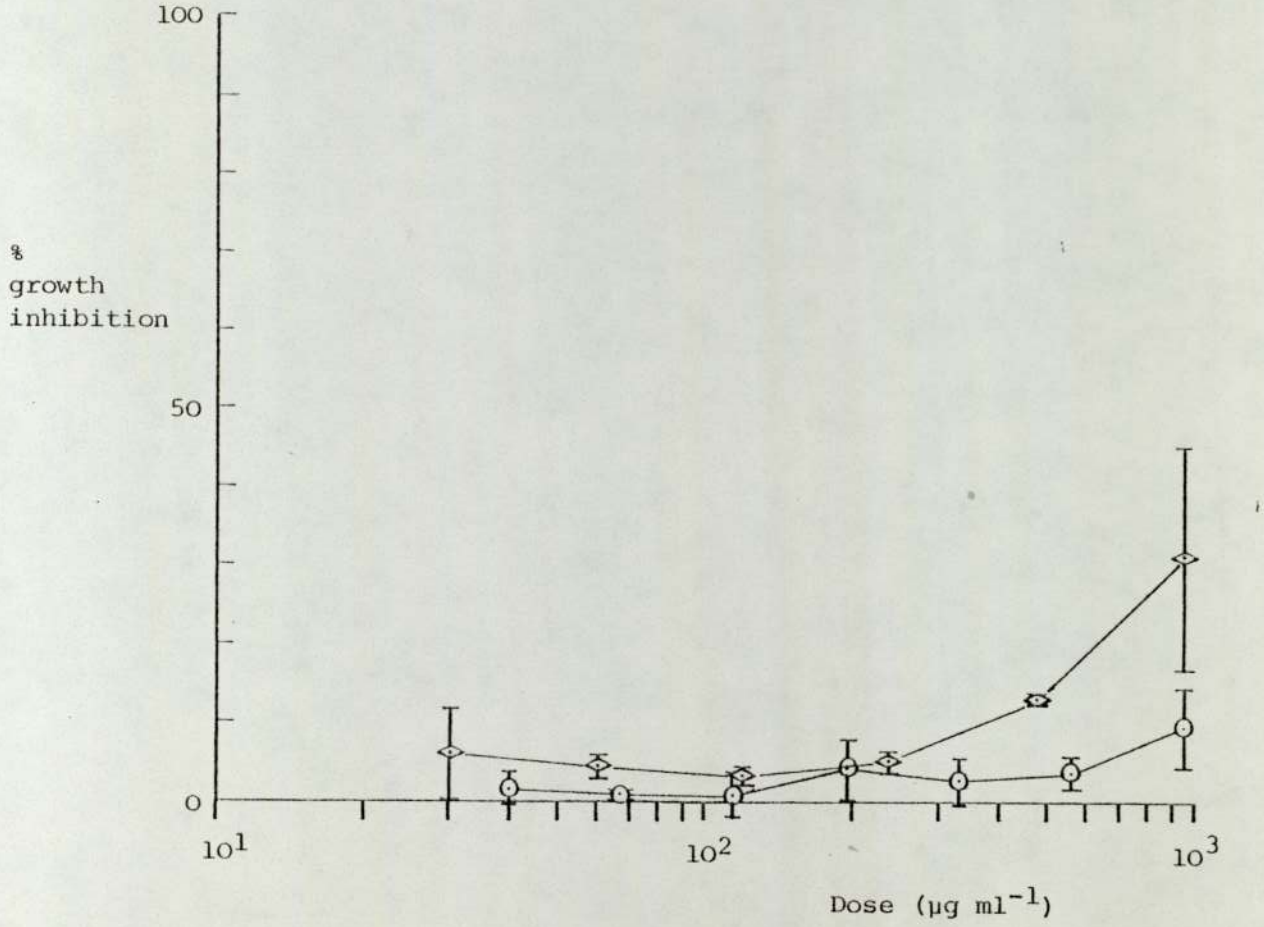

Figure 22 Agents of Table 11 : cytotoxicity in the dark

O 2'-OMe-4'-$NHSO_2Me$, (2.18)

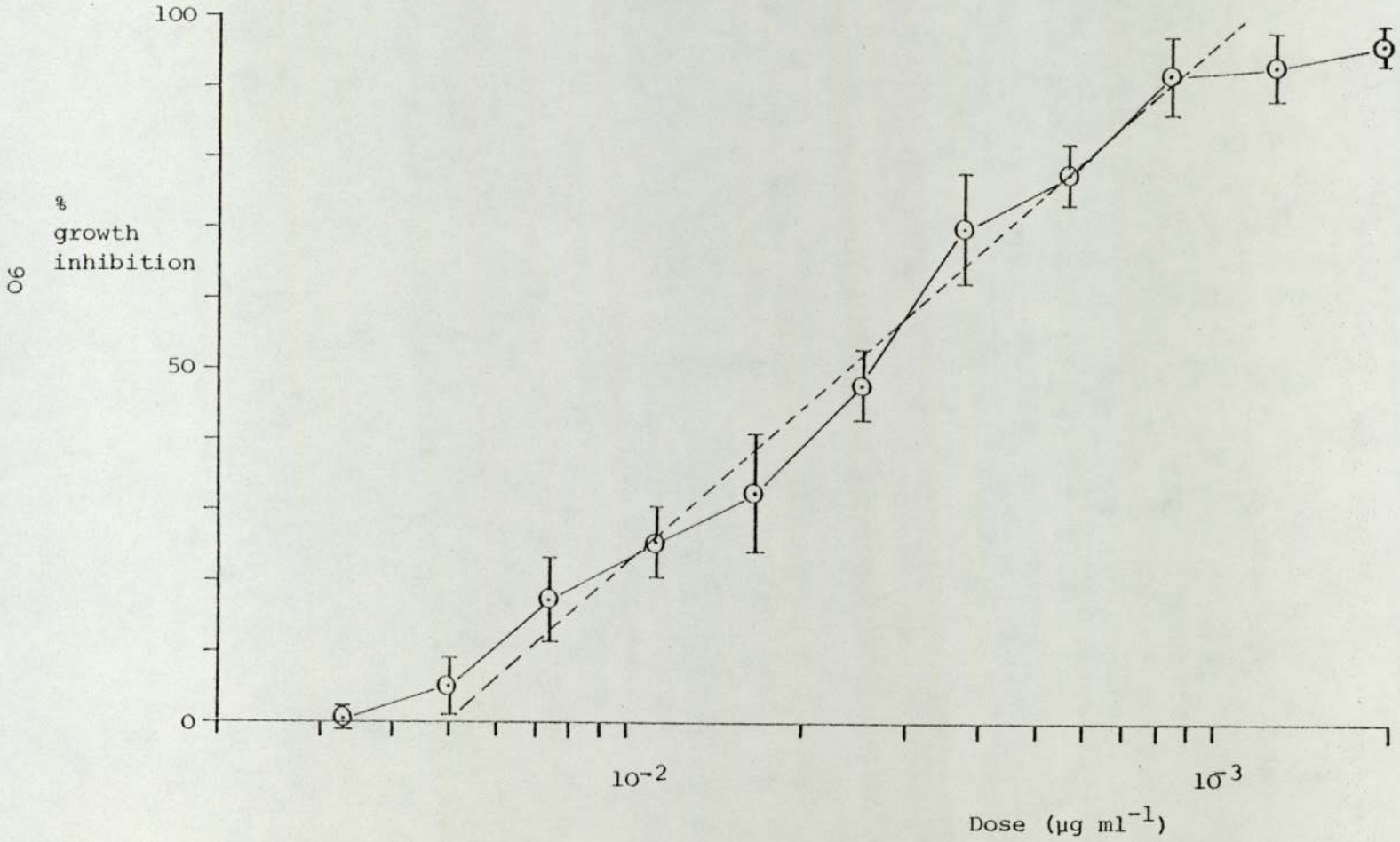

Figure 23 Agents of Table 11 : cytotoxicity in the dark

O Doxorubicin, (7.2)

● Daunorubicin, (7.3)

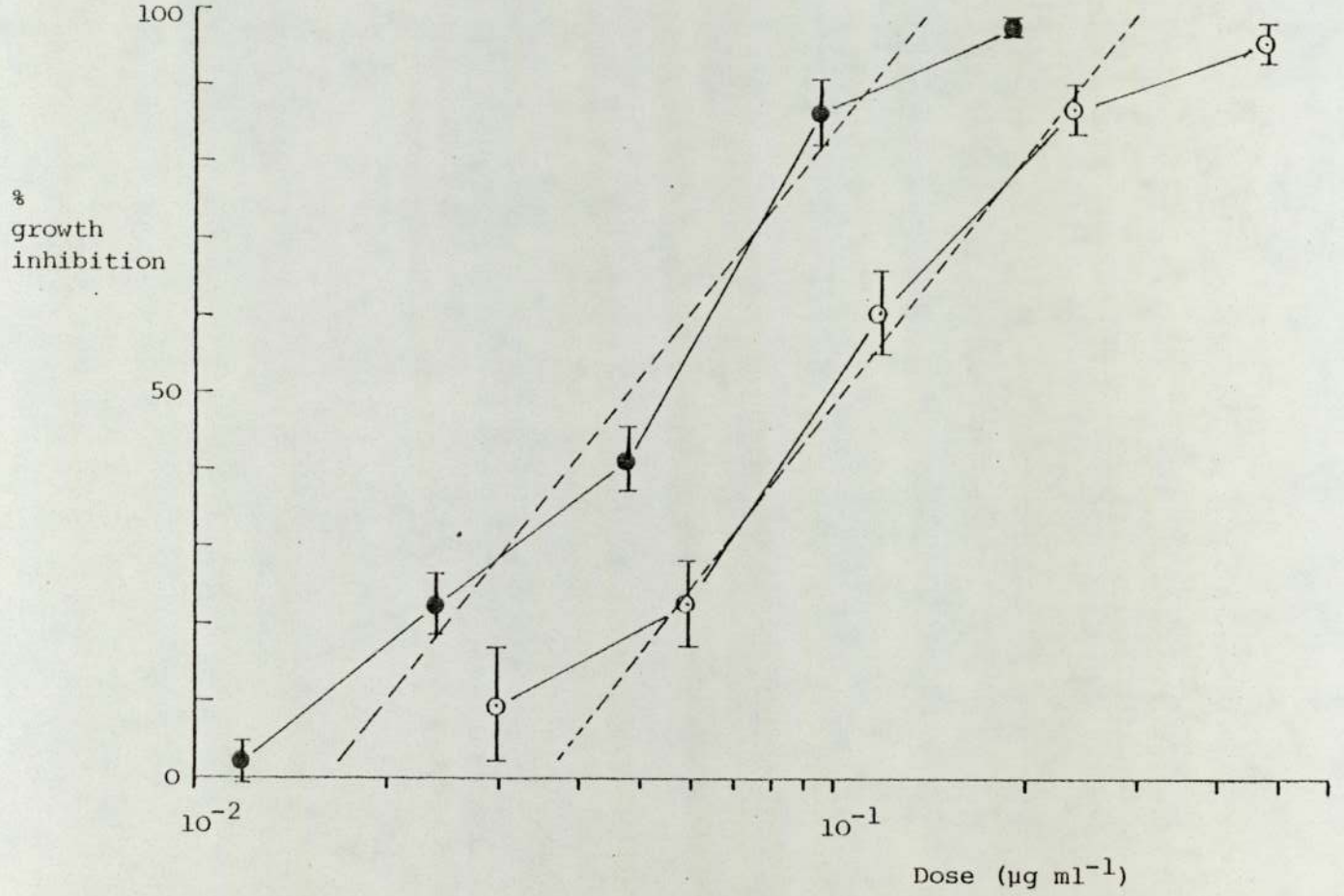

aqueous cell culture medium and often precipitated from the medium during incubation with L1210 cells. The low solubility of these compounds might cast doubt on the validity of their cytotoxicity results since the varying degree of micro-precipitation during incubation would alter their concentrations.

Amino compounds (4.14) - (4.16) were freely soluble in the cell culture medium. The two *p*-amino compounds (4.14) and (4.15) gave similar dose-response characteristics whereas the m-isomer (4.16) was less potent (Figure 19). This potency difference was also found with the azido compounds (4.20) - (4.22) where the two *p*-azido derivatives exhibited almost identical dose-response relationships and the *m*-isomer was again less toxic (Figure 20). Similar observations were evident with the *in vivo* antitumour activities of some of these compounds. The *p*-amino derivative (4.14) was found to be more active than its *m*-amino counterpart in the *in vivo* L1210 screening system[80]. The *p*-azido derivative (4.20) was shown to be marginally active *in vivo* against mouse P388 lymphocytic leukaemia (T/C = 125 at 50 $mgKg^{-1}$) but the *m*-azido compound (4.21) was inactive at the same dose[148].

The azido functions of the substituted anilinoacridines (4.20)-(4.22) themselves were probably not responsible for cytotoxicity *per se* since a model azide, 4-azidobenzenesulphonamide (7.5) showed very low toxicity in the present studies (Figure 21). On the other hand, *m*-AMSA (2.18) —— a known antitumour anilino-acridine which had been proposed to possess an intercalative mode of action[86-88] —— showed high cytotoxicity with high potency (Figure 22). Indeed, other known antitumour agents which are allegedly intercalating agents[149-150] such as doxorubicin (7.2)

and daunorubicin (7.3) also elicited high potent cytotoxicity (Figure 23).

Sulphanilamide (7.6), the metabolic reduction product of azidobenzenesulphonamide[151], and the azepinone (7.7), the major photolytic product[152], were both found to be of low toxicity (Figure 21). These compounds will be discussed in a later section.

7.2 Photosensitizing effect of azido compounds

The aims of the present work were stated in Chapter 3. It was proposed that the anilinoacridinium structure could serve as a carrier of an azido function to the immediate vicinity of a vulnerable target in cells——possibly the nucleic acids. Upon irradiation of cells which had been treated with these azidoanilinoacridines, highly reactive nitrene species might be generated to react covalently and disorganise the nucleic acids. The cytotoxicity of these azidoanilinoacridines and the reference azide, 4-azidobenzenesulphonamide (7.5) in the dark has already been discussed in Section 7.1; the potentiation of the cytotoxic effects of these azides by irradiation are now described. The experimental results are summarised in Tables 27-30 and presented graphically in Figures 24-27.

These results indicate that radiation enhances cytotoxicity in all cases, but the very low toxicity of (7.5) in the dark compared with its high toxicity in light (Figure 27) stimulated the investigation of the cytotoxicity of the photolysis products of these azides generated *in situ* in RPMI cell culture medium. If the cytotoxic species was a short-lived nitrene intermediate it could either react with a cellular component or react with

Table 27 Cytotoxicity of agent (4.20) with irradiation

Dose ($\mu g\ ml^{-1}$)	% inhibition			mean	S.D.
1.43	88.8	99.8	96.4	95.0	5.6
7.1×10^{-1}	71.3	79.2	68.3	72.9	5.6
3.6×10^{-1}	48.0	53.0	44.6	48.5	4.2
1.8×10^{-1}	9.5	10.1	18.4	12.7	5.0
9.0×10^{-2}	5.4	8.7	7.6	7.2	1.7

$ID_{80} = 9.0 \times 10^{-1}\ \mu g\ ml^{-1}$

$ID_{50} = 4.2 \times 10^{-1}$

$ID_{20} = 1.96 \times 10^{-1}$

Table 28 Cytotoxicity of agent (4.21) with irradiation

Dose ($\mu g\ ml^{-1}$)	% inhibition			mean	S.D.
1.43×10^{1}	100.2	99.6	100.8	100.2	0.6
7.14	95.0	87.8	98.9	93.9	5.6
3.60	54.5	48.3	65.1	56.0	8.5
1.80	24.3	29.9	20.7	25.0	4.6
0.89	4.1	9.5	2.1	5.2	3.8

$ID_{80} = 5.5\ \mu g\ ml^{-1}$

$ID_{50} = 3.0$

$ID_{20} = 1.67$

Table 29 Cytotoxicity of agent (4.22) with irradiation

Dose ($\mu g\ ml^{-1}$)	% inhibition			mean	S.D.
3.8	97.4	94.1	96.8	96.1	1.8
1.9	79.6	69.3	78.0	75.6	5.5
9.5×10^{-1}	46.2	34.5	39.3	40.0	5.9
4.8×10^{-1}	21.7	19.2	12.6	17.8	4.7
2.4×10^{-1}	17.2	3.6	9.5	10.1	6.8

$ID_{80} = 2.2\ \mu g\ ml^{-1}$

$ID_{50} = 1.09$

$ID_{20} = 5.3 \times 10^{-1}$

Table 30 Cytotoxicity of agent (7.5) with irradiation

Dose ($\mu g\ ml^{-1}$)	% inhibition			mean	S.D.
9.52×10^{1}	94.5	98.9	96.1	96.5	2.2
6.35×10^{1}	86.9	98.7	92.4	92.7	5.9
4.23×10^{1}	70.6	84.6	76.2	77.1	7.0
2.82×10^{1}	58.3	68.6	63.4	63.4	5.2
1.88×10^{1}	40.1	46.2	34.3	40.2	6.0
1.25×10^{1}	23.9	29.9	14.3	22.7	7.9
8.4	9.2	19.7	16.5	15.1	5.4
5.6	1.3	6.5	3.8	3.9	2.6
3.7	-1.6	5.6	0.9	1.6	3.7

$ID_{80} = 4.34 \times 10^{1}\ \mu g\ ml^{-1}$

$ID_{50} = 2.26 \times 10^{1}$

$ID_{20} = 1.17 \times 10^{1}$

Figure 24

Agent 4'-N_3 , (4.20) of Table 11

● with irradiation

O kept in the dark

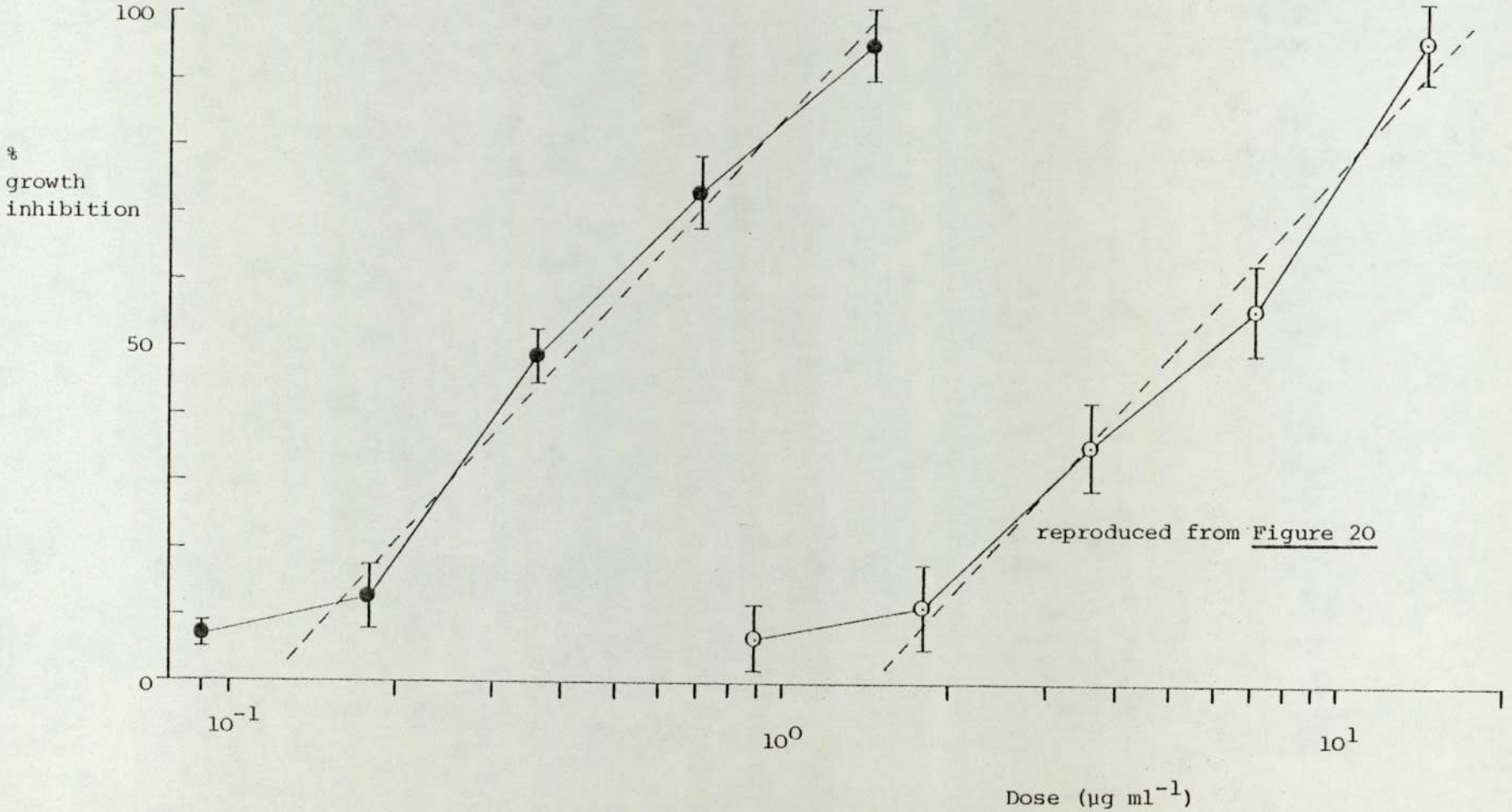

Figure 25

Agent 3'-N_3 , (4.21) of Table 11

● with irradiation

○ kept in the dark

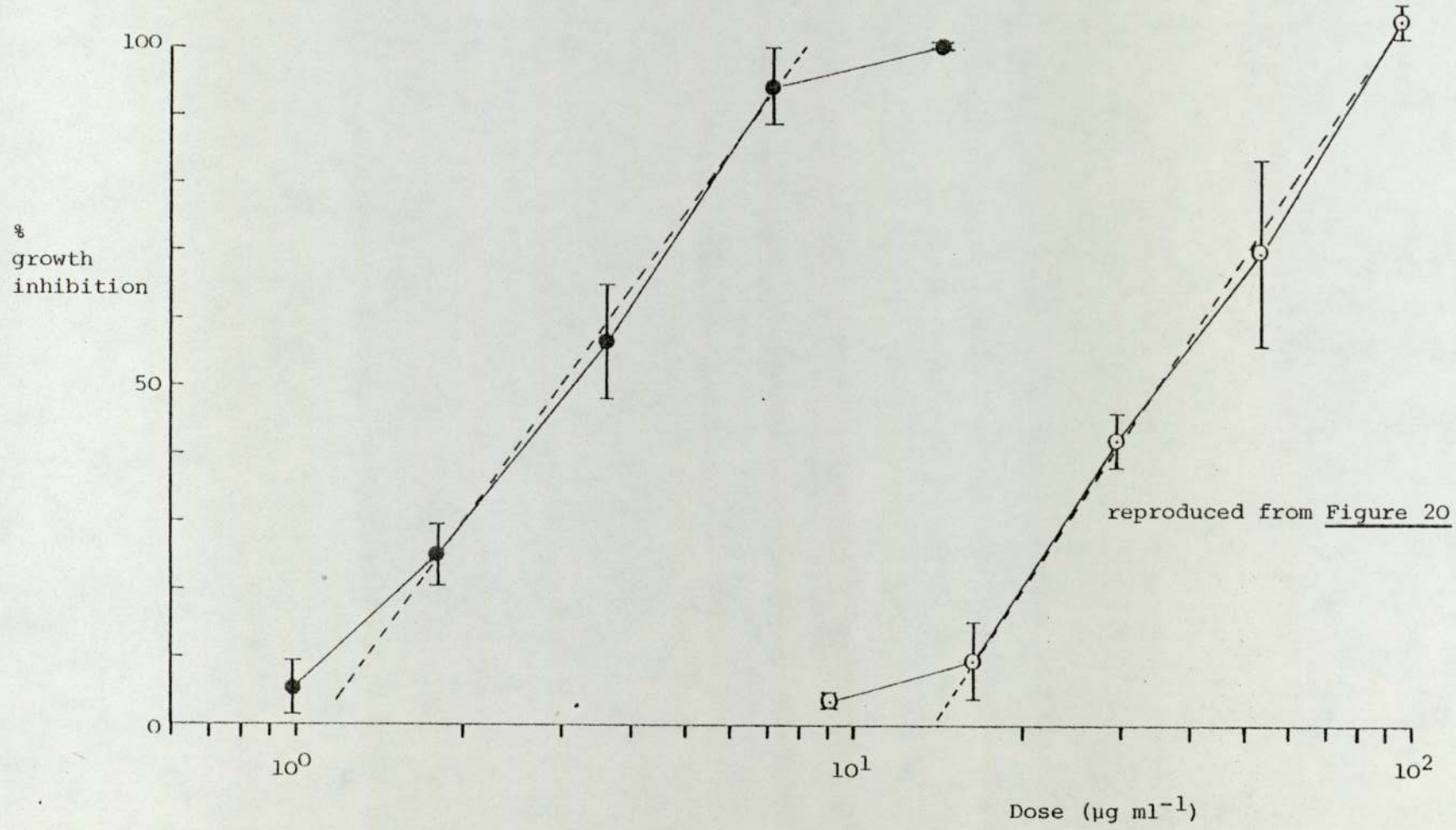

Figure 26 Agent 2'-OMe-4'-N_3 , (4.22) of Table 11

● with irradiation

O kept in the dark

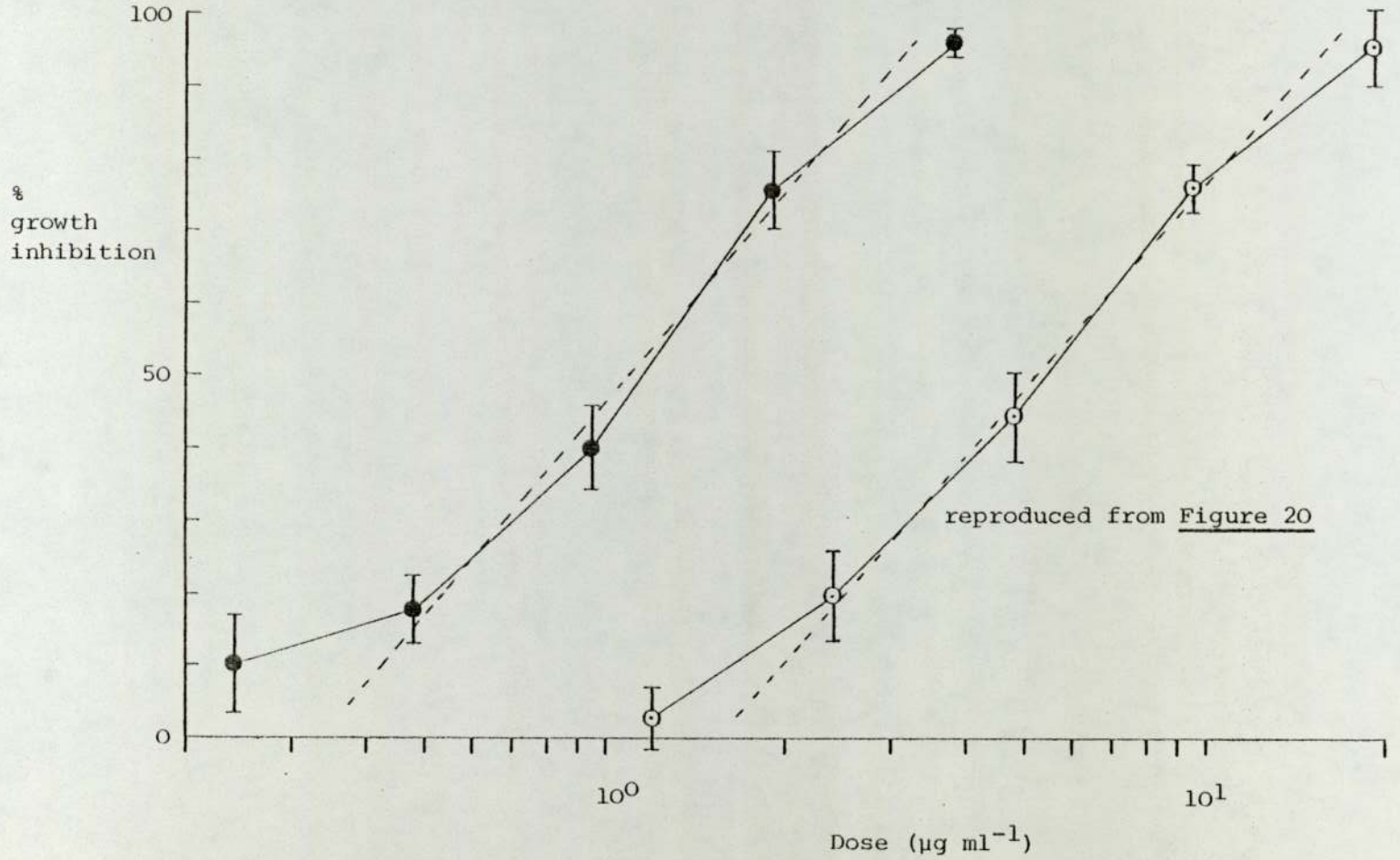

Figure 27

Agent 4-azidobenzenesulphonamide (7.5) of Table 11

● with irradiation

O kept in the dark

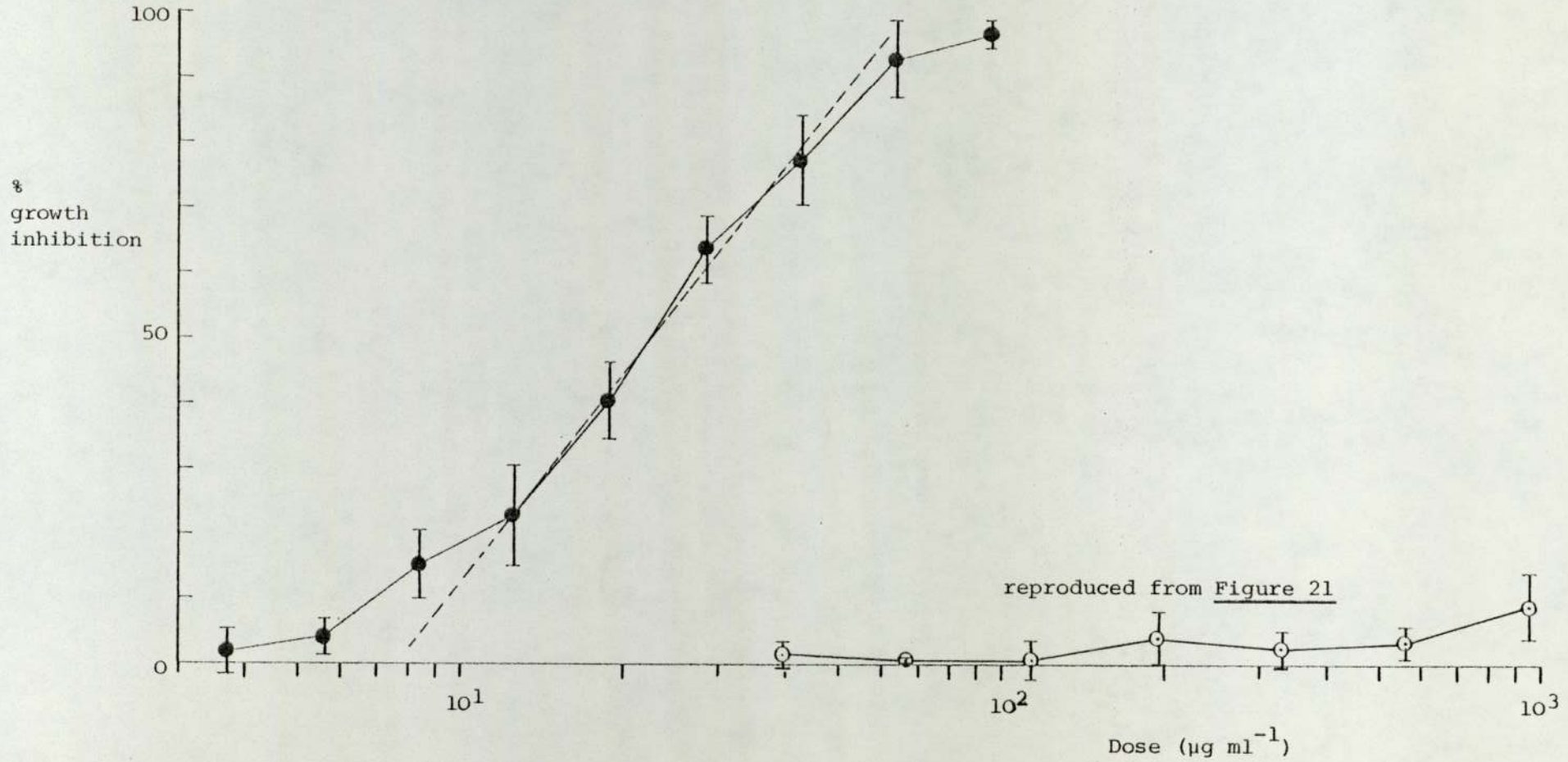

RPMI medium components. Photolyses carried out in RPMI medium in the absence of cells could only allow the latter reaction to occur. An investigation of the cytotoxicity of these reaction products would provide information to show whether the overall cytotoxic effect was due to (stable) photo-products or (short-lived) reactive intermediates. Details of these experiments are given in the Experimental section, their results are reported in Tables 31-38 and presented graphically in Figures 28-31.

The 4'-azide (4.20) showed cytotoxicity with an ID_{80} of 10.90 μg ml^{-1} (see Figure 24), but upon irradiation of a cell culture treated with this compound, the ID_{80} was lowered by over one log-dose difference to 0.90 μg ml^{-1}. However when azide (4.20) was first photolysed in RPMI medium before introducing the L1210 cells, the cytotoxicity of the photolysate was found to be lower than the parent azide with irradiation (Figure 28). This was probably due to incomplete photolysis of the azide during the 5 minutes in the RPMI medium as suggested by the further increase in cytotoxicity when the cell cultures treated with the photolysate were further irradiated. These results implied that cytotoxicity of this azide with irradiation was at least partially due to stable photolysis products.

Greater cytotoxicity enhancement was observed with cell cultures photo-irradiated with the 3'-azide (4.21) as shown in Figure 25: similar investigation of the cytotoxicity of the photolysate of this azide in RPMI medium (Figure 29) showed once again that the photo-products were cytotoxic, but upon further irradiation of the cell cultures treated with the photolysate only a slight increase in cytotoxicity was observed. Similar results were obtained with the 2'-methoxy-4'-azide (4.22) which

Table 31 Cytotoxicity of products of (4.20) generated *in situ* from photolysis in RPMI medium

Dose ($\mu g\ ml^{-1}$)	% inhibition			mean	S.D.
4.76	95.5	94.6	89.0	93.0	3.5
2.38	80.4	72.0	65.3	72.6	7.6
1.20	43.1	38.5	34.3	38.6	4.4
6.0×10^{-1}	9.0	11.6	3.7	8.1	4.0
3.0×10^{-1}	1.9	0.4	-1.8	0.17	1.9

$ID_{80} = 2.8\ \mu g\ ml^{-1}$

$ID_{50} = 1.5$

$ID_{20} = 7.8 \times 10^{-1}$

Table 32 Cytotoxicity of products of (4.20) generated *in situ* from photolysis in RPMI medium with further irradiation during the presence of L1210 cells

Dose ($\mu g\ ml^{-1}$)	% inhibition			mean	S.D.
4.76	99.0	98.4	99.9	99.1	0.8
2.38	93.3	96.6	99.7	96.5	3.2
1.20	78.0	82.1	76.1	78.7	3.1
6.0×10^{-1}	44.4	56.5	58.3	53.1	7.6
3.0×10^{-1}	13.7	23.4	26.6	21.2	6.7

$ID_{80} = 1.2\ \mu g\ ml^{-1}$

$ID_{50} = 5.9 \times 10^{-1}$

$ID_{20} = 2.8 \times 10^{-1}$

Table 33 Cytotoxicity of products of (4.21) generated *in situ* from photolysis in RPMI medium

Dose ($\mu g\ ml^{-1}$)	% inhibition			mean	S.D.
2.86×10^{1}	96.7	94.9	98.5	96.7	1.8
1.90×10^{1}	69.1	81.1	74.6	74.9	0.6
1.27×10^{1}	44.3	48.8	52.7	48.6	4.2
8.5	28.7	29.8	29.8	29.4	0.6
5.6	15.5	19.0	11.3	15.3	3.9
3.8	2.2	5.2	2.2	3.2	1.7
2.5	-1.3	2.8	1.0	0.83	2.1

$ID_{80} = 2.26 \times 10^{1}\ \mu g\ ml^{-1}$

$ID_{50} = 1.22 \times 10^{1}$

$ID_{20} = 6.6$

Table 34 Cytotoxicity of products of (4.21) generated *in situ* from photolysis in RPMI medium with further irradiation during the presence of L1210 cells

Dose ($\mu g\ ml^{-1}$)	% inhibition			mean	S.D.
2.86×10^{1}	101.9	100.6	99.4	100.6	1.4
1.90×10^{1}	89.1	94.7	92.3	92.0	2.8
1.27×10^{1}	66.0	76.2	69.2	70.5	5.2
8.5	47.2	54.7	48.5	50.1	4.0
5.6	25.4	34.1	29.6	29.7	4.4
3.8	12.0	6.5	17.9	12.1	5.7
2.5	3.3	9.4	7.6	6.8	3.1

$ID_{80} = 1.56 \times 10^{1}\ \mu g\ ml^{-1}$

$ID_{50} = 8.4$

$ID_{20} = 4.5$

Table 35 Cytotoxicity of products of (4.22) generated *in situ* from photolysis in RPMI medium

Dose ($\mu g\ ml^{-1}$)	% inhibition			mean	S.D.
7.62	94.0	99.2	89.2	94.1	5.0
3.81	74.3	66.8	74.6	71.9	4.4
1.90	51.9	40.2	45.4	45.8	5.9
9.5×10^{-1}	26.5	14.9	21.8	21.1	5.8
4.8×10^{-1}	0.2	2.0	5.8	2.7	2.9

$ID_{80} = 4.8\ \mu g\ ml^{-1}$

$ID_{50} = 2.1$

$ID_{20} = 9.3 \times 10^{-1}$

Table 36 Cytotoxicity of products of (4.22) generated *in situ* from photolysis in RPMI medium with further irradiation during the presence of L1210 cells

Dose ($\mu g\ ml^{-1}$)	% inhibition			mean	S.D.
7.62	94.3	98.5	93.7	95.5	2.6
3.81	76.9	74.1	73.2	74.7	1.9
1.90	49.4	50.0	39.3	46.2	6.0
9.5×10^{-1}	28.6	13.6	23.3	21.8	7.6
4.8×10^{-1}	5.5	1.9	6.1	4.5	2.3

$ID_{80} = 4.5\ \mu g\ ml^{-1}$

$ID_{50} = 2.0$

$ID_{20} = 9.2 \times 10^{-1}$

Table 37 Cytotoxicity of products of (7.5) generated *in situ* from photolysis in RPMI medium

Dose ($\mu g\ ml^{-1}$)	% inhibition			mean	S.D.
9.52×10^2	21.5	16.4	11.7	16.5	4.9
5.60×10^2	8.9	4.5	2.3	5.2	3.4
3.30×10^2	9.3	2.1	1.1	4.2	4.5
1.94×10^2	10.2	4.8	0.3	5.1	5.0
1.14×10^2	3.6	2.3	-1.2	1.6	2.5
6.7×10^1	-1.8	2.4	-10.4	-3.3	6.5
3.95×10^1	-2.5	-7.6	-13.4	-7.8	5.5
2.32×10^1	-7.4	-11.9	-13.6	-11.0	3.2
1.37×10^1	-9.7	-12.6	-14.5	-12.3	2.4
8.0	-6.8	-12.9	-15.3	-11.7	4.4
4.7	-6.9	-14.2	-20.7	-13.9	6.9

$ID_{80} >> 1 \times 10^3\ \mu g\ ml^{-1}$

$ID_{50} >> 1 \times 10^3$

$ID_{20} > 1 \times 10^3$

Table 38 Cytotoxicity of products of (7.5) generated *in situ* from photolysis in RPMI medium with further irradiation during the presence of L1210 cells

Dose ($\mu g\ ml^{-1}$)	% inhibition			mean	S.D.
9.52×10^2	105.6	104.3	105.2	105.0	0.7
5.60×10^2	106.7	108.9	101.4	105.7	3.9
3.30×10^2	99.7	102.1	100.1	100.6	1.3
1.94×10^2	96.3	99.9	96.7	97.6	2.0
1.14×10^2	83.4	93.4	88.8	88.5	5.0
6.7×10^1	56.5	65.2	74.8	65.5	9.2
3.95×10^1	34.9	49.6	46.5	43.7	7.7
2.32×10^1	21.8	34.7	28.3	28.3	6.5
1.37×10^1	9.7	18.6	17.5	15.3	4.9
8.0	0.3	12.8	6.9	6.7	6.3
4.7	2.4	13.2	5.6	7.1	5.5

$ID_{80} = 1.045 \times 10^2\ \mu g\ ml^{-1}$

$ID_{50} = 4.44 \times 10^1$

$ID_{20} = 1.89 \times 10^1$

Figure 28

Agent 4'-N_3 , (4.20) of Table 11

O cytotoxicity of *in situ* photolysis-products in RPMI medium

● cytotoxicity of *in situ* photolysis-products in RPMI medium with a further 5 minutes irradiation in the presence of the L1210 cells

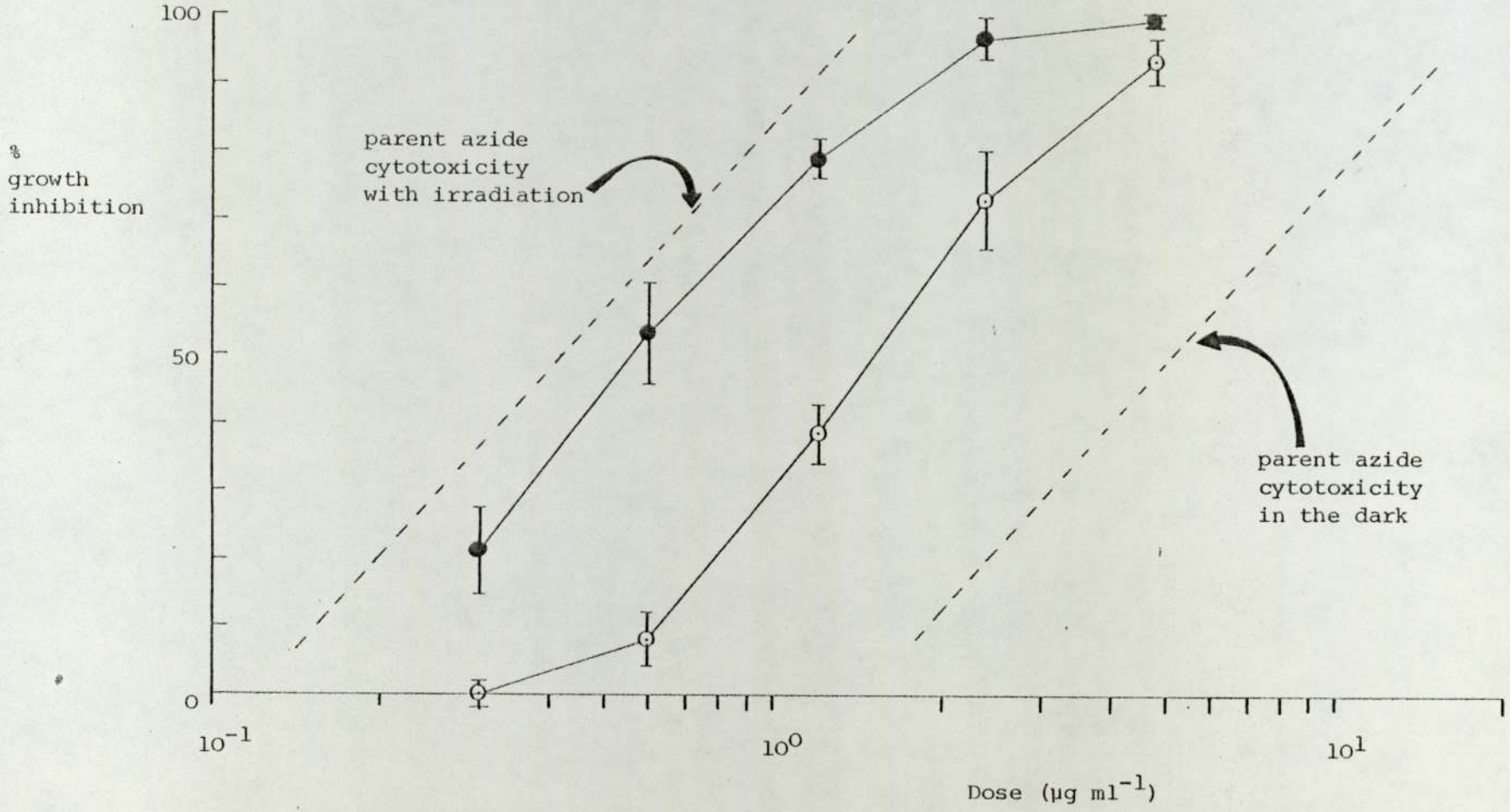

Figure 29

Agent 3'-N_3 , (4.21) of Table 11

O cytotoxicity of *in situ* photolysis-products in RPMI medium

● cytotoxicity of *in situ* photolysis-products in RPMI medium with a further 5 minutes irradiation in the presence of the L1210 cells

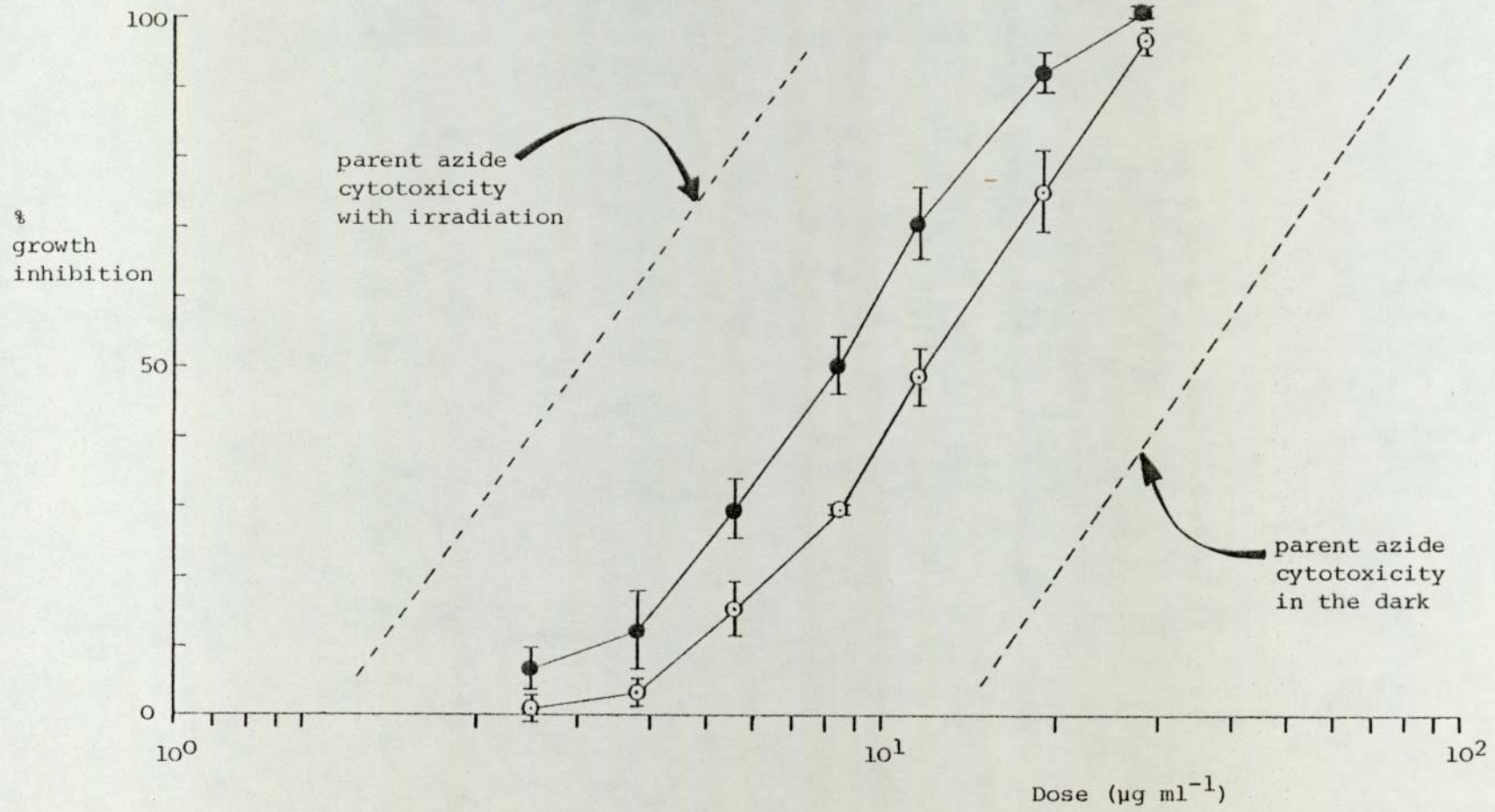

Figure 30

Agent 2'-OMe-4'-N_3 , (4.22) of Table 11

O cytotoxicity of *in situ* photolysis-products in RPMI medium

● cytotoxicity of *in situ* photolysis-products in RPMI medium with a further 5 minutes irradiation in the presence of the L1210 cells

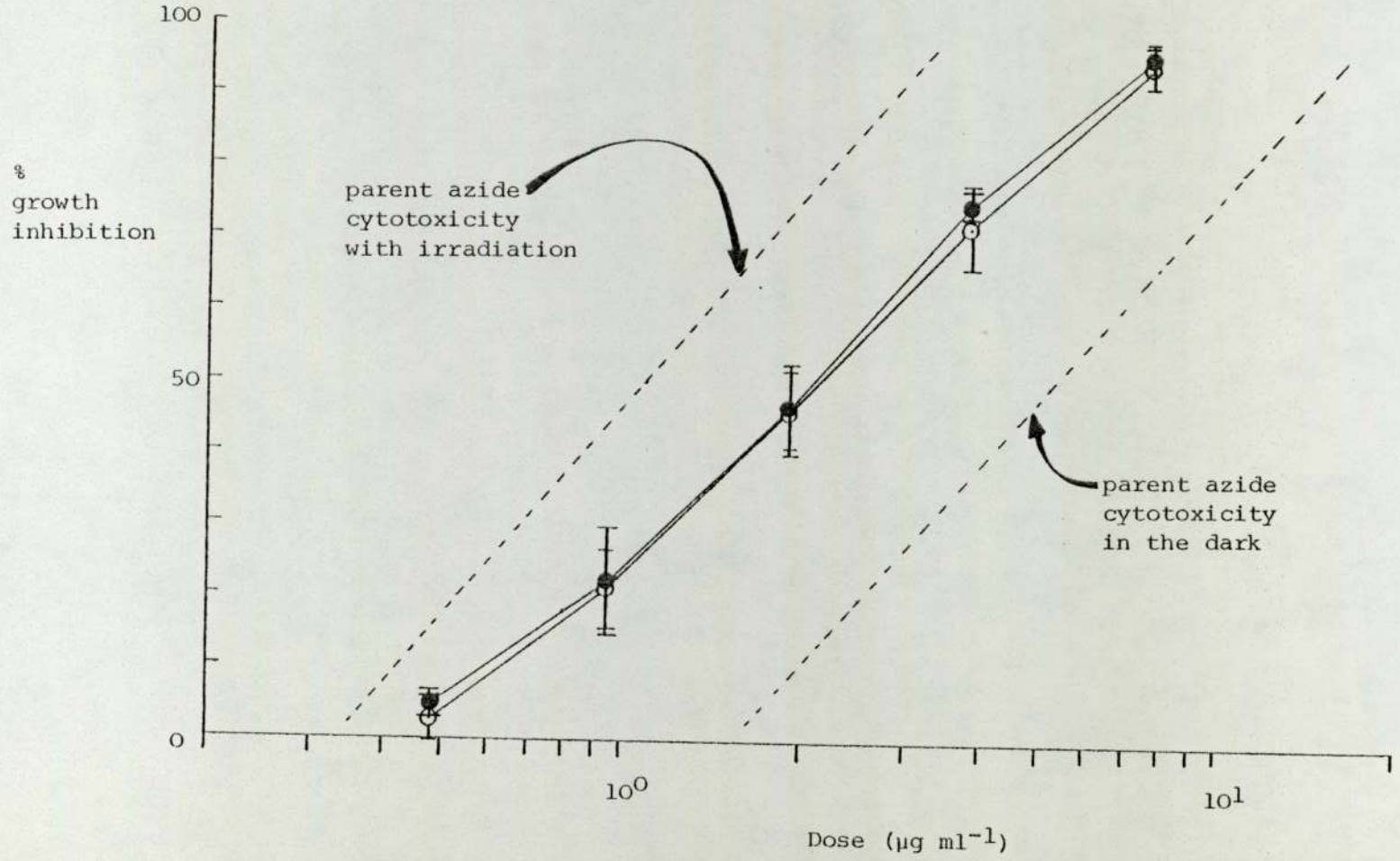

Figure 31

Agent 4-azidobenzenesulphonamide (7.5) of Table 11

○ cytotoxicity of *in situ* photolysis-products in RPMI medium

● cytotoxicity of *in situ* photolysis-products in RPMI medium with a further 5 minutes irradiation in the presence of the L1210 cells

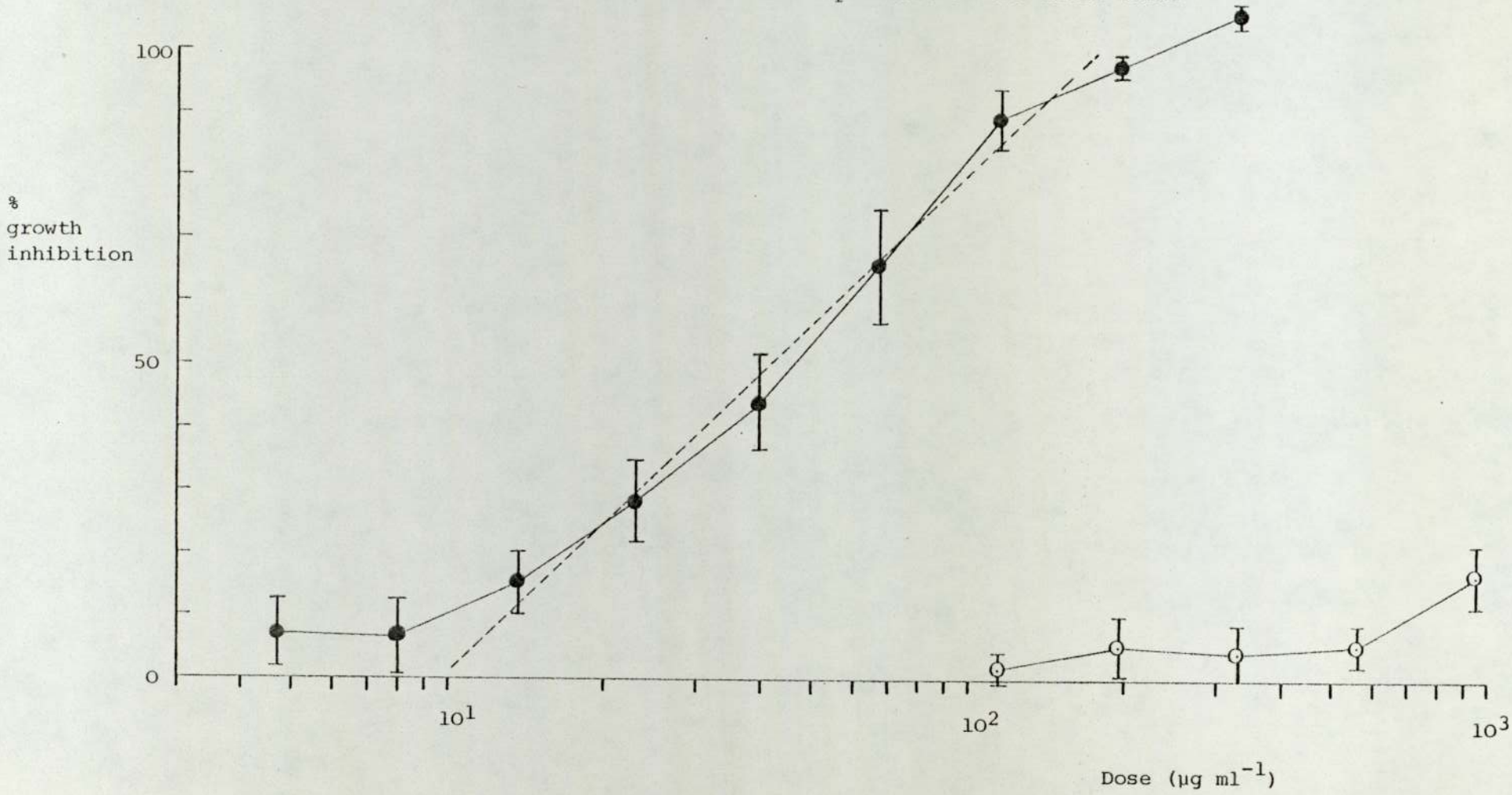

are presented in Figures 26 and 30 except that this compound afforded a lesser degree of cytotoxicity potentiation by irradiation.

The fact that the RPMI photolysates of the azides (4.20) - (4.22) were less toxic compared with the high cytotoxicity of the corresponding azides in light (see Figures 28-30) suggested that the overall cytotoxicity might be partly due to direct reactions of reactive (nitrene) intermediates with cellular components resulting in cell death. In order to investigate this hypothesis, a non-toxic model azide which afforded non-toxic photo-products was required. Then it should be possible to establish if short-lived nitrene species were indeed implicated in cytotoxicity.

The compound 4-azidobenzenesulphonamide (7.5) seemed to satisfy the mentioned requirements since this azide in the dark was non-toxic (Figure 21) and its main photolysis product in an aqueous medium —— 5-sulphonamido-3H-azepin-2(1H)-one (7.7) —— also exhibited low toxicity (Figure 21). When L1210 cells treated with azide (7.5) were irradiated during incubation, high cytotoxicity was apparent (Figure 27): but, if this azide was pre-photolysed in RPMI medium before treating L1210 cells with the photolysate low cytotoxicity was evidenced (Figure 31). However if these cell cultures in the photolysate were further irradiated, high cytotoxicity was again observed. Therefore only when irradiation was applied did this azide show high toxicity.

7.3 Photosensitization/irradiation time relationship of azido compounds

It has been established in Section 7.2 that irradiation of cells treated with azido compounds afforded photosensitization.

If the cytotoxic species was indeed photogenerated, the degree of photosensitization should be a function of irradiation time. A dose for each one of the azido compounds was chosen such that in the dark this dose of the agent gave a low % growth inhibition, but the same dose exhibited a high % growth inhibition when the treated cell cultures were irradiated. This dose (in $\mu g\ ml^{-1}$) was called Z and was selected from Figures 24-27 to suit the mentioned criteria. The azide (7.5) allowed the use of three Z values because of its low toxic effect in the dark.

The experimental details are described in the Experimental section and the results in Tables 39-42 and are presented graphically in Figures 32-35. The irradiation time selected for all the photosensitization experiments in Section 7.2 was 300 seconds. This time was chosen so that the maximum biological response was reached; further irradiation of the azide-treated cell cultures gave no further increase in cytotoxicity until the exponential increase due to damage by prolonged irradiation itself took over (see Chapter 6, Section 6.3). The behaviour of the three azido-anilinoacridines (4.20) - (4.22) demonstrated that the degree of photosensitization was indeed proportional to the irradiation time until a maximum "plateau" level of response was reached. This maximum level of % growth inhibition was characteristic of the particular azide and served as a convenient index of the photo-sensitization ability or potential of that azide (Figures 32-34).

The model azide, 4-azidobenzenesulphonamide (7.5) showed low toxicity in the dark at doses up to $1 \times 10^{3}\ \mu g\ ml^{-1}$, but at $> 1 \times 10^{2}\ \mu g\ ml^{-1}$ in light, this compound elicited 100% growth inhibition of L1210 cell culture (see Figure 27). By employing three Z values, it was interesting to discover (Figure 35) that

Table 39 Photosensitization/irradiation time relationship of agent (4.20) in L1210 cells

Irradiation time (s)	% inhibition			mean	S.D.
0	6.6	12.5	9.8	9.6	3.0
10	29.2	39.7	36.9	35.3	5.4
20	43.0	54.8	49.5	49.1	5.9
30	57.9	67.2	62.0	62.4	4.7
40	65.8	76.2	68.3	70.1	5.4
50	68.6	78.5	76.4	74.5	5.2
60	70.7	84.8	81.3	78.9	7.3
80	83.6	90.3	86.6	86.8	3.4
100	84.2	91.2	88.2	87.9	3.5
150	87.0	93.5	89.1	89.9	3.3
200	87.7	94.9	91.7	91.4	3.6

where Z = 1.43 $\mu g\ ml^{-1}$

Table 40 Photosensitization/irradiation time relationship of agent (4.21) in L1210 cells

Irradiation time (s)	% inhibition			mean	S.D.
0	8.5	10.6	16.2	11.2	4.0
10	24.5	26.1	36.9	29.2	6.7
20	36.8	39.2	48.6	38.0	1.7
30	46.4	50.8	57.1	51.4	5.4
40	54.9	61.2	67.7	61.3	6.4
50	61.4	76.2	76.8	71.5	8.7
60	66.2	76.3	85.5	76.0	9.7
80	77.6	86.4	93.3	85.8	7.9
100	87.5	92.1	98.9	92.8	5.7
150	97.2	100.0	100.3	99.2	1.7
200	99.5	102.1	105.1	102.2	2.8

where Z = 1.43×10^{1} $\mu g\ ml^{-1}$

Table 41 Photosensitization/irradiation time relationship of agent (4.22) in L1210 cells

Irradiation time (s)	% inhibition			mean	S.D.
0	1.19	19.6	4.32	8.4	9.9
10	22.3	22.1	24.2	22.9	1.2
20	25.4	25.9	28.5	26.6	1.7
40	31.5	29.0	36.4	32.3	3.8
60	33.3	36.8	38.9	36.3	2.8
80	36.4	40.1	43.3	39.9	3.5
100	41.7	43.1	44.5	43.1	1.4
140	42.6	44.5	47.3	44.8	2.4
180	45.9	47.6	51.7	48.4	3.0
300	47.6	51.7	52.6	50.6	2.7
720	57.9	62.3	63.4	61.2	2.9

where $Z = 1.43 \times 10^{1}$ µg ml^{-1}

Table 42 Photosensitization/irradiation time relationship of agent (7.5) in L1210 cells

(a) where Z = 9.52×10^{1} µg ml^{-1}

Irradiation time (s)	% inhibition			mean	S.D.
0	6.4	3.8	2.9	4.4	1.8
15	14.9	9.9	1.8	8.9	6.6
30	18.3	23.2	26.6	22.7	4.2
45	27.6	32.8	38.7	33.0	5.6
60	41.8	42.2	41.0	41.7	0.6
90	67.4	64.5	61.2	64.4	3.1
120	81.3	77.6	73.7	77.5	3.8
180	97.5	93.6	93.4	94.8	2.3
300	102.5	101.8	98.9	101.1	1.9

(b) where Z = 2.857×10^{2} µg ml^{-1}

Irradiation time (s)	% inhibition			mean	S.D.
0	14.2	12.3	23.7	16.7	6.1
15	19.6	25.4	32.1	25.7	6.3
30	43.5	47.8	54.7	48.7	5.7
45	62.3	67.4	71.4	67.0	4.6
60	76.9	80.5	82.8	80.1	3.0
90	94.6	95.6	97.0	95.7	1.2
120	99.8	102.7	103.2	101.9	1.8

(c) where Z = 9.524×10^{2} µg ml^{-1}

Irradiation time (s)	% inhibition			mean	S.D.
0	14.5	13.6	16.8	15.0	1.7
15	37.5	33.6	42.9	38.0	4.7
30	69.4	64.2	75.8	69.8	5.8
45	93.4	96.5	88.7	92.9	3.9
60	99.9	99.8	92.6	97.4	4.2
90	99.8	99.7	102.5	100.7	1.6

Figure 32

Photosensitization/irradiation time relationship

Agent 4'-N_3 , (4.20) of Table 11

O Z = 1.43 μg ml^{-1}

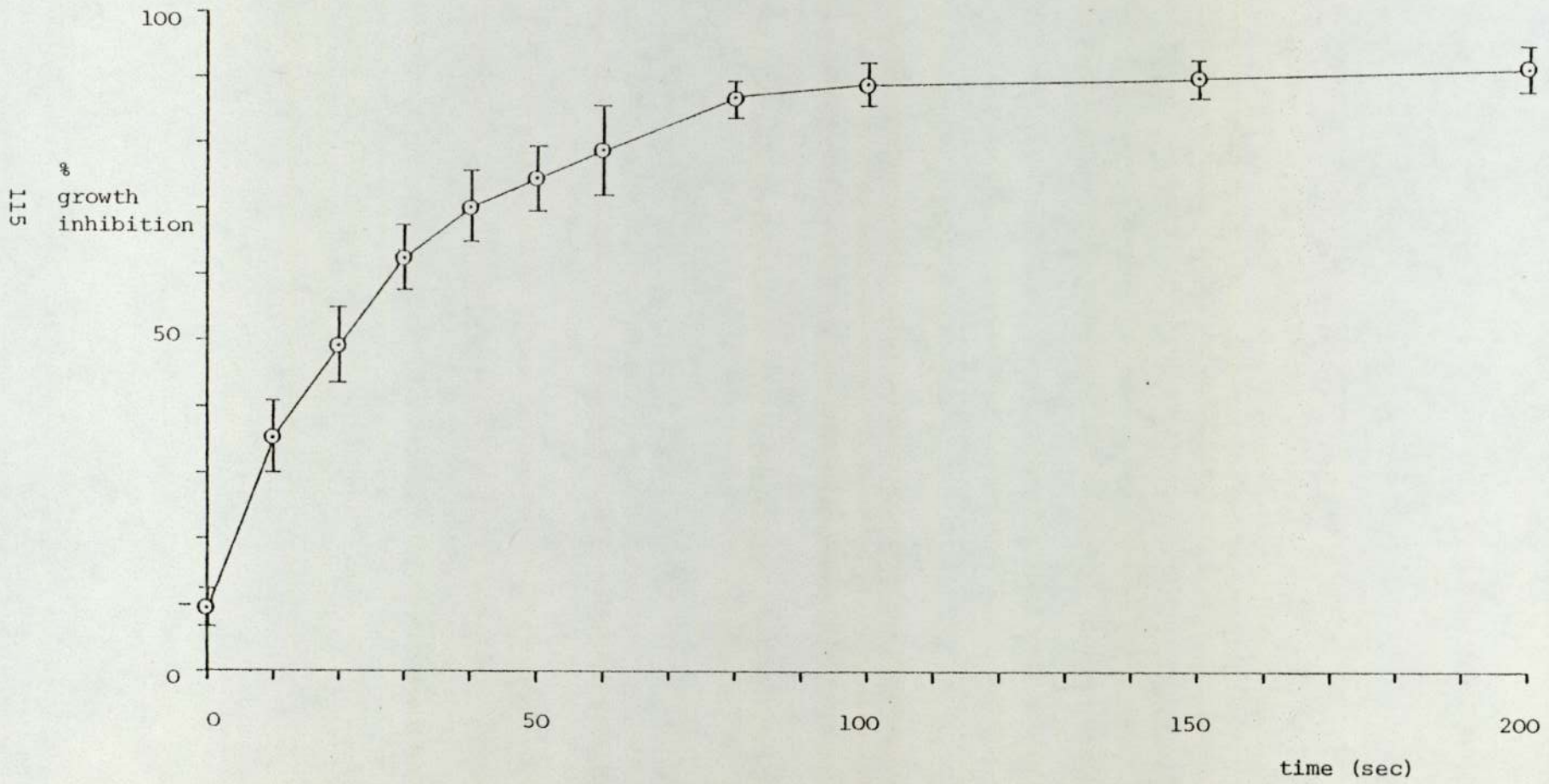

Figure 33

Photosensitization/irradiation time relationship

Agent 3'-N_3 , (4.21) of Table 11

O Z = 14.3 μg ml^{-1}

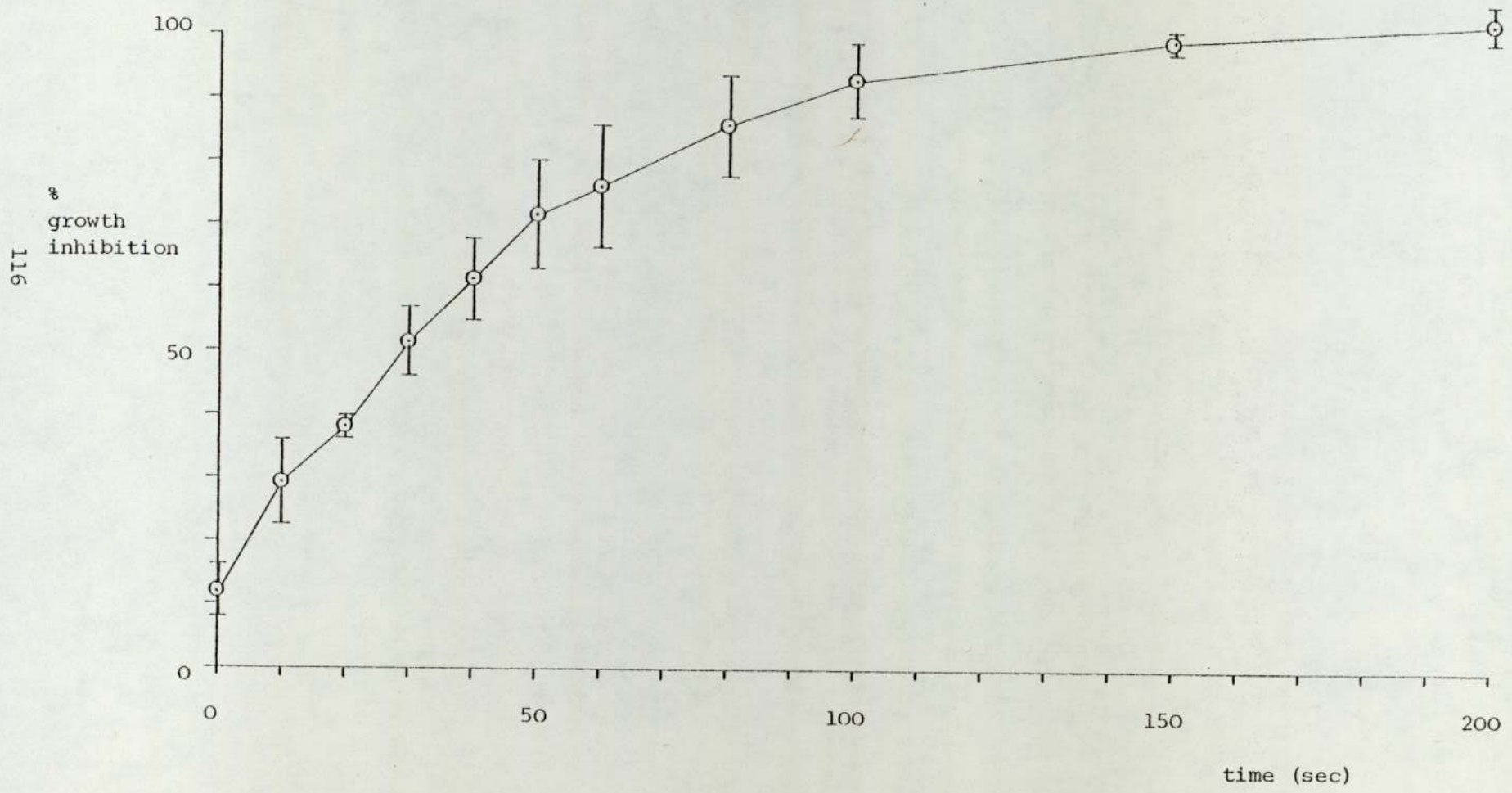

Figure 34

Photosensitization/irradiation time relationship

Agent 2'-OMe-4'-N_3 , (4.22) of Table 11

O Z = 14.3 μg ml^{-1}

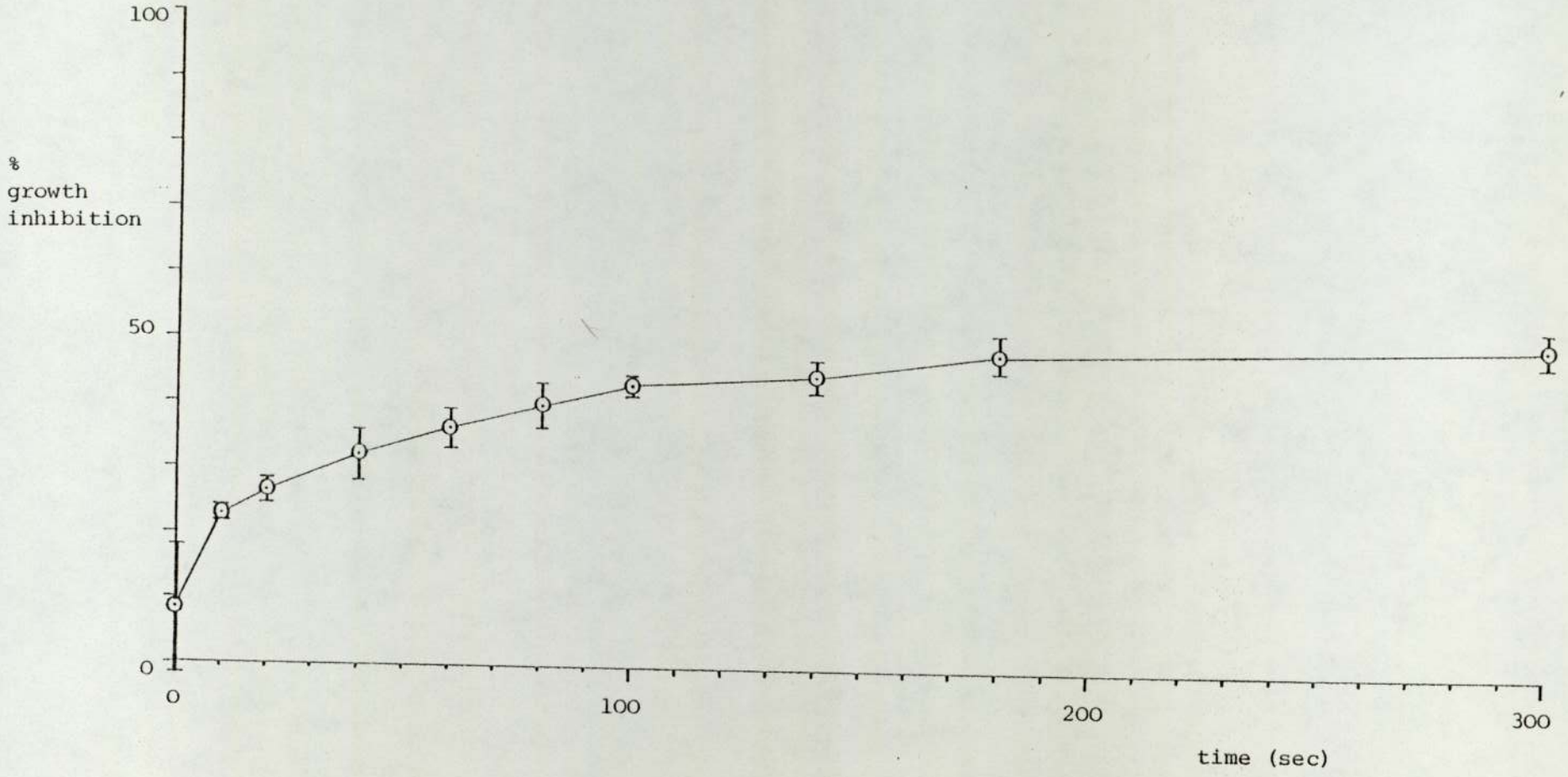

Figure 35

Photosensitization/irradiation time relationship

Agent 4-azidobenzenesulphonamide (7.5) of Table 11

○ Z = 952.4 μg ml^{-1} ; ● Z = 285.7 μg ml^{-1} ;

□ Z = 95.2 μg ml^{-1}

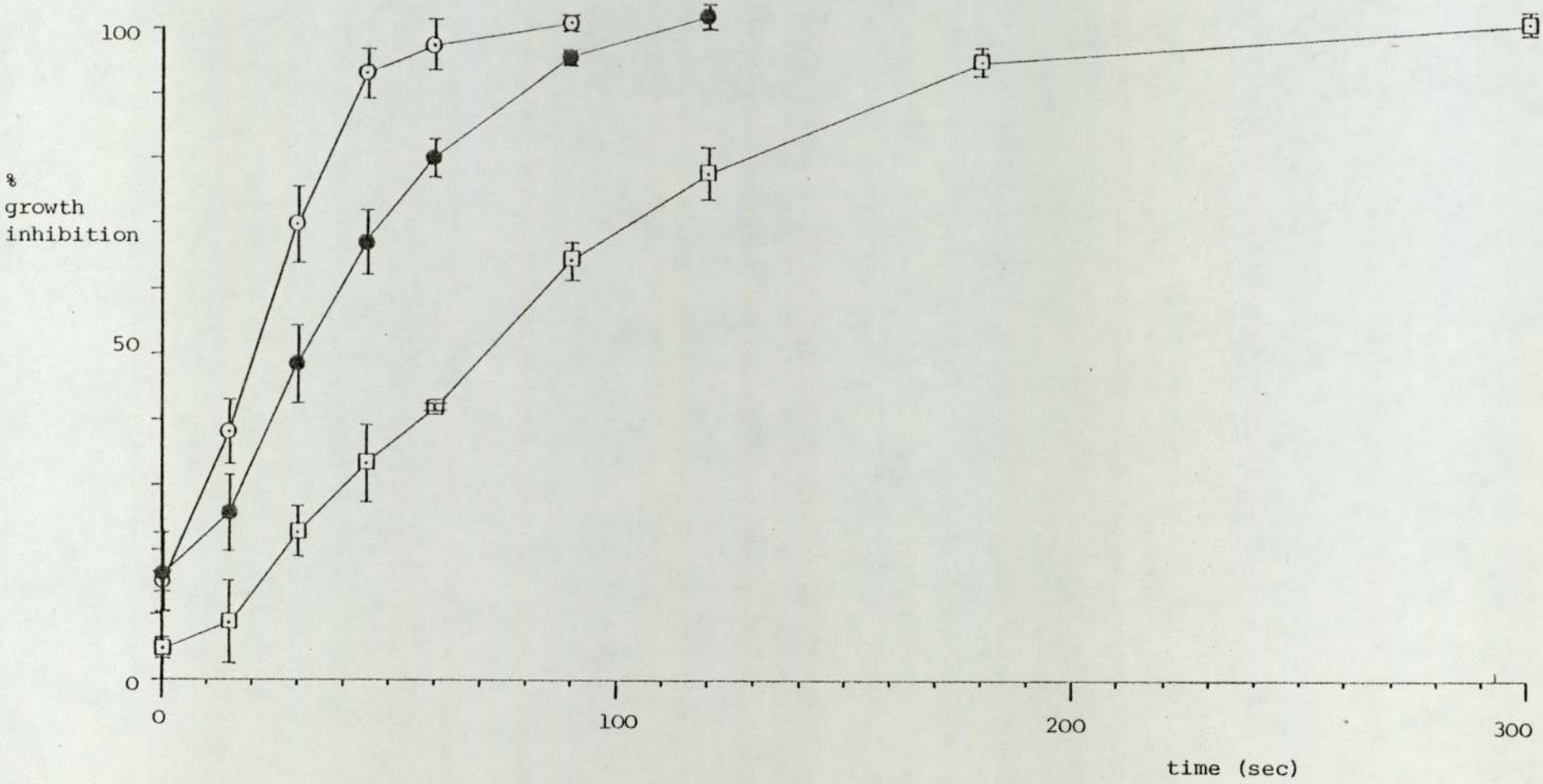

the higher the concentration of this azide in the cell culture being irradiated, the greater the degree and rate of photosensitization. This fact together with the knowledge that the photolysis products of this azide were of low toxicity (see Section 7.2) lent further support to the proposition that a nitrene intermediate was the cytotoxic species.

7.4 A further investigation of the cytotoxicity of the photolysis products of azido compounds

The problem encountered in isolating the photolysis products of azidoanilinoacridines has been outlined in Chapter 5, Section 5.1, and the cytotoxicity of products generated *in situ* in the photolysis of these azides in RPMI medium were discussed in Section 7.2 of this chapter. This present discussion is concerned with the cytotoxicity of the photolysates of azido compounds after prolonged photolysis in Tris buffer. In this pH 7.4 buffer, the photo-decomposition of the azido compounds should be similar to that in a biological environment, but the reaction of the proposed nitrene intermediates would most likely to be that with the solvent, i.e. water.

The azide solutions were photolysed in sealed glass ampoules (which allowed the transmission of 366 nm radiation) for 2 hours. The photolysates were then screened for cytotoxicity. They were also tested for further photoactivated cytotoxicity. Details of the experimental methods are given in the Experimental section and the results are reported in Tables 43-50 and presented graphically in Figures 36-39. The prolonged photolysis time of 2 hours was expected to be adequate to fully decompose the azides. This appeared to be the case with azides (4.20)and (4.22) (Figures 36 and 38), but the photolysate of 3'-azide (4.21) afforded a

Table 43 Cytotoxicity of products of (4.20) generated *in situ* from photolysis in Tris buffer

Dose ($\mu g\ ml^{-1}$)	% inhibition			mean	S.D.
1.91	101.2	98.7	97.0	99.0	2.1
9.5×10^{-1}	89.9	68.3	79.1	79.1	10.8
4.8×10^{-1}	67.2	56.8	45.4	56.5	10.9
2.4×10^{-1}	26.6	19.8	16.5	21.0	5.2
1.2×10^{-1}	13.6	11.5	6.3	10.5	3.8

$ID_{80} = 9.7 \times 10^{-1}\ \mu g\ ml^{-1}$

$ID_{50} = 4.5 \times 10^{-1}$

$ID_{20} = 2.2 \times 10^{-1}$

Table 44 Cytotoxicity of products of (4.20) generated *in situ* from photolysis in Tris buffer with further irradiation during the presence of L1210 cells

Dose ($\mu g\ ml^{-1}$)	% inhibition			mean	S.D.
1.91	99.7	99.2	97.2	98.7	1.3
9.5×10^{-1}	93.9	82.3	77.6	84.6	8.4
4.8×10^{-1}	62.7	62.3	52.1	59.0	6.0
2.4×10^{-1}	32.8	21.7	23.9	26.1	5.9
1.2×10^{-1}	19.1	7.6	8.5	11.7	6.4

$ID_{80} = 8.3 \times 10^{-1}\ \mu g\ ml^{-1}$

$ID_{50} = 4.1 \times 10^{-1}$

$ID_{20} = 2.1 \times 10^{-1}$

Table 45 Cytotoxicity of products of (4.21) generated *in situ* from photolysis in Tris buffer

Dose ($\mu g\ ml^{-1}$)	% inhibition			mean	S.D.
1.43×10^{1}	89.1	79.5	86.3	85.0	4.9
7.1	51.3	53.7	48.0	51.0	2.9
3.6	18.2	23.6	17.6	19.8	3.3
1.8	6.9	9.9	11.7	9.5	2.4
9.0×10^{-1}	3.7	1.4	3.0	2.7	1.2

$ID_{80} = 1.29 \times 10^{1}\ \mu g\ ml^{-1}$

$ID_{50} = 6.9$

$ID_{20} = 3.6$

Table 46 Cytotoxicity of products of (4.21) generated *in situ* from photolysis in Tris buffer with further irradiation during the presence of L1210 cells

Dose ($\mu g\ ml^{-1}$)	% inhibition			mean	S.D.
1.43×10^{1}	99.8	98.3	99.5	99.2	0.8
7.1	86.7	92.0	87.2	88.6	2.9
3.6	49.3	51.2	44.9	48.5	3.2
1.8	27.5	28.7	29.8	28.7	1.2
9.0×10^{-1}	10.6	2.6	5.6	6.3	4.0

$ID_{80} = 6.3\ \mu g\ ml^{-1}$

$ID_{50} = 3.2$

$ID_{20} = 1.6$

Table 47 Cytotoxicity of products of (4.22) generated *in situ* from photolysis in Tris buffer

Dose ($\mu g\ ml^{-1}$)	% inhibition			mean	S.D.
3.8	96.0	86.6	92.6	91.7	4.8
1.9	84.7	74.9	81.2	80.3	5.0
9.5×10^{-1}	59.4	50.2	47.5	52.4	6.2
4.8×10^{-1}	31.7	12.0	15.1	19.6	10.6
2.4×10^{-1}	14.2	0.3	9.4	8.0	7.1

$ID_{80} = 1.85\ \mu g\ ml^{-1}$

$ID_{50} = 9.4 \times 10^{-1}$

$ID_{20} = 4.7 \times 10^{-1}$

Table 48 Cytotoxicity of products of (4.22) generated *in situ* from photolysis in Tris buffer with further irradiation during the presence of L1210 cells

Dose ($\mu g\ ml^{-1}$)	% inhibition			mean	S.D.
3.8	99.8	94.1	96.8	96.9	2.9
1.9	92.6	81.6	82.9	85.7	6.0
9.5×10^{-1}	65.3	57.5	53.3	58.7	6.1
4.8×10^{-1}	46.1	19.5	21.0	28.9	14.9
2.4×10^{-1}	23.4	2.7	4.6	10.2	11.4

$ID_{80} = 1.63\ \mu g\ ml^{-1}$

$ID_{50} = 7.9 \times 10^{-1}$

$ID_{20} = 3.8 \times 10^{-1}$

Table 49 Cytotoxicity of products of (7.5) generated *in situ* from photolysis in Tris buffer

Dose ($\mu g\ ml^{-1}$)	% inhibition			mean	S.D.
9.52×10^2	101.0	100.5	102.7	101.4	1.2
3.81×10^2	57.8	43.6	62.3	54.6	9.8
1.52×10^2	14.5	9.8	27.5	17.2	9.2
6.1×10^1	2.6	2.4	12.2	5.7	5.6
2.44×10^1	-1.4	-2.1	4.5	0.3	3.6
9.8	-6.5	-4.5	-0.1	-3.7	3.3
3.9	-4.8	1.6	1.2	-0.7	3.6

$ID_{80} = 6.182 \times 10^2\ \mu g\ ml^{-1}$

$ID_{50} = 3.213 \times 10^2$

$ID_{20} = 1.67 \times 10^2$

Table 50 Cytotoxicity of products of (7.5) generated *in situ* from photolysis in Tris buffer with further irradiation during the presence of L1210 cells

Dose ($\mu g\ ml^{-1}$)	% inhibition			mean	S.D.
9.52×10^2	101.5	106.2	110.0	105.9	4.3
3.81×10^2	101.1	101.4	105.5	102.7	2.5
1.52×10^2	99.8	99.9	100.6	100.1	0.4
6.1×10^1	95.7	93.5	98.6	95.9	2.6
2.44×10^1	74.6	60.7	73.5	69.6	7.7
9.8	29.9	35.8	42.0	35.9	6.1
3.9	19.8	17.2	12.3	16.4	3.8

$ID_{80} = 3.65 \times 10^1\ \mu g\ ml^{-1}$

$ID_{50} = 1.33 \times 10^1$

$ID_{20} = 4.8$

Figure 36

Agent 4'-N_3 , (4.20) of Table 11

O cytotoxicity of *in situ* photolysis-products in Tris buffer

● cytotoxicity of *in situ* photolysis-products in Tris buffer with a further 5 minutes irradiation in the presence of the L1210 cells

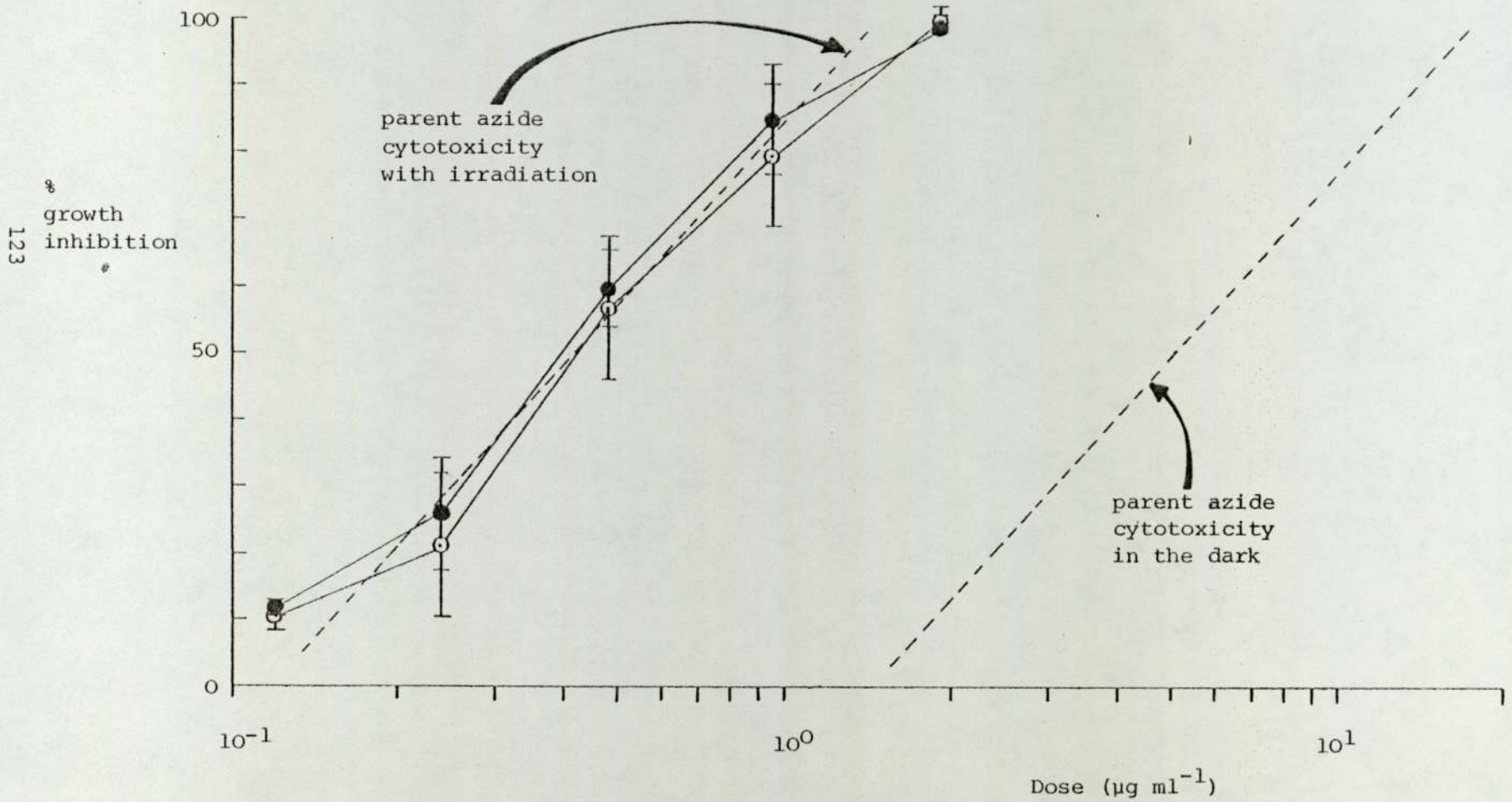

Figure 37

Agent 3'-N_3 , (4.21) of Table 11

O cytotoxicity of *in situ* photolysis-products in Tris buffer

● cytotoxicity of *in situ* photolysis-products in Tris buffer with a further 5 minutes irradiation in the presence of the L1210 cells

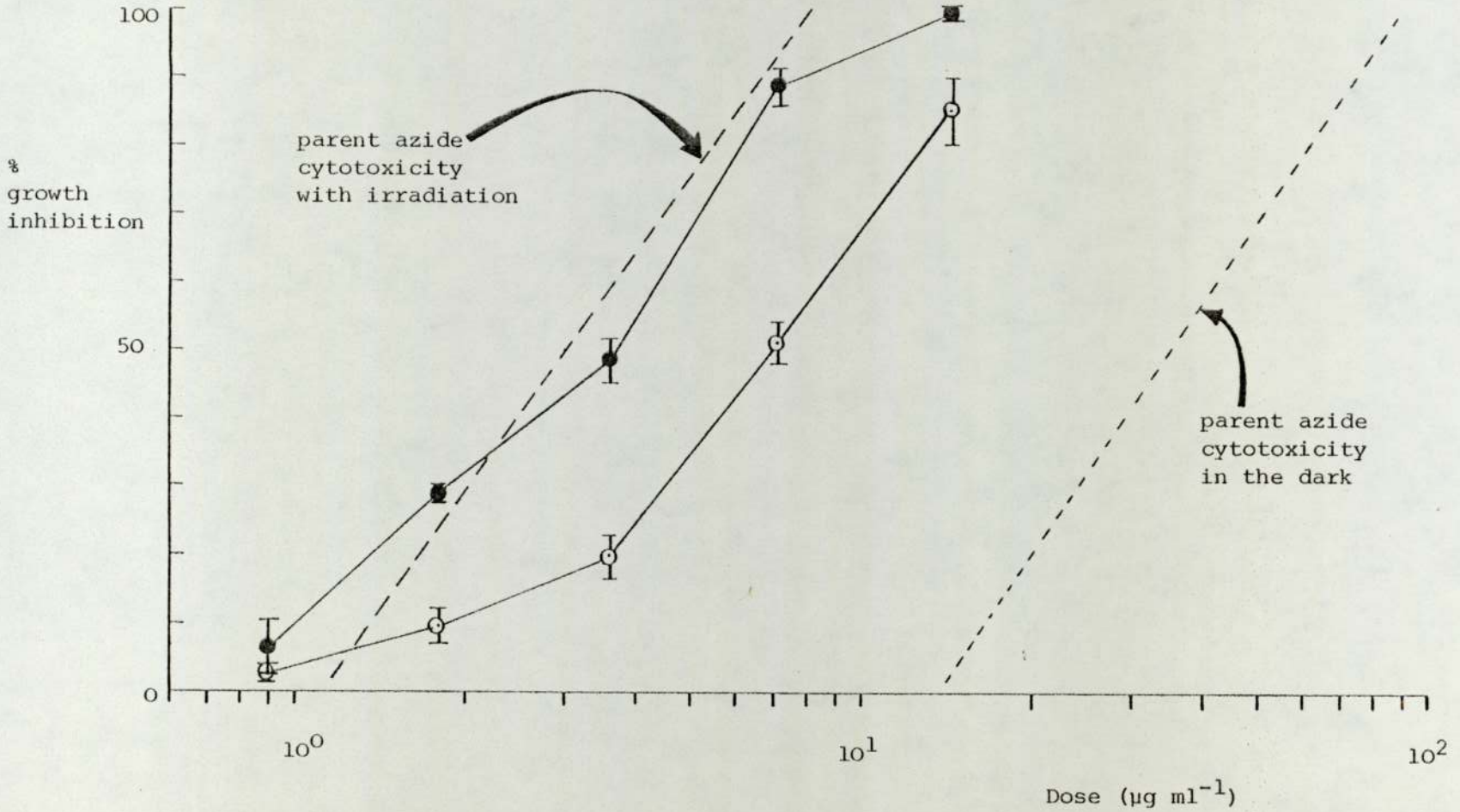

Figure 38

Agent 2'-OMe-4'-N_3 , (4.22) of Table 11

O cytotoxicity of *in situ* photolysis-products in Tris buffer

● cytotoxicity of *in situ* photolysis-products in Tris buffer with a further 5 minutes irradiation in the presence of the L1210 cells

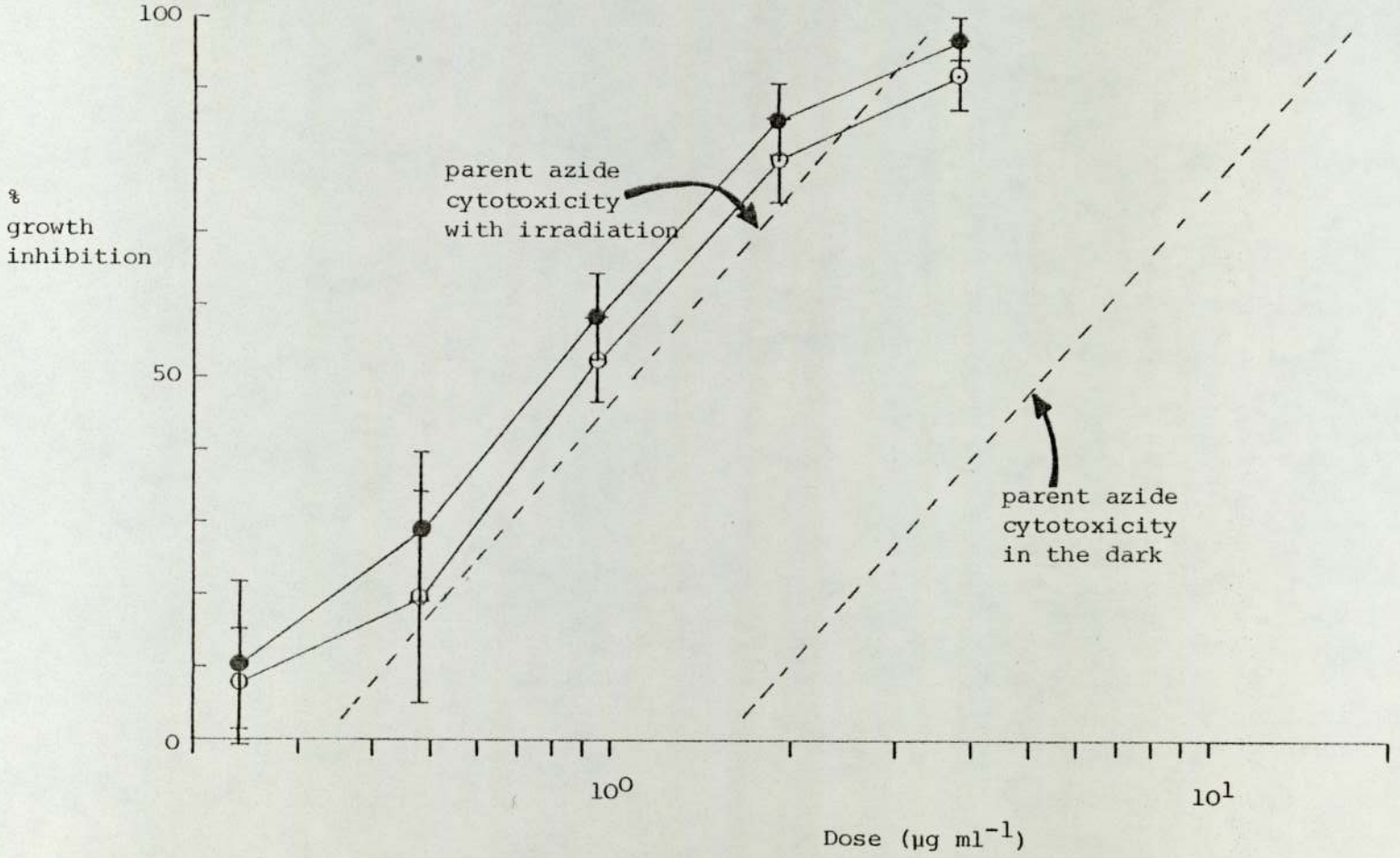

Figure 39

Agent 4-azidobenzenesulphonamide (7.5) of Table 11

O cytotoxicity of *in situ* photolysis-products in Tris buffer

● cytotoxicity of *in situ* photolysis-products in Tris buffer with a further 5 minutes irradiation in the presence of the L1210 cells

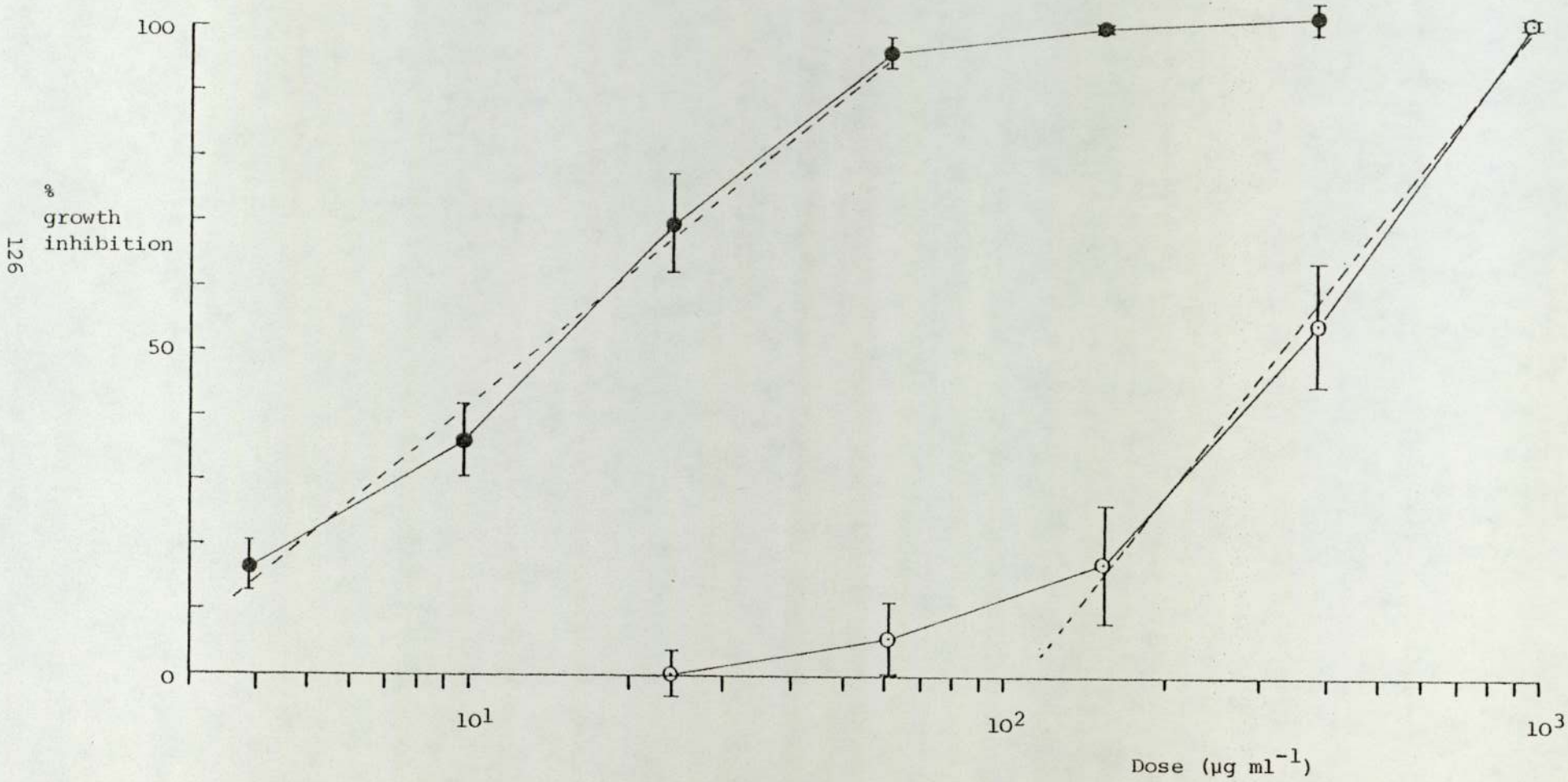

dose-response curve indicative of incomplete photolysis. After a further 5 minutes of irradiation of cells treated with this photolysate, a cytotoxicity level similar to the photosensitised cytotoxicity level of the parent azide was achieved (Figure 37).

The prolonged photolysis time of 2 hours caused the non-toxic 4-azidobenzenesulphonamide (7.5) to form more toxic products with an ID_{80} of 618.2 μg ml^{-1} (Figure 39). The photolysing solution was observed to change from colourless to a dark amber. These highly coloured by-products[152] might well be responsible for some of the observed toxicity. The cytotoxicity of the photolysate was lower than the cytotoxicity of the parent azide in light (Figure 39). This was considered as indicative of incomplete photolysis of this azide in Tris buffer after 2 hours. However another 5 minutes of irradiation of cells treated with the photolysate afforded high cytotoxicity. This might well be due to an additive effect of the cytotoxicity of the photolysate and the cytotoxicity due to photosensitization.

7.5 Conclusion

The objectives of this project have substantially been realised since the photosensitizing properties of azide compounds has been established although only *in vitro*. A tentative interpretation of the cytotoxicity results and photosensitization by the model azide, 4-azidobenzenesulphonamide (7.5) is presented in Scheme 8 where the involvement of a short-lived nitrene intermediate is proposed. The position is less clear in interpreting the nature of the cytotoxic species in irradiated azidoanilinoacridine-treated L1210 cells since photolysis of azidoanilinoacridines did produce stable cytotoxic compounds

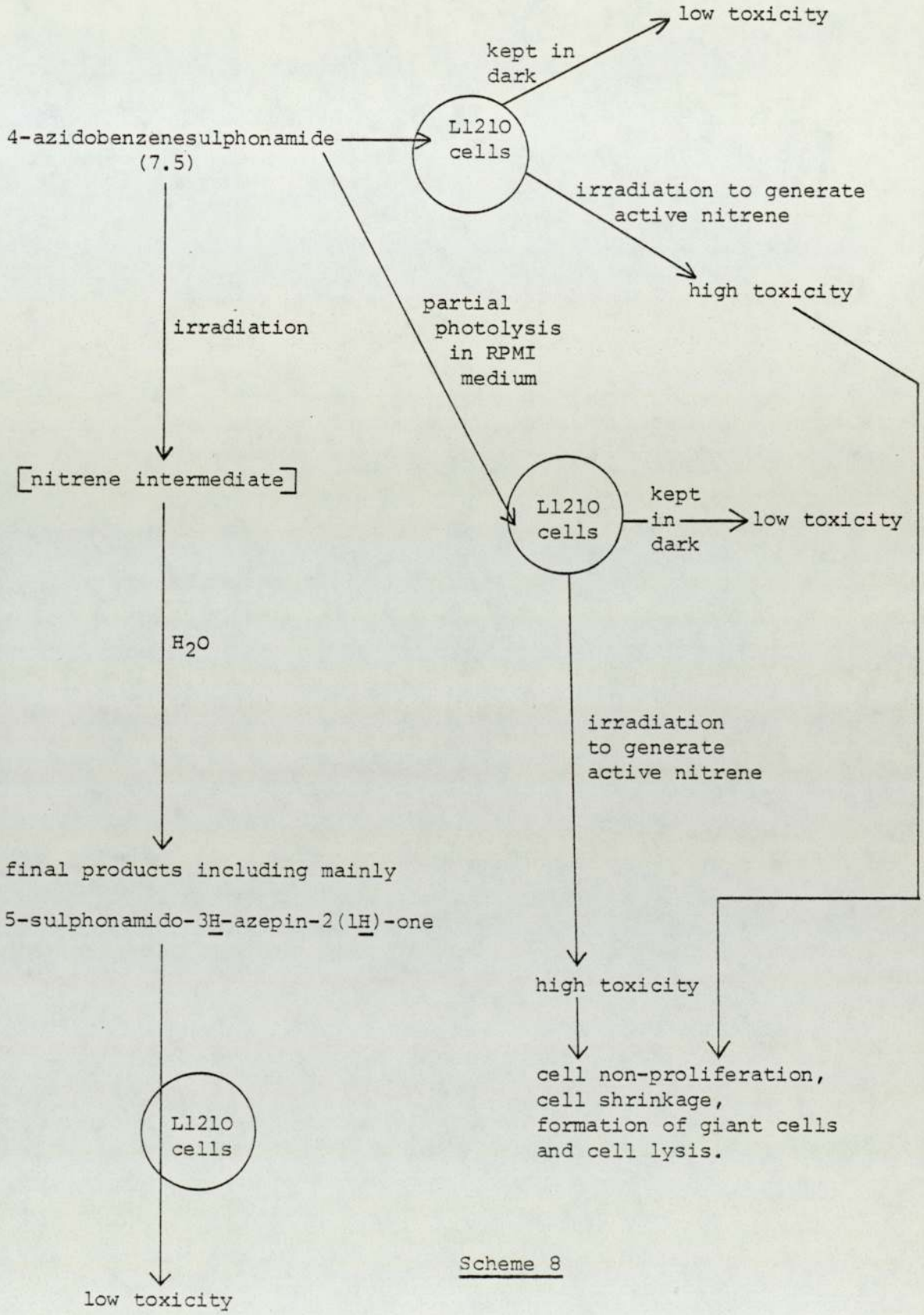
low toxicity
kept in dark
4-azidobenzenesulphonamide (7.5)
L1210 cells
irradiation to generate active nitrene
high toxicity
irradiation
partial photolysis in RPMI medium
[nitrene intermediate]
L1210 cells
kept in dark
low toxicity
H_2O
irradiation to generate active nitrene
final products including mainly
5-sulphonamido-3H-azepin-2(1H)-one
high toxicity
cell non-proliferation, cell shrinkage, formation of giant cells and cell lysis.
L1210 cells
low toxicity

Scheme 8

such as the amine (4.4) (see Chapter 5, Section 5.1) which no doubt contributed to the overall cytotoxicity of these azides in the photosensitization experiments. The cytotoxic effects of these azidoanilinoacridines may follow the pattern summarised in Scheme 9.

It is interesting to speculate about the different photo-generation pathways of different nitrene species from the azides examined. A singlet nitrene might be involved in the photo-sensitised cytotoxicity of 4-azidobenzenesulphonamide (7.5) since its major photo-product was 5-sulphonamido-3H-azepin-2(1H)-one (7.7), a singlet-derived product[152]. In a separate preparative-scale photolysis of 4-azidobenzenesulphonamide (7.5), the expected triplet-derived products[99], sulphanilamide (7.6), the hydrazo compound (7.8) or the azo compound (7.9) were not detected[152]. The reactive species involved in the photosensitised cytotoxicity

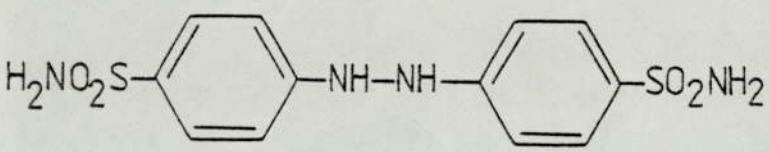

the hydrazo compound (7.8)

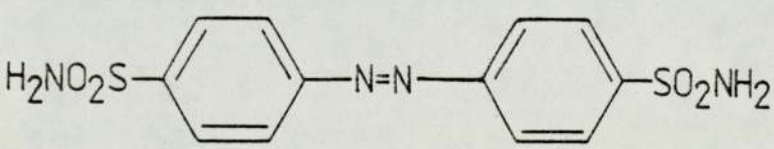

the azo compound (7.9)

of azidoanilinoacridines might on the other hand be a triplet nitrene since photolysis of azidoanilinoacridines gave a triplet-derived product, the amine (4.4).

The "plateau" level (discussed in Section 7.3) of the photosensitization potential of the examined azido compounds at

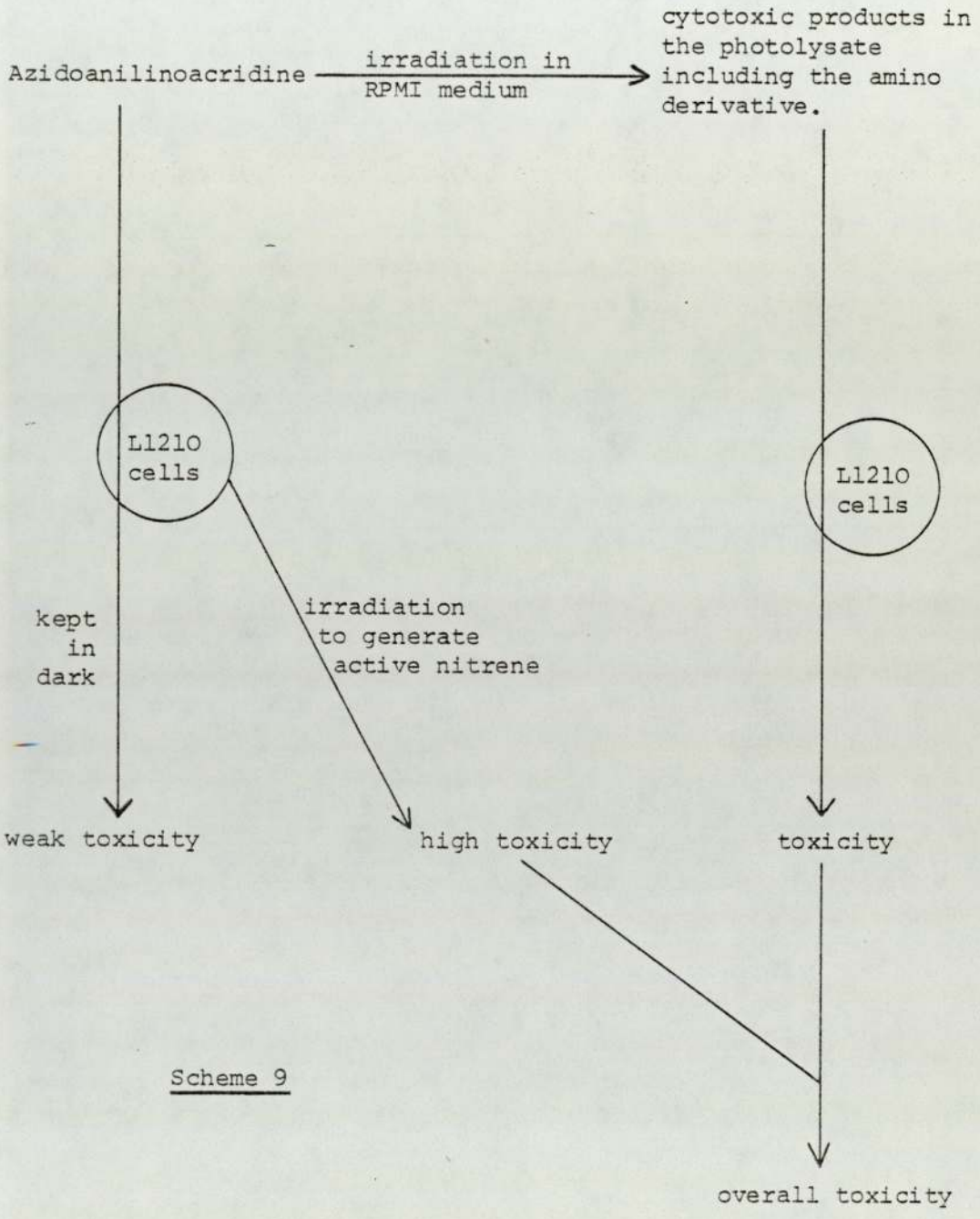
Azidoanilinoacridine
irradiation in
RPMI medium
cytotoxic products in
the photolysate
including the amino
derivative.
L1210
cells
L1210
cells
kept
in
dark
irradiation
to generate
active nitrene
weak toxicity
high toxicity
toxicity
overall toxicity

Scheme 9

a particular Z dose are summarised in Table 51 together with the % growth inhibition due to this dose Z in the dark.

Table 51

Azide	Z(μg ml^{-1})	% growth inhibition	
		dark	plateau level at irradiation time = 200 s (determined graphically)
4.20	1.43	9.6 ± 3.0	92
4.21	14.3	11.8 ± 4.0	100
4.22	14.3	8.4 ± 9.9	50
7.5	95.2	4.4 ± 1.8	97
	285.7	16.7 ± 6.1	100
	952.4	15.0 ± 1.7	100

These results suggested that the azide (7.5) was superior as a photosensitizer to the azidoanilinoacridines (4.20) - (4.22), especially if the low toxicity of azide (7.5) was also taken into account. However, the azidoanilinoacridines might have higher selectivity for the nucleic acids of tumour cells *in vivo*, in which case both azides (4.20) and (4.21) may prove more useful as antitumour photosensitizers. Azide (4.22) on the other hand appears to have no claim as a photosensitizer of high effectiveness.

In Section 7.4, solutions of azidoanilinoacridines were photolysed for a prolonged (2 hour) period and the azides were expected to be completely decomposed to form stable photo-products. Azides (4.20) and (4.22) did in fact show no further photosensitization effects (Figures 36 and 38), but the photolysate of azide (4.21)

retained certain photosensitization potential (Figure 37): a further 5 minutes of irradiation of cells treated with this photolysate afforded enhanced cytotoxicity. Since only a period of 5 minutes was needed to give this enhancement, this was considered as a further support to the hypothesis that reactive (nitrene) intermediates were at least partly responsible for their cytotoxicity. The high photosensitization potential of the reactive species generated *in situ* from the azide (7.5) further substantiated this inference (Figure 39).

It is not pretended that antitumour agents with absolute selectivity have resulted from the present work, however it is hoped that this series of experiments has demonstrated that photosensitization or radiosensitization with azido derivatives of antitumour agents may afford an additional degree of selectivity to existing therapeutic methods. This type of radiosensitizers containing an azido function can be activated by radiation irrespective of the oxygen concentration in the surrounding areas of the tumour which has been the obstacle in the successful employment of earlier radiosensitizers described in Chapter 1. This then paved the way and set the target for a more effective combination of radiotherapy with chemotherapy.

In future work, the metabolism of the azidoanilinoacridines must be investigated. The model azide, 4-azidobenzenesulphonamide (7.5) was found to be metabolised in rats to the amine[151] sulphanilamide (7.6) which was non-toxic to L1210 cells (Figure 21 and Table 25). If the azidoanilinoacridines were also metabolised to the corresponding amines, the selectivity afforded by radiosensitization using these azides would be modified by the tumour selectivity of these amines. However, evidence in Chapter 3

suggested that the azido function itself did not impart undue instability to organic molecules in their metabolism in man[114].

The present *in vitro* photosensitization experiments have, of course, to be extended to *in vivo* systems. The radiation employed to activate the azido compounds and generate short-lived nitrene intermediates was short wavelength visible light (366 nm) of limited penetrative power; future developments should endeavour to extend to employing *X* and Y-radiation to generate active nitrene intermediates in the treatment of tumour in the deep viscera. Finally the mode of the antitumour action of the azidoanilinoacridines must also be elucidated. To this end, collaborative studies employing DNA-fibre *X*-ray diffraction techniques have been initiated[153]. These studies would help to discover if azidoanilinoacridines do intercalate DNA and form covalent complexes with nucleotides when activated by radiation.

Part 3

Experimental

Part 3 Experimental

Chapter 8 Chemical Studies

8.1 Synthesis of substituted 9-anilinoacridines

Method A

The appropriate aniline derivative (0.01 mole) was dissolved in anhydrous methanol (100 ml) and the solution heated to reflux. 9-Chloroacridine (2.14 g) was then added in small portions to the refluxing solution over 30 minutes and the mixture heated for a further 60 minutes. The solution was then allowed to cool to room temperature. Excess ether was added to precipitate the anilinoacridine hydrochloride. The product was collected and dried in a vacuum desiccator. The yield in most cases approached theoretical. The compounds were all recrystallised from ethanol-ether.

(a) 9-(4-Aminoanilino)acridine hydrochloride (4.4), m.p. 314-316° (Lit.,[80] m.p. 315-317°) as brown flakes.

ν_{max} 3320 and 3410 cm^{-1} (NH_2)

(b) 9-(3-Aminoanilino)acridine hydrochloride (4.5), m.p. 296-298° (Lit.,[80] m.p. 299-301°) as brown flakes.

ν_{max} 3290 and 3420 cm^{-1} (NH_2)

(c) 9-(2-Aminoanilino)acridine hydrochloride (4.6), m.p. 318-321° (Lit.,[80] m.p. 320-322°) as amber flakes.

ν_{max} 3290 and 3420 cm^{-1} (NH_2)

(d) *9-(4-Nitroanilino)acridine hydrochloride* (4.7), m.p. 319-321°, as orange rosettes.

Found C, 64.6; H, 3.9; N, 12.0%;

$C_{19}H_{14}N_3O_2Cl$ requires C, 64.9; H, 4.0; N, 12.0%.

ν_{max} 1335 and 1510 cm^{-1} (NO_2)

(e) *9-(3-Nitroanilino)acridine hydrochloride* (4.8),

m.p. 316-317°, as orange rosettes

Found C, 64.5; H, 4.1; N, 11.8%;

$C_{19}H_{14}N_3O_2Cl$ requires C, 64.9; H, 4.0; N, 12.0%

ν_{max} 1350 and 1530 cm^{-1} (NO_2)

Method B

The appropriate disubstituted aniline (0.01 mole) was dissolved in acetonitrile (50 ml) and the solution heated to reflux. 9-Chloroacridine (2.14 g) was then added in small portions to the refluxing solution over 20 minutes. When all the 9-chloroacridine had been added, the mixture was refluxed for a further 40 minutes. The solution was then allowed to cool to room temperature and ether (20 ml) added. The precipitated anilinoacridine hydrochloride was collected and dried in a vacuum desiccator. The yields were in the range 60-90%. The compounds were recrystallised from acetonitrile-ether.

(a) *9-(2-Methoxy-4-nitroanilino)acridine hydrochloride* (4.9),

m.p. 254-255°, as yellow flakes.

Found C, 63.0; H, 4.6; N, 11.3%;

$C_{20}H_{16}N_3O_3Cl$ requires C, 62.9; H, 4.2; N, 11.0%.

ν_{max} 1350 and 1530 cm^{-1} (NO_2)

1025 cm^{-1} (C-O)

(b) *9-(2-Methoxy-5-nitroanilino)acridine hydrochloride* (4.10),

m.p. 247°, as yellow flakes.

Found C, 62.7; H, 4.1; N, 10.6%;

$C_{20}H_{16}N_3O_3Cl$ requires C, 62.9; H, 4.2; N, 11.0%.

ν_{max} 1350 and 1530 cm^{-1} (NO_2)

1015 cm^{-1} (C-O)

(c) *9-(2-Amino-5-nitroanilino)acridine hydrochloride* (4.11), m.p. 289-291°, as yellow flakes.

Found C, 62.5; H, 4.2; N, 15.7%;

$C_{19}H_{15}N_4O_2Cl$ requires C, 62.2; H, 4.1; N, 15.3%.

ν_{max} 1330 and 1520 cm^{-1} (NO_2)

3300 and 3450 cm^{-1} (NH_2)

(d) *9-(2-Amino-5-nitroanilino)acridine hydrochloride hydrate* (4.12), m.p. 306°(dec), as red crystals.

Found C, 59.7; H, 4.1; N, 14.3%;

$C_{19}H_{15}N_4O_2Cl.1H_2O$ requires C, 59.3; H, 4.4; N, 14.6%.

ν_{max} 1330 and 1520 cm^{-1} (NO_2)

3300 and 3450 cm^{-1} (NH_2)

8.2 Reduction of nitro-substituted 9-anilinoacridines.

Raney nickel-hydrazine hydrate reduction.

The nitro compound (0.01 mole) was dissolved in a minimum volume of DMSO (15-20 ml) at reflux temperature with constant stirring. An excess (≈ 3 g) of Raney nickel was added to the stirring solution. Hydrazine hydrate (5-10 ml) was then added dropwise to the mixture over a 30 minute period. The hot mixture was filtered quickly through a celite filter pad. The (red) amine solution was cooled to room temperature and again filtered.

The amine solution was added to a ten-fold volume of water (200-300 ml). This solution was basified with ammonia (to pH 11) and the amine free base was extracted into chloroform. The aqueous layer was discarded while the chloroform fraction was then re-extracted into 100 ml of water by acidification to pH 5 (with 10*N*-hydrochloric acid). This aqueous solution was shaken with

ether to remove traces of 9-acridanone. The amine base was liberated by basification of the acid solution and extracted into chloroform. The chloroform was distilled off to leave an amine residue which was re-dissolved in a minimum volume of anhydrous methanol. On removing the methanol, the amine free base was obtained. Alternatively, the methanolic solution could be acidified with dry hydrogen chloride to give the amine hydrochloride. The volume of methanol was reduced by evaporation to promote crystallisation and an equal volume of dry ether was added to complete the precipitation. The product was collected and dried in a vacuum desiccator. The yields were 60-70%.

(a) 9-(4-Aminoanilino)acridine dihydrochloride (4.14), m.p. 309-311°, as yellow plates.

Found C, 59.2; H, 5.3; N, 11.0%;

$C_{19}H_{17}N_3Cl_2.1\frac{1}{2}H_2O$ requires C, 59.2; H, 5.2; N, 10.9%.

(b) *9-(4-Amino-2-methoxyanilino)acridine dihydrochloride* (4.15), m.p. 240-243°, as amber flakes.

Found C, 56.1; H, 5.0; N, 10.0%;

$C_{20}H_{19}N_3OCl_2.2H_2O$ requires C, 56.6; H, 5.4; N, 9.9%.

ν_{max} 1030 cm^{-1} (C-O)

(c) *9-(5-Amino-2-methoxyanilino)acridine dihydrochloride* (4.16), m.p. 258-260°, as brown flakes.

Found C, 58.2; H, 4.8; N, 9.6%;

$C_{20}H_{19}N_3OCl_2.1\frac{1}{2}H_2O$ requires C, 57.8; H, 5.3; N, 10.1%.

ν_{max} 1010 cm^{-1} (C-O)

8.3 Diazotisation of amino-substituted 9-anilinoacridine hydrochlorides and the subsequent synthesis of the azido derivatives.

The amino compound (0.1 mole) was dissolved in a minimum

volume of water (50-100 ml) at reflux temperature. The solution was then cooled in an ice bath to 0-5° and this low temperature was maintained throughout the preparation. The suspension was stirred constantly with a magnetic stirrer. 5 ml of 10*N*-hydrochloric acid (or 5 ml of 40% tetrafluoroboric acid if the diazonium tetrafluoroborate was to be isolated) was added to the suspension. An aqueous solution of sodium nitrite (1.1 mol. equiv., 0.76 g in 5 ml) was then added dropwise to the mixture over a period of 15 minutes. The suspension was allowed to stir for a further 30-45 minutes.

The diazonium tetrafluoroborate was collected and dried between sheets of filter paper before further drying in a vacuum desiccator.

(a) *4-[N-(Acridin-9-yl)amino]phenyldiazonium tetrafluoroborate hydrotetrafluoroborate* (4.17),

m.p. 271-273°(dec), as brown flakes (from acetonitrile-ether).

Found C, 48.9; H, 3.1; N, 12.0%;

$C_{19}H_{14}N_4B_2F_8$ requires C, 48.4; H, 3.0; N, 11.9%.

ν_{max} 2260 cm^{-1} (N_2^+)

(b) *3-[N-(Acridin-9-yl)amino]phenyldiazonium tetrafluoroborate hydrotetrafluoroborate* (4.18),

m.p. 96-98°(dec) as brown flakes (from acetonitrile-ether).

Found C, 48.0; H, 3.4; N, 11.7%;

$C_{19}H_{14}N_4B_2F_8$ requires C, 48.4; H, 3.0; N, 11.9%.

ν_{max} 2320 cm^{-1} (N_2^+)

(c) *9-(4-Azidoanilino)acridine hydrochloride* (4.20),

m.p. 201-203°(dec) as amber flakes (from methanol-ether).

Found C, 48.0; H, 3.4; N, 11.7%;

$C_{19}H_{14}N_5Cl.1\frac{1}{2}H_2O$ requires C, 60.9; H, 4.5; N, 18.7%.

ν_{max} 2120 cm^{-1} (N_3)

(d) *9-(3-Azidoanilino)acridine hydrochloride* (4.21),

m.p. 209-211°(dec) as brown flakes (from methanol-ether).

Found C, 62.3; H, 4.0; N, 19.0%;

$C_{19}H_{14}N_5Cl.1H_2O$ requires C, 62.4; H, 4.4; N, 19.1%.

ν_{max} 2130 cm^{-1} (N_3)

(e) *9-(4-Azido-2-methoxyanilino)acridine hydrochloride* (4.22),

m.p. 220-221°(dec) as yellow flakes (from methanol-ether).

Found C, 60.5; H, 4.5; N, 17.3%;

$C_{20}H_{16}N_5OCl.1H_2O$ requires C, 60.7; H, 4.6; N, 17.7%.

ν_{max} 2150 cm^{-1} (N_3)

8.4 Synthesis of *9-(benzotriazol-1-yl)acridine* (4.28).

9-(2-Aminoanilino)acridine hydrochloride (0.01 mol. equiv., 3.2 g) was diazotised in aqueous hydrochloric acid as in Section 6.3. The benzotriazolylacridine was precipitated, collected after 1 hour, washed with a small quantity of cold water and dried in a vacuum desiccator in the dark. It was recrystallised from aqueous DMF.

m.p. 255-256°(dec) as cream white flakes.

Found C = 77.4; H = 4.2; N = 18.9%;

$C_{19}H_{12}N_4$ requires C = 77.0; H = 4.1; N = 18.9%.

8.5 Synthesis of sodium *4-[N-(acridin-9-yl)amino]phenyl diazotate* (4.23).

A solution of 4-[N-(acridin-9-yl)amino]phenyldiazonium chloride hydrochloride was prepared as described in Section 6.3. This was poured slowly into an ice-cold sodium hydroxide solution (10*N*, 100 ml) with continuous stirring. The rate of addition was

such that the temperature of the mixture never rose above 10^{o}. The product precipitated out and was washed with a large volume of water. The diazotate was collected, dried initially between sheets of filter paper and further dried in a vacuum desiccator in the dark. The product was of brick-red colouration and showed a characteristic infra red absorption band ν_{max} 2110 cm^{-1} (N_2O^-).

Found C, 67.3; H, 4.1; N, 16.2%;

$C_{19}H_{13}N_4ONa$ requires C, 67.9; H, 3.9; N, 16.7%.

8.6 Photolysis of azido-substituted 9-anilinoacridines.

The compounds investigated were the three azides (4.20), (4.21) and (4.22).

The azido derivative (0.010 g) was dissolved in DMSO to form a 2.0 mg ml^{-1} solution. A sonicator was used to assist dissolution. This solution was then diluted to 30.0 µg ml^{-1} with one of the following solvents: (a) pH 7.4 buffer, (b) pH 4 buffer, (c) pH 11 buffer, or (d) ethanol. (See Notes on materials for details on these buffers.)

3 ml of this solution was placed in a (1 cm^2 path) quartz cell and stoppered. Photolysis of the solution was carried out in a light box fitted with a fluorescent tube. Three types of fluorescent tubes of different emission wavelengths, namely (a) 253.7 nm, (b) 366 nm and (c) visible range were used. The quartz cell was positioned 5 cm from the centre of the fluorescent tube.

Nine sets of experimental conditions of different solvent/ irradiation wavelength combinations were employed.

Solvent	Irradiation wavelength λ (nm)
ethanol	253.7, 366, visible.
pH 7.4 buffer	253.7, 366, visible.
pH 4 buffer	235.7, visible.
pH 11 buffer	253.7.

Ultra violet/visible spectra (275-600 nm) were taken at intervals until there were no further hypsochromic and hypo/hyperchromic changes (e.g. Figures 8-10). The analytical wavelength used was 420 nm in all cases except for 3'-azide (4.21) in ethanol, pH 7.4 and pH 11 buffers where the analytical wavelength was 325 nm.

The absorbance of the solution at time-zero was taken as 100% relative to the absorbance at time - ∞ (i.e. when no further hypo/hyperchromic changes) taken as 0%. Intermediary absorbances were expressed as a % of the time-zero absorbance. Half-lives of the azides in solution under the set conditions were obtained graphically from a plot of log absorbance against time of irradiation.

8.7 Photolysis of 9-(benzotriazol-1-yl)acridine (4.28).

The benzotriazolo derivative (0.010 g) was dissolved in ethanol to form a 20.0 μg ml^{-1} solution. A sonicator was used to assist dissolution. This was further diluted to 1.5 μg ml^{-1} in ethanol; 3 ml of this solution was placed in a 1 cm^2 quartz cell and stoppered. Photolysis of the solution was carried out in a light box fitted with fluorescent tubes of various emission wavelengths, namely (a) 253.7 nm, (b) 366 nm, or (c) visible range. The quartz cell was placed at the same position in each experiment and was 5 cm from the centre of the fluorescent tube.

Ultra violet spectra (200-450 nm) were taken at intervals over a period of time as before (see Figure 13). The analytical wavelength chosen was 360 nm.

The method for determining the half-lives of the benzotriazolo derivative under various experimental conditions (i.e. different irradiation wavelengths) were the same as described in the last section, that is graphically from a plot log absorbance against time of irradiation.

8.8 Thermolysis of 9-(benzotriazol-1-yl)acridine (4.28).

100 mg of the benzotriazole was vacuum-sublimed in a "cold finger" sublimation apparatus at 250-300°. The sublimation was complete after 60 minutes and the yellow deposit on the inner core was collected. The yellow compound was identified as *7*3*H*-*quin*[*4,3,2-kl*]*acridine* (5.4),

m.p. 270-272° as yellow flakes.

Found C, 84.6; H, 4.8; N, 10.3;

$C_{19}H_{12}N_2$ requires C, 85.1; H, 4.5; N, 10.4.

Chapter 9 Biological materials and methods

9.1 L1210 mouse lymphocytic leukaemic cell culture

Medium : RPMI-1640 with 25 mM Hepes buffer, L-glutamine and 10% ($^{v}/_{v}$) horse serum supplied by Gibco Biocult.

Antibiotics: Penicillin and stretomycin solution, 5000 units each ml^{-1} supplied by Gibco Biocult.

Aeration: 10% carbon dioxide and 90% air.

Maintenance of the stock culture

The stock was maintained in 10 ml of aerated medium in a sealed culture flask. The cell density of the stock was not allowed to exceed 1×10^{6} cell ml^{-1}; when this density was approached, the stock was subcultured. 2×10^{5} cells were resuspended in 10 ml of fresh medium, 0.1 ml (i.e. 1% $^{v}/_{v}$) of antibiotics added and the suspension was then aerated for 1 minute. The stock was kept in an incubator at 37^{o}. Cell density in all cell culture experiments was monitored and determined with a Coulter Counter calibrated for L1210 cells.

Growth of L1210 cells

A calculated number of cells (2×10^{6}) were taken from the stock and transferred to a universal tube. They were spun down in a bench centrifuge to form a pellet and the supernatant discarded. The pellet was resuspended in 50 ml of fresh medium in a sterile culture flask at a density of approximately 4×10^{4} cells ml^{-1}. Antibiotics (50 µl, i.e. 1% $^{v}/_{v}$) was added and the suspension was mixed by vortexing.

Replicates of 2 ml fractions of the suspension were pipetted

into each of the 24 wells of a Repli dish, this was termed "plating-out". Cells in two wells were counted immediately after plating-out and these figures were taken as the initial density or the time-zero cell density. The 2.0 ml cell suspension was diluted with 18.0 ml of Isoton (an isotonic solution) and the diluted suspension was counted. A volume of 0.5 ml was sucked through the Coulter counter during counting hence the resultant particle-number was multiplied by 20 to give the cell density in cells ml^{-1}.

The remaining cell suspensions in the Repli dish were then incubated in a gassing incubator at 37^{o} in an atmosphere of 10% carbon dioxide/90% air. Duplicate of 2.0 ml cell suspensions from the Repli dish were counted every 10-15 hours; the cell density and the time of counting were recorded. A plot of log cell density against time gave a sigmoid curve (Figure 14).

9.2 Effect of DMSO on cell growth

A calculated number of cells (2×10^{6}) were taken from the stock and transferred to a universal tube. They were pelleted by centrifugation and resuspended in 14 ml of fresh medium, then mixed by vortexing. The suspension was then aerated. Meanwhile, universal tubes with 300 µl of the calculated DMSO/medium solution were prepared:

DMSO x(µl)	0	25	50	75	100	125	150	175	200	225
medium (µl)	300	275	250	225	200	175	150	125	100	75

To each tube 1.0 ml of the cell suspension was added followed by gentle aeration before these tubes were sealed. These preparations

were incubated at 37° for 60 minutes. At the end of this period, cells in each tube were pelleted, supernatant removed and 5 ml of fresh medium plus 50 µl of antibiotics were added and mixed by vortexing.

The cell suspensions were then plated out in a Repli dish at 2.0 ml per well and 2 wells per DMSO/medium dilution (i.e. in duplicate). The 1 ml suspensions left in each tube were then pooled. A 2.0 ml sample of the pooled suspension was counted and this value was the initial count, when multiplied by 20 gave the initial density (which should be around 2.86×10^4 cells ml^{-1}). The Repli dish of cells was incubated in a gassing incubator at 37° in an atmosphere of 10% carbon dioxide/90% air for 45-50 hours or when the cell density had reached 6-10 times the initial density. Each well of cells was then counted as described in the last section and the result recorded. Final density was expressed as:

$$\text{final density} = (\text{cell count} \times 20) - \text{initial density.}$$

Since 300 µl of DMSO/medium solution were added to each of the 1.0 ml cell suspensions, the real DMSO concentration was:

$$\frac{1000 \times}{1000 + 300} = \underline{\underline{0.7692 \times}}$$

% Growth inhibition was a term referred to:

$$\left(1 - \frac{\text{final density of treated population}}{\text{final density of control population}}\right) \times 100$$

A graph of % growth inhibition against DMSO concentration was plotted (Figure 15).

9.3 Effect of 366 nm radiation on cell growth

A number of cells (2×10^6) were taken from the stock, transferred to a universal tube, centrifuged to form a pellet and resuspended in 14 ml of fresh medium, then mixed and aerated. To a series of (twelve) universal tubes 1.0 ml per tube of the cell suspension was pipetted and 50 µl of DMSO was added to each tube followed by aeration before these tubes were sealed. The series of tubes of cells was irradiated for a series of fixed periods in the specially constructed light box, then incubated for a further period at 37° in the dark. The sum of the irradiation time and the incubation period was a total of 60 minutes.

When this irradiation/incubation was complete (i.e. after the 60 minutes), cells in each tube were pelleted, supernatant removed and 5 ml of fresh medium plus 50 µl of antibiotics were added and mixed by vortexing.

The cell suspensions were then plated out at 2.0 ml per well and 2 wells per sample (i.e. in duplicate) of a particular irradiation period. Initial density and final densities were determined as in the last section. % Growth inhibition was calculated from these values as:

$$\left(1 - \frac{\text{final density of irradiated population}}{\text{final density of non-irradiated population}}\right) \times 100$$

A graph of % growth inhibition against irradiation time was plotted (Figure 17).

9.4 L1210 cytotoxicity screening system

A calculated number of cells (2×10^6) were taken from the stock and transferred to a universal tube. They were pelleted by

centrifugation and resuspended in 14 ml of fresh medium, then mixed by vortexing. The suspension was then aerated. Meanwhile, a series of universal tubes each containing 50 µl of a serial dilution of a test compound was prepared. To each tube, 1.0 ml of the cell suspension was pipetted followed by aeration before these tubes were sealed. These preparations were incubated at 37° for 60 minutes (in the dark). At the end of the 60 minutes, cells in each tube were pelleted, supernatant removed and 5 ml of fresh medium plus 50 µl of antibiotics were added and mixed by vortexing.

The cell suspensions were then plated out at 2.0 ml per well and 2 wells per sample (i.e. in duplicate) of a particular serial dilution. Initial density and final densities were determined as described in Section 9.4. % Growth Inhibition was calculated from these values also as indicated in Section 9.2. The % Growth Inhibition against log dose plots were constructed (see Figures 18-23), these were termed dose/response curves.

The structures of the 15 compounds which have been screened in this system are given in Table 11 (see also Chapter 8 for the chemical composition of the anilinoacridines). Compound (2.18) was in the free base form.

9.5 Photosensitizing effect of azido compounds

(a) Cytotoxicity in (366 nm) light

The procedures for investigating the cytotoxicity due to test compounds in (366 nm) light were similar to those set out in Section 9.4 except that during the 60 minutes incubation time the tubes containing 1.0 ml of cell suspension and 50 µl of the test compound solution were irradiated in the specially constructed

light box for exactly 5 minutes under conditions described in Section 9.3.

When this irradiation/incubation was complete, cells in each tube were pelleted, supernatant removed and 5 ml of fresh medium plus 50 µl of antibiotics were added and mixed by vortexing.

The cell suspensions were then plated out and dose/response curves were constructed (see Figures 24-27) following the same plating-out procedures set out in Section 9.4. Azido compounds (4.20)-(4.22) and (7.5) were screened under the experimental procedures of this section.

(b) Relationship between photosensitization and irradiation time

The procedures for investigating the relationship between photosensitization by azido compounds (4.20)-(4.22) and (7.5) of Table 11 were similar to those set out in Section 9.3 except that the 50 µl of DMSO was replaced by 50 µl of a fixed concentration of the test compound —— at Z µg ml^{-1}, and at the end of each irradiation period, the tubes were not further incubated, the remaining plating-out procedures were followed. Z was chosen based on the results from experiments of Sections 9.4 and 9.5a on the azido compounds concerned, the criteria for selecting the value Z could be found in the "Results and Discussion" section.

Plots of % Growth Inhibition against log (irradiation time) were constructed (see Figures 32-35).

9.6 Cytotoxicity of photolysis products of azido compounds

(a) Cytotoxicity of products generated *in situ* from photolysis in RPMI medium

A calculated number of cells (2×10^6) were taken from the

stock, transferred to a universal tube, centrifuged to form a pellet and resuspended in 14 ml of fresh medium. They were then mixed by vortexing and aerated. The cell suspension was pipetted (at 1.0 ml per tube) to a series of universal tubes, the cells in each tube were then pelleted and supernatant removed. Meanwhile, another series of universal tubes each containing 1.0 ml of medium and 50 µl of a serial dilution of the test azido compound was prepared. The tubes containing RPMI medium and the test compound serial dilutions were irradiated in the light box (with 366 nm light) for 5 minutes. Each irradiated solution was then added to the corresponding universal tube containing the cell-pellet, then mixed by vortexing and aerated. These preparations were then incubated at 37° for 60 minutes in the dark. At the end of the 60 minutes, cells in each tube were pelleted, supernatant removed and 5 ml of the fresh medium plus 50 µl of antibiotics were added and mixed by vortexing.

The cell suspensions were then plated-out and dose/response curves were constructed (see Figures 28-31) following the same plating out procedures set out in Section 9.4.

(b) The procedures for investigating the photosensitizing effect of the photo-products generated *in situ* from photolysis in RPMI medium were the same as those set out in Section 9.6a except that the tubes containing the L1210 cell suspension and the irradiated solution were further irradiated for 5 minutes (with 366 nm light) before being incubated at 37° for 55 minutes instead of 60 minutes.

(c) Cytotoxicity of products generated *in situ* from photolysis in Tris-ethanol buffer

Test compound solutions were prepared as follows:

(i) Azide (4.20) ----- a 2.0 mg ml^{-1} solution in DMSO was prepared, this was further diluted in Tris-ethanol buffer to 40.0 µg ml^{-1}. 50 µl of this solution added to 1.0 ml of cell suspension would give a final concentration of,

$$\frac{50}{1000 + 50} \times 40 = 1.9 \text{ µg ml}^{-1}$$

(ii) Azide (4.21) ----- a 2.0 mg ml^{-1} solution in DMSO was prepared, this was further diluted in Tris-ethanol buffer to 300.0 µg ml^{-1}. 50 µl of this solution added to 1.0 ml of cell suspension would give a final concentration of,

$$\frac{50}{1000 + 50} \times 300 = 14.3 \text{ µg ml}^{-1}$$

(iii) Azide (4.22) ----- a final concentration of 1.9 µg ml^{-1} of this compound in Tris-ethanol buffer was prepared in the same manner as azide (4.20) in (i) above.

(iv) Azide (7.5) ----- a 20.0 mg ml^{-1} solution in Tris-ethanol buffer was prepared. 50 µl of this solution added to 1.0 ml of cell suspension would give a final concentration of,

$$\frac{50}{1000 + 50} \times 20000 = 952.4 \text{ µg ml}^{-1}$$

2.0 ml of each of these solutions were sealed in plain glass ampoules and irradiated in the light box at 366 nm for 2 hours. The resultant photolysis products solutions were then used to form the corresponding serial dilutions and their cytotoxicity screened in accordance to procedures in Section 9.4.

(d) The procedures for investigating the photosensitizing effect of the photo-products generated *in situ* from photolysis in Tris-ethanol buffer were the same as those set out in Section 9.6c except that the tubes containing the L1210 cell suspension and the irradiated solution were further irradiated for 5 minutes with 366 nm light before being incubated at 37° for 55 minutes instead of 60 minutes.

Notes on instruments, abbreviations, materials and methods.

(1) Infra red spectra were recorded on a Pye Unicam SP 200 spectrophotometer (as KBr discs).

(2) Ultra violet spectra were recorded on a Pye Unicam SP 8000 spectrophotometer, the solvent used was ethanol unless specified otherwise.

(3) Mass spectra were recorded on a *Vg* micromass 12B single focusing mass spectrometer.

(4) Photolyses were conducted in a light box fitted with an 8W fluorescent tube. The emission wavelengths of the three types of fluorescent tubes were (a) 253.7 nm; (b) 366 nm; and (c) the visible range. Samples were placed at a fixed distance (5 cm) from the centre of the fluorescent tube. When the light box was employed for biological experiments, the 366 nm tube was used.

(5) Preparative photolyses were carried out in a Hanovia photochemical reactor fitted with a 100W medium-pressure arc and a quartz jacket (water cooled).

(6) Cell numbers were determined with a Coulter counter Z_{B1} fitted with a 100 μ orifice tube calibrated for L1210 mouse leukaemic cells.

(7) Cell cultures were inspected with an Olympus inverted microscope model CK.

(8) Melting points (m.p.) were uncorrected.

(9) Elemental analyses were obtained from The Butterworth Microanalytical Consultancy Ltd.

(10) Absolute alcohol referred to commercial "100% ethanol".

(11) Ethanol referred to 95% ethanol which was benzene free.

(12) DMF referred to dimethylformamide.

(13) DMSO referred to dimethylsulphoxide.

(14) Buffers for photolysis experiments contained 52.63% of 95% ethanol (equivalent to 50% ethanol) and were made up to 100% with distilled water.

(a) pH 7.4 buffer contained 5 mM Tris, also used in the biological experiments as a photolysis medium; this buffer was abbreviated as the Tris-ethanol buffer.

(b) pH 11 buffer contained 25 mM sodium carbonate/bicarbonate, and

(c) pH 4 buffer contained 50 mM sodium citrate.

(15) Thin layer chromatography on silica plates was used for routine checks on the purity of compounds and for studying photolysis and thermolysis products. Three solvent systems were used to cross-examine results.

(a) a very polar system: Chloroform 80, Methanol 20, Ammonia 1;

(b) a system of intermediate polarity: Toluene 80, Methanol 20, Ammonia 1; and

(c) a routine system: Benzene 90, Methanol 10.

Common by-products such as acridine, 9-acridanone and 9-aminoacridine were used as reference compounds.

(16) All linear regression and other statistical calculations were carried out on a Texas Instruments TI 51 III machine.

Bibliography

Bibliography

1. Roe F. J. C., in "The Biology of Cancer", chapter 1, *Van Nostrand*, London, (1966).
2. Vander A. J., Sherman J. H. and Luciano D. S., "Human Physiology", p. 126, *McGraw-Hill*, New York, (1970).
3. Burch P. R. J., "The Biology of Cancer", *MTP Press*, Lancaster, (1976).
4. Priestman T. J., "Cancer Chemotherapy", chapter 1, *Montedison Pharmaceuticals*, Barnet, (1977).
5. Pierce G. B., Shikes R. and Fink M., "Cancer: A Problem of Developmental Biology", p. 159 and p. 174, *Prentice-Hall*, Englewood Cliff., N.J., (1978).
6. Albert A., "Selective Toxicity", 5th edition, *Chapman-Hall*, London, (1973).
7. Korolkovas A. and Burckhalter J. H., "Essentials of Medicinal Chemistry", p. 543, *Wiley-Interscience*, New York, (1976).
8. Carter S. K., Bakowski M. T. and Hellmann K., "Chemotherapy of Cancer", p. 17, *Wiley Medical*, New York, (1977).
9. Carter S. K., Bakowski M. T. and Hellmann K., "Chemotherapy of Cancer", p. 328-329, *Wiley Medical*, New York, (1977).
10. Mayers F. H., Jawetz E. and Goldfien A., "Review of Medical Pharmacology", 5th edition, p. 471, *Lange Medical Publications*, Los Altos, Calif., (1976).
11. Priestman T. J., "Cancer Chemotherapy", p. 72-75, *Montedison Pharmaceuticals*, Barnet, (1977).
12. Foye W. O., "Principles of Medicinal Chemistry", p. 138, *Lea & Febiger*, Philadelphia, (1974).
13. Stenlake J. B., "Foundations of Molecular Pharmacology, Vol. 2, The Chemical Basis of Drug Action", chapters 1 and 3, *Athlone Press*, London, (1979).

14. Chapman J. D., Reuvers A. P., Borsa J., Henderson J. S. and Migliore R. D., *Cancer Chemother. Rep. Part 1, 58,* 559, (1974).

15. Schulman S. G., *J. Pharmaceutical Sci., 62,* 1745, (1973).

16. Doggett R. L. S., Bagshaw M. A. and Kaplan H. S., in "Modern Trends in Radiotherapy", Eds.: Deeley & Wood, p. 109, *Butterworths,* London, (1967).

17. Bridges B. A., *Advan. Radiation Biol., 3,* 123, (1969).

18. Mitchell J. S., in "Modern Trends in Radiotherapy", Eds.: Deeley & Wood, p. 194, *Butterworths,* London, (1967).

19. Mitchell J. S. and Simon-Reuss I., *Nature, 160,* 98, (1947).

20. Gray L. H., Conger A. D., Ebert M., Hornsey S. and Scott O. C. A., *Brit. J. Radiol., 26,* 638, (1953).

21. Adams G. E., Dische S., Fowler J. F. and Thomlinson R. H., *Lancet, 1,* 186, (1976).

22. Churchill-Davidson I., Sanger C. and Thomlinson R. H., *Lancet, 1,* 1091, (1955).

23. Fowler J. F., Denekamp J., Sheldon P. W., Smith A. M., Begg A. C., Harris S. R. and Page A. L., *Brit. J. Radiol., 47,* 781, (1974).

24. Howes A. E., Page A. and Fowler J. F., *Brit. J. Radiol., 45,* 250, (1971).

25. Hallowes R. C., West D. G. and Hellmann K., *Nature, 247,* 487, (1974).

26. Peters L. J., *Brit. J. Radiol., 49,* 708, (1976).

27. Thomlinson R. H., Dische S., Gray A. J. and Errington L. M., *Clin. Radiol., 27,* 167 (1976).

28. Urtasum R., Band P., Chapman J. D., Feldstein M. L., Mielke B. and Fryer C., *N. Engl. J. Med., 294,* 1364, (1976).

29. Chapman J. D., Reuvers A. P., Borsa J., Petkau A. and McCalla D., *Cancer Research, 32*, 2616, (1972).

30. Wilson R. L. and Searle A. J. F., *Nature, 255*, 498, (1975).

31. Chapman J. D., Greenstock C. L., Reuvers A. P., McDonald E. and Dunlop I., *Radiat. Res., 53*, 190, (1973).

32. Andrews J. R., "The Radiobiology of Human Cancer Radiotherapy", 2nd edition, p. 136, *University Park Press*, Baltimore,(1978).

33. Doggett R. L. S., Bagshaw M. A. and Kaplan H. S., in "Modern Trends in Radiotherapy", Eds.: Deeley & Wood, p. 121, *Butterworths*, London, (1967).

34. Szybalski W., *Cancer Chemother. Rep. Part 1, 58*, 539, (1974).

35. Erikson R. L. and Szybalski W., *Biochem. Biophys. Res. Commun., 4*, 258, (1961).

36. Lozeron H. and Szybalski W., *J. Mol. Biol., 30*, 277, (1967).

37. Heidelberger C., *Prog. Nucleic Acid Res. Mol. Biol., 4*, 1 (1965).

38. Erikson R. L. and Szybalski W., *Cancer Research, 23*, 122, (1963).

39. Morrison R. T. and Boyd R. N., "Organic Chemistry", 3rd edition, p. 21, *Allyn and Bacon*, Boston, (1973).

40. Graebe C. and Caro H., *Chem. Ber., 3*, 746 (1870).

41. Albert A., "The Acridines", 2nd edition, *Arnold*, London, (1966).

42. Acheson R. M., "Acridines", 2nd edition, *Interscience*,New York,(1973).

43. Smiles J. and Taylor A. E. R., *Nature, 179*, 306, (1957).

44. DeBruyn P. P. H., Robertson R. C. and Farr R. S., *Anat. Record, 108*, 279, (1950).

45. DeBruyn P. P. H., Farr R. S., Banks H. and Morthland F. W., *Exp. Cell Research, 4*, 174, (1953).

46. Browning C. and Gilmour W., *J. Path. Bact.*, *18*, 144 (1913).

47. McIlwain H., *Biochem. J.*, *35*, 1311, (1941).

48. Hurwitz J., Furth J., Malamy M. and Alexander M., *Proc. Nat. Acad. Sci.*, *48*, 1222, (1962).

49. Albert A., Rubbo S. and Burvill M., *Brit. J. Exp. Path.*, *30*, 159, (1949).

50. Elliott W., *Biochem. J.*, *86*, 562, (1963).

51. Waring M., *Mol. Pharmacol.*, *1*, 1, (1965).

52. Peacocke A. R. and Skerrett J. N. H., *Trans. Farad. Soc.*, *52*, 261, (1956).

53. Stone A. and Bradley D., *J. Amer. Chem. Soc.*, *83*, 3627, (1961).

54. Lerman L. S., *J. Mol. Biol.*, *3*, 18, (1961).

55. Lerman L. S., *J. Mol. Biol.*, *10*, 367, (1964).

56. Lerman L. S., *Proc. Nat. Acad. Sci.*, *49*, 94, (1963).

57. Waring M. J., *J. Mol. Biol.*, *54*, 247, (1970).

58. Cohen G. and Eisenberg H., *Biopolymers*, *8*, 45, (1969).

59. Waring M. J. and Chisholm J. W., *Biochim. Biophys. Acta.*, *262*, 18, (1972).

60. Waring M. J. and Henley S. M., *Nucleic Acids Res.*, *2*, 567, (1975).

61. Reinert K. E., *J. Mol. Biol.*, *72*, 593, (1972).

62. Luck G., Triebel H., Waring M. and Zimmer Ch., *Nucleic Acids Res.*, *1*, 503, (1974).

63. Wartell R. M., Larson J. E. and Wells R. D., *J. Biol. Chem.*, *249*, 6719, (1974).

64. Kohn K. W., Waring M. J., Glaubiger D. and Friedman C. A., *Cancer Research*, *35*, 71, (1975).

65. LePecq. J.-B., Xuong N. D., Gosse C. and Paoletti C., *Proc. Nat. Acad. Sci.*, *71*, 5078, (1974).

66. LePecq J.-B. and Paoletti C., *J. Mol. Biol.*, *27*, 87, (1967).

67. LePecq J.-B., LeBret M., Barbet J. and Roques B., *Proc. Nat. Acad. Sci.*, *72*, 2915, (1975).

68. Peck R. M., O'Connel A. P. and Creech H. J., *J. Med. Chem.*, *9*, 217, (1966).

69. Davis M. A. and Soloway A. H., *J. Med. Chem.*, *10*, 730, (1967).

70. Ledochowski A., *Materia Medica Polona*, *8*, 237, (1976).

71. Konopa J., *Materia Medica Polona*, *8*, 258, (1976).

72. Boyland E. and Nery R., *Analyst*, *89*, 95, (1964).

73. Konopa J., Koldej K. and Pawlak J. W., *Chem.-Biol. Interactions*, *13*, 99, (1976).

74. Gieldanowski J., *Materia Medica Polona*, *8*, 252, (1976).

75. Piotrowska-Sowinska J., *Materia Medica Polona*, *8*, 266, (1976).

76. Kwasniewska-Rokicinska C., Swiecki J. and Drosik K., *Materia Medica Polona*, *8*, 289, (1976).

77. Rogalski E., Domagala J. and Kolodziej J., *Materia Medica Polona*, *8*, 311, (1976).

78. Bratkowska-Seniow B., Oleszkiewicz L., Kozak E. and Krizar T., *Materia Medica Polona*, *8*, 323, (1976).

79. Cain B. F., Atwell G. J. and Seelye R. N., *J. Med. Chem.*, *14*, 311, (1971).

80. Atwell G. J., Cain B. F. and Seelye R. N., *J. Med. Chem.*, *15*, 611, (1972).

81. Albert A. and Ritchie B., *J. Chem. Soc.*, 458, (1943).

82. Cain B. F. and Atwell G. J., *J. Med. Chem.*, *19*, 1409, (1976).

83. Cain B. F., Atwell G. J. and Denny W. A., *J. Med. Chem.*, *20*, 987, (1977).

84. Cain B. F., Seelye R. N. and Atwell G. J., *J. Med. Chem.*, *17*, 922, (1974).

85. Cain B. F., Atwell G. J. and Denny W. A., *J. Med. Chem.*, *19*, 772, (1976).

86. Waring M. J., *Euro. J. Cancer*, *12*, 995, (1976).

87. Gromley P. E., Sethi V. S. and Cysyk R. L., *Cancer Research*, *38*, 1300, (1978).

88. Furlong N. B., Sato J., Brown T., Chavez F. and Hurlbert R. B., *Cancer Research*, *38*, 1329, (1978).

89. Hall, D., Swann D. A. and Waters T. N., *J.C.S. Perkin II*, 1334, (1974).

90. Cain B. F., Atwell G. J. and Denny W. A., *J. Med. Chem.*, *18*, 1110, (1975).

91. Wilson W. R., Cain B. F. and Baguley B. C., *Chem.-Biol. Interactions*, *18*, 163, (1977).

92. Cain B. F., Wilson W. R. and Baguley B. C., *Mol. Pharmacol.*, *12*, 1027, (1976).

93. Cain B. F. and Atwell G. J., *J. Med. Chem.*, *19*, 1124, (1976).

94. Legha S. S., Gulterman J. U., Hall S. W., Benjemin R. S., Burgess M. A., Valdivieso M. and Bodey G. P., *Cancer Research*, *38*, 3712, (1978).

95. Von Hoff D. D., Howser D., Gormly P., Bender R. A., Glanbiger D., Levine A. S., and Young R. C., *Cancer Treatment Rep.*, *62*, 1421, (1978).

96. Rose F. L., *Nature*, *215*, 1492, (1967).

97. Reiser A., Terry G. C. and Willets F. W., *Nature*, *211*, 410, (1966).

98. Gilchrist T. L. and Rees C. W., "Carbenes, Nitrenes and Arynes", *Nelson*, London, (1969).

99. Smith P. A. S., in "Nitrenes", Ed.: Lwowski W., *Interscience-Wiley*, New York, (1970).

100. Abramouitch R. A. and Scriven E. F. V., *Chem. Commun.*, *787*, (1970).

101. Odum R. A. and Aaronson A. M., *J. Amer. Chem. Soc.*, *91*, 5680, (1969).

102. Odum R. A. and Wolf G., *J. Chem. Soc. Chem. Commun.*, 360, (1973).

103. Von E. Doering W. and Odum R. A., *Tetrahedron*, *22*, 81, (1966).

104. Sundberg R. J. and Smith R. H., *J. Org. Chem.*, *26*, 295, (1971).

105. Hall J. H., Hill J. W. and Fargher J. M., *J. Amer. Chem. Soc.*, *90*, 5313, (1968).

Hall, J. H., Hill J. W. and Tsai H. C., *Tetrahedron Lett.*, 2211, (1965).

106. Abramovitch R. A. and Kyba E. P., in "The Chemistry of the Azido group", Ed.: Patai S., p. 221, *Interscience*, New York, (1971).

107. Reiser A. and Wagner H. M., in "The Chemistry of the Azido group", Ed.: Patai S., p. 441, *Interscience*, New York, (1971).

108. Johnson B. F., *Clin. Pharmacol. Ther.*, *11*, 77, (1970).

109. Knoll J., Furst S. and Kelemen K., *J. Pharm. Pharmac.*, *25*, 929, (1973).

110. Ning R. Y., Sternbach L. H., Pool W. and Randall L. O., *J. Med. Chem.*, *16*, 879, (1973).

111. Knoll J., Furst S. and Maklett S., *J. Pharm. Pharmac.*, *27*, 99, (1975).

112. Bradshaw D., Butchart G. A. M., Hemsworth B. A. and Stevens M. F. G., *J. Pharm. Pharmac.*, *26* (Suppl.), 123P, (1974).

113. Clark S. C., Jasinski D. R., Pevnick J. S. and Griffth J. D., *Clin. Pharmacol. Therapeutics*, *19*, 295, (1976).

114. Cone E. J., *Xenobiotica, 8*, 301, (1978).

115. Michel M. F., Van Waardhuizen J. P. and Kerrebijn K. F., *Chemotherapy, 18*, 77, (1973).

116. Willner D., Holdrege C. T., Baker S. R. and Cheney L. C., *J. Antibiot., 25*, 64, (1972).

117. Fleet G. W. J., Porter R. R. and Knowles J. R., *Nature, 224*, 511 (1969).

118. Fleet G. W. J., Knowles J. R. and Porter R. R., *Biochem. J., 128*, 499, (1972).

119. Smith R. A. G. and Knowles J. R., *Biochem. J., 141*, 51, (1974).

120. Kiefer H., Lindstrom J., Lennox E. S. and Singer S. J., *Proc. Nat. Acad. Sci., 67*, 1688, (1970).

121. Escher E. and Schwyzer R., *Febs. Letters, 46*, 347, (1974).

122. Perry M. B. and Heung L. L. W., *Canad. J. Biochem., 50*, 510, (1972).

123. Winter B. A. and Goldstein A., *Mol. Pharmacol., 8*, 601, (1972).

124. Das Gupta U. and Rieska J. S., *Biochem. Biophys. Res. Commun., 54*, 1247, (1973).

125. White W. E. and Yielding K. L., *Biochem. Biophys. Res. Commun., 52*, 1129, (1973).

126. Katzenellenbogen J. A., Myers H. N. and Johnson H. J., *J. Org. Chem., 38*, 3525, (1973).

127. Schwartz I. and Ofengand J., *Proc. Nat. Acad. Sci., 71*, 3951, (1974).

128. Seela F. and Cramer F., *Hoppe-Seyler's Z. Physiol. Chem., 356*, S.1185, (1975).

129. Trenin A., in "The Chemistry of the Azido group", Ed.: Patai S., p. 3, *Interscience*, New York, (1971).

130. Knowles J. R., *Accounts of Chem. Res.*, *5*, 155, (1972).

131. Lawley P. D., *Prog. in Nucleic Acid Res. & Mol. Biol.*, *5*, 89, (1966).

132. Bayley H. and Knowles J. R., *Methods Enzymol.*, *46*, 69, (1977).

133. Zollinger H., "Azo and Diazo Chemistry", p. 147 and 65, *Interscience*, New York, (1961).

134. *Mass Spectral Data*, *2*, No. 639, (1951).

135. Wentrup C., *Tetrahedron*, *26*, 4969, (1970).

136. Crow W. D. and Wentrup C., *Tetrahedron Letters*, 4379, (1967).

137. Rutherford K. G., Redmond W. and Rigamonti J., *J. Org. Chem.*, *26*, 5149, (1961).

138. Albert A., "The Acridines", 2nd edition, p. 179, *Arnold*, London, (1966).

139. Scriven E. F. V. and Thomas D. R., *Chem. & Ind.*, 385, (1978).

140. Albert A. and Serjeant E. P., "The Determination of Ionisation Constants", *Chapman-Hall*, London, (1971).

141. Clark J. and Perrin D. D., *Quart. Revs.*, *18*, 295, (1964).

142. Butchart G. A. M., "Selective Toxicity and The Covalent Bond", Ph.D. thesis, p. 96, *University of Aston*, (1975).

143. Eastham S. J., "Studies on antitumour acridines", Pharmacy B.Sc. project report, *University of Aston*, (1979).

144. Tsujimoto K., Ohashi M. and Yonezawa T., *Bull. Chem. Soc. Japan*, *45*, 515, (1972).

145. Gibson M. S., *J. Chem. Soc.*, 1076, (1956).

146. Rammler D. H. and Zaffaroni A., *Ann. N.Y. Acad. Sci., 141*, 131, (1967).

147. Maddock C. L., Green M. N. and Brown B. L., *Proc. Am. A. Cancer Res., 7*, 46, (1966).

148. Unpublished screening data from the *National Cancer Institute*, Bethesda, U.S.A.

149. Pigram W. J., Fuller W. and Hamilton L. D., *Nature New Biology, 235*, 17, (1972).

150. Schwartz H. S., *Biomedicine, 24*, 317, (1976).

151. Bliss, E. A., Brown T. B., Stevens M. F. G. and Wong C. K., *J. Pharm. Pharmacol.*, in print.

152. Stevens M. F. G., personal communication.

153. Pigram W. J., Physics Department, *University of Keele*, personal communication.